

**INFLUENCE OF CORTICAL  
DESCENDING PATHWAYS ON  
NEURONAL ADAPTATION IN THE  
AUDITORY MIDBRAIN**

**BENJAMIN ROBINSON**

**UCL**

**PHD NEUROSCIENCE**

**2014**

# DECLARATION

I, Benjamin Robinson, confirm that the work presented in this thesis is my own. Where information has been derived from other sources, I confirm that this has been indicated in the thesis.

.....

Date: 7<sup>th</sup> February 2014

# ABSTRACT

---

Adaptation of the spike rate of sensory neurones is associated with alteration in neuronal representation of a wide range of stimuli, including sound level, visual contrast, and whisker vibrissa motion. In the inferior colliculus (IC) of the auditory midbrain, adaptation may allow neurones to adjust their limited representational range to match the current range of sound levels in the environment. Two outstanding questions concern the rapidity of this adaptation in IC, and the mechanisms underlying it. I hypothesise that the descending, corticofugal system, a major pathway of the auditory system, plays a role in neuronal adaptation to sound level statistics in the IC.

I recorded single unit responses in guinea pig IC to a broadband stimulus which switched every 5s between two distributions of sound level. I then deactivated auditory cortex bilaterally using cooling cryoloops. During cooling, adapted neuronal rate-vs.-sound level functions shifted rightwards, with thresholds tending to increase. This resulted in attenuation of the improvement in neuronal representation of mean sound levels associated with adaptation. In addition, the population of IC neurones adapted more slowly to the switching stimulus during cooling. The data suggest that cortex is not necessary for the generation of midbrain spike-rate adaptation, but that adaptation appears to be a property intrinsic to IC neurones and/or inherited from more peripheral sites. Nonetheless, corticofugal activity appears to be important in midbrain neural coding of sound level, altering adaptation and improving neuronal representation of sound levels around the most common levels in the stimulus.

# CONTENTS

---

<b>1</b>	<b>INTRODUCTION</b>	<b>9</b>
1.1	The Inferior Colliculus	9
1.2	Adaptation of neuronal responses	11
1.3	Corticofugal pathways	12
1.3.1	Anatomy of corticofugal pathways	12
1.3.2	Physiological effects of corticofugal pathways	16
1.3.3	Corticofugal pathways and neuronal plasticity	21
1.4	Adaptation to sound level statistics	23
1.4.1	Functions of adaptation	21
1.4.2	Mechanisms of adaptation	24
1.5	Summary	25
<b>2</b>	<b>METHODS: THE CRYOLOOP</b>	<b>26</b>
2.1	Introduction	26
2.2	The cryoloop	28
2.2.1	Cryoloop components	28
2.2.2	Surgery and cryoloop positioning	30
2.2.3	Cryoloop operation	30
2.3	Cryoloop calibration: methods	31
2.3.1	Temperature probe	32

2.3.2	Cortical temperature measurement	33
2.3.3	IC temperature measurement	33
2.3.4	Simultaneous neuronal and temperature measurement	34
2.3.5	Cooling cortex overlying IC	34
2.4	Cryoloop calibration data	37
2.4.1	Loop and cortex temperatures	37
2.4.2	IC temperature during cooling	40
2.4.3	Auditory cortex evoked neuronal activity during cooling	42
2.4.4	Effects of cooling IC without cooling auditory cortex	44
2.5	Discussion	47
<b>3</b>	<b>METHODS: TIME COURSE OF ADAPTATION</b>	<b>49</b>
<hr/>		
3.1	Introduction	49
3.2	Surgery	50
3.3	Sound delivery	51
3.4	Physiological recordings	52
3.5	Stimulus design and presentation	52
3.6	Cryoloop operation with respect to stimulus presentation	54
3.7	Data analysis	56
<b>4</b>	<b>CORTICAL COOLING AND MIDBRAIN SOUND-EVOKED NEURONAL RESPONSES</b>	<b>59</b>
<hr/>		
4.1	Introduction	59
4.2	Rate-vs.-level functions and the switching stimulus	61
4.3	Observations on bilateral auditory cortex cooling	64

4.4	Cooling non-auditory cortex	65
4.5	Effects of cortical cooling on rate-vs.-level functions	69
4.6	Baseline rate-vs.-level functions	75
4.7	Recovery of rate-vs.-level functions	77
4.8	Quantification of rate-vs.-level functions	78
4.8.1	Threshold, saturation, and other measures	78
4.8.2	Assessing suprathreshold alterations	85
4.9	Coding measures of rate-vs.-level function shift	91
4.10	Unilateral cooling	95
4.10.1	Contralateral cooling	95
4.10.2	Ipsilateral cooling	96
4.10.3	Ipsi- and contralateral cooling comparisons	98
4.11	Summary	99
<b>5</b>	<b>COOLING EFFECTS ON ADAPTATION TIME COURSE</b>	<b>101</b>
<hr/>		
5.1	Introduction	101
5.2	Stimuli and recordings	102
5.3	Time course without cortical cooling	102
5.3.1	Rapid, asymmetrical adaptation	102
5.3.2	Time course of adaptation and stimulus time scales	106
5.4	Time course of adaptation during cortical cooling	106
5.4.1	Adaptation of mean spike rates	106
5.4.2	Time constants of adaptation during cortical cooling	111
5.4.3	Adjustments of rate-vs.-level functions over time	119
5.4.4	Adaptation time constants and neuronal characteristic frequency	122
5.4.5	A slow component of adaptation	123

5.5	Discussion	124
<b>6</b>	<b>DISCUSSION</b>	<b>126</b>
6.1	Introduction	126
6.2	Cryoloop apparatus	127
6.3	General observations during cortical cooling	129
6.4	Effects of cortical cooling on rate-vs.-level functions	130
6.4.1	Cooling-associated threshold shifts	130
6.4.2	Cooling-associated modulation of suprathreshold levels	131
6.4.3	Saturation and dynamic range	133
6.4.4	Adaptation state and rate-vs.-level function shift on cooling	134
6.4.5	Laterality of cortical input	135
6.4.6	Cortical influence on midbrain neuronal coding of sound level	138
6.5	Spike rate adaptation and cortical cooling	139
6.5.1	Cortical influence on depth of adaptation	139
6.5.2	Cortical influence on time course of adaptation	139
6.5.3	Adaptation to a reduction in mean sound level	143
6.5.4	Relation of adaptation time course to characteristic frequency	144
6.5.5	Multiple time scales of adaptation in IC	145
6.6	Neuronal recovery post-cooling	145
6.7	Mechanisms of adaptation and corticofugal modulation	147
6.8	Anatomy of corticofugal effects	150
6.9	Limitations of study	151
6.9.1	Urethane anaesthesia	151

6.9.2	Control experiments: temperature	152
6.9.3	Data limitations	153
6.9.4	Analysis limitations	153
6.9.5	Interpretation of function	154
6.10	Summary model and future work	155

**BIBLIOGRAPHY** **159**

---

**ACKNOWLEDGEMENTS** **169**

---

# 1

## INTRODUCTION: THE AUDITORY MIDBRAIN, ADAPTATION, AND THE DESCENDING PATHWAYS

---

### ***1.1 The Inferior Colliculus***

The inferior colliculus (IC) is the site of converging inputs within the ascending auditory pathway, and as such is considered the principal auditory nucleus in the midrain (Malmierca and Hackett, 2010). Sound stimuli in the environment lead to activation of IC neurones via the following steps: pressure changes in the air (sound waves) are transmitted mechanically through the outer and middle ear to the cochlea within the inner ear, on which are arrayed the inner hair cells (IHCs) whose function, in response to cochlear motion, is to generate receptor potentials which in turn activate auditory nerve neurones that synapse the IHCs. The first auditory relay, the cochlear nucleus, is the site of termination of auditory nerve

neurones, and, from here, the ascending auditory pathway becomes complex, projecting to the nuclei of the lateral lemniscus and the Superior Olivary Complex bilaterally (Pickles, 1984; Malmierca and Hackett, 2010). This divergent pathway then converges on the IC, whose inputs include: the lateral superior olive (LSO) bilaterally; the medial superior olive (MSO) ipsilaterally; the nuclei of the lateral lemniscus; the contralateral dorsal cochlear nucleus (DCN) the contra-teal posteroventral nucleus, and the contralateral anteroventral nucleus (Adams, 1979).

Despite the complexity of inputs to the IC, its anatomical structure follows a set pattern across small mammal species (including the mouse, the ferret, the rat, and the guinea pig): IC in these species is a tripartite structure, with a central nucleus (ICC) overlain dorsally by the dorsal cortex (DCIC) and surrounded laterally and rostrally by the external cortex (ECIC; Malmierca et al. 1995). The central nucleus of the IC (ICC) is tonotopically organised, characterised by the presence of fibrodendritic laminae consisting of parallel layers of afferent lemniscal fibres and neurones with disk-shaped cells with flat dendritic arbours orientated in the plane of any given lamina (Malmierca and Hackett, 2010). These laminae consist of iso-frequency sheets of cells, and it is this arrangement which gives rise to the progressive, gradual, frequency changes with depth observed in sound-evoked neural recordings, which, in ICC, are usually short-latency, robust, and display a distinct characteristic frequency (Pickles, 1984; Malmierca and Hackett, 2010). By contrast, the ECIC receives strong connections from somatosensory structures as well as auditory input via the ICC and the nuclei of the lateral lemniscus, and appears to be an integrative area rather than a predominantly auditory relay, having broad tuning curves with indistinct best frequencies (Pickles, 1984). The DCIC may be particularly important in

corticofugal feedback, as it receives the main input from the cortex, much denser than that of the ICC (see section 1.2.1).

## ***1.2 Adaptation of neuronal responses***

Adaptation, a form of plasticity observed as the decline in neuronal firing rate over the course of sustained sensory stimulation (Adrian 1926), appears to be a ubiquitous property of sensory neurones, occurring across species and sensory modalities. It has, in several cases, been associated with adjustments in neuronal coding to take account of stimulus statistics, including in the visual (Ohzawa et al. 1985; Brenner et al. 2000) and somatosensory (Maravall et al. 2007) systems. Similarly, in the auditory system, adaptation has been associated with an improvement in neuronal coding of sound levels around the mean level encountered in the environment, serving to match the limited neuronal dynamic range to the range of commonly occurring sound levels (Dean et al. 2005; Wen et al. 2009). This process of adaptive improvement in neuronal coding operates in the cortex (Watkins & Barbour 2008; Watkins & Barbour 2010), the midbrain inferior colliculus (IC; Dean et al. 2005), and even, to a lesser extent, the auditory nerve (Wen et al. 2009). However, it is not known whether adaptation is a local mechanism in IC, whether it is inherited from more peripheral sites, whether it is initiated or modulated in a top-down fashion via descending inputs from cortex, or whether it results from an interaction of these mechanisms (Tzounopoulos & Kraus 2009). This thesis attempts to address that question, investigating the extent to which adaptation to sound level statistics in the IC occurs in the absence of inputs from cortex, and to what extent it is cortically influenced. Driven in part by previous work suggesting that the influence of cortex on IC may affect

temporal aspects of the neuronal response as well as spike-rates (Popelár et al., 2003; Nakamoto et al., 2010), the present study also examines the time course of the adaptation to sound-level statistics in the IC before, during, and after cortical deactivation.

## **1.3 Corticofugal pathways**

### **1.3.1 Anatomy of corticofugal pathways**

Central to the notion that cortex may influence the function of subcortical structures is the anatomical description of massive neuronal projections from wide areas of sensory cortex to structures throughout the thalamus and brainstem. Over the last half-century, the anatomy of the corticofugal pathways from auditory cortex has been examined in a variety of species, including monkey (Jasper et al. 1952; Winer et al. 2002), cat (Diamond et al. 1969; Adams 1980; Winer et al. 2002; Wong & Kelly 1981; Aitkin & Phillips 1984; Winer & Prieto 2001), ferret (Bajo et al. 2007), opossum (Linden & Rocha-Miranda 1983), guinea pig (Feliciano & Potashner 1995; Schofield & Coomes 2005; Coomes et al. 2005; Meltzer & Ryugo 2006; Schofield & Coomes 2006; Lim & Anderson 2007; Motts & Schofield 2009; Schofield 2009; Schofield 2010), gerbil (Bajo & Moore 2005), rat (Arnault & Roger 1987; Moriizumi & Hattori 1991; Romanski & LeDoux 1993; Saldaña et al. 1996; Meltzer & Ryugo 2006), and mouse (Meltzer & Ryugo 2006). Physiological work on these species, and on bats, is described in Section 1.3

The majority of studies examining cortical descending systems have examined projections to the thalamus, the inferior colliculus (IC), or both, and have elucidated several important anatomical principles. First, corticocollicular pathways can be bilateral (Huffman & Henson 1990), and recent work using fluorescent retrograde tracers suggests that about half of the contralateral

projecting neurones project ipsilaterally also (Coomes et al. 2005). This implies that both cortices might influence a given IC neurone. Second, the site of termination of corticocollicular fibres in the IC is not uniform, but appears greater in the dorsal cortex and the external nucleus of the IC than in the central nucleus (Schofield 2009). This observation is important given that the present study aims to record in the central nucleus (ICC). In contrast with earlier studies employing axonal degeneration techniques and suggesting no direct cortical input to the ICC (Huffman & Henson 1990), several studies using retrograde tracers have now confirmed that, in guinea pigs, the central nucleus does receive a direct input from cortex (Feliciano & Potashner 1995; Coomes et al. 2005). A third anatomical finding is that the origin of cortical fibres projecting to IC is restricted to layers V and VI of auditory cortex, with the majority deriving from layer V. Almost all corticocollicular fibres contacting the ICC derive from layer V (Schofield 2009). Thus any method aiming to deactivate descending pathways through deactivating their cortical origin will only be effective in if it deactivates layers V and VI of cortex.

A fourth anatomical principle is that, in addition to a direct corticocollicular pathway, cortex may influence IC via indirect routes such as via the cochlear nucleus (Schofield & Coomes 2005). The possibility that this pathway could have an indirect effect on the IC is strengthened by the recent finding that a subset of CN neurones which receive descending input, project directly to IC, ipsilaterally, contralaterally, or bilaterally (Schofield & Coomes 2005). Those IC neurones receiving a direct cortical input can themselves send centrifugal projections to CN neurones (Schofield & Coomes 2006). Another indirect pathway from cortex to IC is through contralateral IC, via the commissure of the inferior colliculus (Aitkin & Phillips 1984).

Other polysynaptic pathways from cortex to IC run via non-auditory brain areas. For example, auditory cortex sends possibly excitatory projections to two midbrain tegmental nuclei: the pedunculo-pontine tegmental nucleus (PPT) and the laterodorsal tegmental nucleus (LDT; Schofield & Motts 2009). These nuclei are part of a general arousal system, and have been identified as the source of cholinergic inputs to the IC (Motts & Schofield 2009). The possibility that cortical neurones can elicit cholinergic effects in the midbrain is strengthened by the finding that PPT and LDT neurones receiving cortical input also project to IC, both ipsilaterally and contralaterally (Schofield 2009).

Other non-auditory targets of the auditory cortex include the amygdala (Romanski & LeDoux 1993) and the striatum (Moriizumi & Hattori 1991), as well as a variety of other non-auditory areas (Winer et al. 2005). Of further note is the finding that the corticocollicular pathway in rat sends collaterals to the basal ganglia, suggesting a possible role for this pathway in coordinating audition and movement (Moriizumi & Hattori 1991).

Similar to the indirect cholinergic pathway via the midbrain tegmentum, several lines of evidence suggest that the direct pathway from cortex to IC is also excitatory. In cat and rat, corticocollicular axon terminals contain round synaptic vesicles and make asymmetric synaptic junctions (Saldaña et al. 1996). In addition, ablation of corticocollicular fibres depressed electrically-evoked calcium dependent release of D-asp, associated with glutamatergic synapses, in the IC (Feliciano & Potashner 1995). Finally, short-latency post-synaptic potentials were observed in the central nucleus of the cat IC when AC was stimulated (Mitani et al. 1983). A sixth anatomical principle is that multiple areas of auditory cortex project to IC – with up to eleven separate projection sites from cat AC (Winer 2005; Winer & Lee 2007). Finally, it appears that corticocollicular,

unlike corticothalamic, projections maintain tonotopic relationships (Lim & Anderson 2007).

To summarise, anatomical studies of corticocollicular fibres lead to the view of an excitatory projection whose origin is layers V and VI across a wide range of auditory cortical regions and whose paths are multiple, both polysynaptic and monosynaptic, encompassing auditory and non-auditory areas on their passage to both ipsilateral and contralateral IC. This view has implications for the current study. First, it suggests a multiplicity of function of the pathways, and therefore any consistent physiological results across neurones may be surprising – although the predominantly excitatory nature of the pathway may suggest that it generally tends to counteract adaptation. This prediction can however easily be challenged by invoking polysynaptic pathways through inhibitory, GABAergic interneurons, common within the IC (Oliver et al. 1994). More importantly, these anatomical data have driven my approach to the method of cortical deactivation: the current study is, to my knowledge, the first to deactivate reversibly both auditory cortices simultaneously, an important advance considering the bilateral nature of the projections. In addition, the cryoloops employed to deactivate cortex are designed to cover and deactivate core and belt areas of auditory cortex to ensure that all descending projections from cortex are deactivated (Wallace et al 2000; Coomber et al 2011). Finally, in interpreting the data, it is important to bear in mind that there are many pathways from cortex to IC, such that specific claims cannot be made concerning the function of corticocollicular pathways *per se*, as others have been able to do (Bajo et al. 2010), but must restrict conclusions as pertaining to corticofugal pathways in general.

### **1.3.2 Physiological effects of corticofugal pathways**

To probe the function of the descending pathways, investigators have stimulated or deactivated cortex, and therefore its efferents, whilst recording the activity of neurones located in subcortical structures of interest. Methods of cortical inactivation include surgical aspiration (Murphy & Sillito 1987), spreading depression (Buresova et al. 1964), cooling with a neoprene bladder (Orman & Humphrey 1981), with a Peltier device (Hashemi-Nezhad et al. 2003), or with a cryoloop (e.g. Lomber et al. 1999, Coomber et al. 2011), application of pharmacological agents such as lidocaine (Jen et al. 2001) or tetrodotoxin (Popelár et al. 2003). Studies approaching the question of corticofugal function by stimulating cortex electrically are legion (e.g. Torterolo et al. 1998; Suga et al. 2000; Jen et al. 2001). The cortical excitation approach, whilst useful, may be less physiologically relevant than deactivation paradigms, given that the latter provide the opportunity to examine ‘pure’ afferent responses in the absence of cortical feedback. Nonetheless, both kinds of studies have provided valuable data, as discussed below.

One early deactivation study found that 48% of rat IC neurones exhibited altered tone-driven activity when cortex was inactivated by spreading depression (Buresova et al. 1964). Of interest to the current study, the authors found that in most neurones the greatest alterations occurred in the final 0.4s of a 2s stimulus; in no cases were the main effects of cortical inactivation to be found within the first 0.4s of sound-driven stimulation. This is consistent with the notion that corticofugal circuits have a longer latency, but it is also consistent with the idea that corticofugal influences are most potent when neurones have adapted to a stimulus – an idea which applies to the current study. Using tetrodotoxin, Popelár and colleagues also inactivated ipsilateral rat AC and observed increases in firing rate (40%), decreases (44%) or no change (16%) in IC single units (Popelár et al.

2003). In accord with the data of Buresova et al (1964), Popelár and colleagues found that the onset part of the neuronal peri-stimulus time histogram (PSTH) was often preserved unchanged during cortical inactivation, whereas the latter 75ms underwent either excitatory or inhibitory changes. It was never the case that only the onset part of the PSTH was altered, without an attendant change in the sustained segment. As with the data of Buresova et al (1964), this finding suggests that corticofugal effects may be more pronounced when spike-rates have adapted.

In addition to examining corticofugal effects on neuronal spike rates, several groups have investigated temporal aspects of the neuronal response within subcortical structures during cortical deactivation. For example, an active cortex appears to enhance the difference in temporal responses to two harmonic complexes presented simultaneously, in single neurones in guinea pig IC (Nakamoto et al. 2010). Further evidence for a role of corticofugal pathways in spike-timing has been found in guinea pig thalamic Medial Geniculate Body (MGB), where descending input from cortex improves neuronal synchronization (Villa et al. 1999). This temporal function has also been found in the visual system, where corticofugal pathways appear to increase the precision with which lateral geniculate nucleus (LGN) responses are locked to stimulus features (Andolina et al. 2007). In addition, corticothalamic pathways appear to improve synchronization of relay cells in thalamus whose receptive fields underlie the creation of orientation-tuning in cortex, thereby facilitating firing of their cortical target neurones (Sillito et al. 1994; see also Murphy and Sillito (1987) for role of corticofugal feedback in the generation of length tuning in the LGN). This temporal aspect of corticofugal function may serve a gating function (Villa et al. 1991). In the present study, I assess the temporal effects of corticofugal pathways

by examining the time course of adaptation before, during, and after cortical cooling.

In addition to IC, auditory cortex sends projections to other subcortical areas. Effects of cooling cortex on activity in the thalamus appear to be similar to those occurring during decreased arousal (Orman & Humphrey 1981), which may suggest a role for these pathways in modulating subcortical structures according to the state of wakefulness of the animal. However, effects of cortical inactivation on thalamus responses are complex, with decreases in spontaneous rate in 60% of neurones, increases in 20%, and a variety of alterations in frequency tuning and synchronization, as mentioned above (Villa et al. 1991). In addition to thalamus and IC, corticofugal pathways have been found to alter responses in cochlear nucleus (Luo et al. 2008) and even, via the medial olivocochlear bundle, hair-cell responses in the cochlear (Xiao & Suga 2002). This last observation is supported by a study in humans that reported altered otoacoustic emissions (OAEs) during stimulation of auditory cortex in the course of surgery for refractory epilepsy (Perrot et al. 2006). It has been suggested that, in line with decreased density of anatomical inputs, corticofugal influence diminishes at each successive station towards the periphery (Luo et al. 2008), but this has not been confirmed by direct comparisons within single experiments.

In contrast to these deactivation techniques, other groups have stimulated auditory cortex whilst recording subcortically. Syka and colleagues stimulated rat auditory cortex with ball electrodes whilst recording in ipsilateral IC (Syka & Popelár 1984). ~50% of neurones displayed altered activity during cortical stimulation. Of those neurones whose activity did change, 61/84 underwent excitatory action potential bursts with latencies of 3-15ms, followed by longer periods of inhibition of spontaneous or sound-evoked activity. The authors did not

present data from contralateral stimulation, but stated that it appeared similar. However, a more recent study directly comparing ipsi- and contralaterally stimulated cortical influences in guinea pig IC found that the ipsilateral pathway tended to induce excitatory responses, and the contralateral pathway inhibitory responses, though with a high degree of overlap (Tortorolo et al. 1998).

What effects might these changes in excitability have on neuronal input-output functions? Using an ipsilateral excitation paradigm in big brown bat, Sun and colleagues (1996) recorded rate-vs.-level functions in midbrain and found that cortical excitation resulted in reduced excitability and rightward shift of rate-vs.-level functions, whereas blocking cortex using lidocaine resulted in a leftward shift of rate-vs.-level functions, suggesting that the corticofugal system may decrease midbrain sensitivity to incoming sounds (Sun et al. 1996). However, the tonal stimulus used was only 4ms in duration, delivered at 1Hz; the results of Popelár et al. (2003) and Buresova (1964) suggest that to gain a comprehensive picture of corticofugal pathway action a stimulus two to three orders of magnitude longer in duration would be necessary. Indeed, Popelár et al. observed a wide variety of alterations in rate-vs.-level functions, obtained by recording IC single unit responses to 100ms tones at characteristic frequency (CF). These alterations with ipsilateral cortical deactivation include: right- and leftward shifts in rate-vs.-level function position with attendant alterations in threshold; shape changes; and depression of overall rate – a wider variety of alterations than that of Sun and colleagues.

Thus the corticofugal pathways appear either to increase or decrease excitability with an attendant variety of alterations to input-output functions. This variety of responses to cortical manipulation is consistent with anatomical evidence demonstrating multiple possible pathways of corticofugal information

flow. One such pathway may be the cortex→external nucleus of IC→central nucleus of IC pathway (central nucleus: ICC; external nucleus: ICx). In big brown bat, the cortex-ICx pathway is excitatory and uses NMDA receptors; the ICx-ICC pathway is inhibitory and mediated in part through GABA-A receptors (Jen et al. 2001). Thus, cortex could facilitate ICx, which would lead to an indirect inhibitory action in ICC. This pathway, in addition to the direct excitatory AC-ICC pathway, could explain the finding of excitation and inhibition across different IC cells and even within the same neurone. A segregation of corticofugal effect (excitatory or inhibitory) between the two kinds of ascending auditory pathway may also occur in rodents: nonlemniscal neurones in the auditory thalamus of the guinea pig are predominantly inhibited by corticofugal feedback, whereas lemniscal neurones are generally facilitated by cortical feedback (He 2003a; He 2003b).

Two recent studies have suggested that corticofugal pathways play a role in human audition. First, the work of Perrot and colleagues (2006) suggests that human auditory cortex stimulation can alter otoacoustic emissions (OAEs), which reflect the activity of cellular amplification processes in the cochlea. Second, de Boer and Thornton's elegant study on speech-in-noise discrimination found that subjects' task performance was predicted by the degree of activity in the medial olivocochlear bundle (MOCB). The MOCB, originating in the brainstem and terminating in the cochlea, is the route by which corticofugal influences reach the inner ear (Guinan, 2006; Xiao and Suga, 2002; Perrot et al., 2006). The authors found that MOCB activity altered over the course of learning the task, increasing most in those subjects whose initial MOCB activity, and whose task-scores, were lowest (de Boer and Thornton, 2008).

### ***1.3.3 Corticofugal pathways and neuronal plasticity***

The importance of the corticofugal pathways in plasticity was emphasised by two recent studies investigating interaural level differences (ILD). The first study demonstrated that neuronal ILD sensitivity in IC is altered by reversible cortical deactivation: Nakamoto and colleagues (2008) found a striking array of changes to neuronal ILD-response functions during cooling, including a complete cessation of response in 8% of neurones, as well as changes in shape of functions and increases or decreases in firing rate that tended to preserve shape. The variety of changes precluded any broad conclusions about their function or that of the corticofugal system in regards to ILD coding. However, a more recent study has confirmed that plasticity of ILD representation is a behaviourally important aspect of corticofugal action. Bajo and colleagues trained ferrets on an auditory spatial task involving interaural level, and then plugged one ear to alter interaural level cues (Bajo et al. 2010). Ferrets with corticocollicular pathways intact were able to relearn spatial position relationships despite the ear-plug. However, when corticocollicular pathways were inactivated, the animals could no longer relearn spatial positions, suggesting that corticocollicular pathways are necessary for long-duration plasticity in the ferret auditory system.

Another potentially important role for the corticofugal systems has been suggested by cortical stimulation studies in bats and mice, which have led to the notion that cortical neurones of a given BF facilitate subcortical responses at that frequency, and suppress responses to other frequencies, resulting in modulation of frequency-tuning curves (e.g. Suga 2008), and that this principle applies also to other parameters such as duration tuning (Ma & Suga 2007). This ‘egocentric selection’ may explain the observation of increases and decreases in the excitation of IC neurones when cortex is stimulated over large areas, as opposed to over small areas of limited frequency. It appears that the degree of BF shift as a result

of ‘egocentric selection’ is proportional to the difference in BF between the collicular and the cortical neurone, up to a certain point (Yan & Ehret 2002). It has also been suggested that when collicular and cortical BFs do not match, cortical excitation leads to higher neuronal thresholds and smaller neuronal dynamic ranges, but that when BFs are similar, the opposite may be true (Yan & Ehret 2002). It is worth noting, however, that these stimulation studies often use paradigms of electrical stimulation of cortex lasting tens of minutes to induce subcortical plasticity, and it is far from clear whether such paradigms reflect natural brain processes – though attempts have been made to show that sound stimuli alone can induce similar plasticity (Gao & Suga 2000).

These cortical stimulation studies have led to the view that plasticity lasting for several hours or longer in subcortical structures depends on cortical feedback. Adaptation to sound level statistics, which I investigate in the current study, is a form of plasticity lasting milliseconds to seconds: it may be the case that all forms of plasticity depend on cortical feedback, or, alternatively, it may be that shorter-lasting forms such as adaptation are driven completely or partly by intrinsic IC processes or by ascending inputs to IC cells. This question has been addressed in the medial geniculate body (MGB) of the auditory thalamus in recent deactivation studies. Antunes and Malmierca (2011), using cryoloop deactivation in rat, found that stimulus-specific adaptation (SSA), lasting on the order of hundreds of milliseconds, was unaltered by cortical feedback, whereas Bäuerle et al. (2011) found, using muscimol deactivation in gerbil, that SSA in MGB was altered by cortical deactivation. My study examines the extent to which adaptation in IC depends on descending inputs from cortex.

## **1.4 Adaptation to sound level statistics**

### **1.4.1 Functions of adaptation**

Perceptible sound levels in nature vary from 0dB SPL to above 120dB SPL, and the human auditory system is able to represent such sounds with decibel precision over the entire range. In electrophysiological experiments, neural representation of sound level is often visualised by plotting input-output functions relating sound level to neural response. However, in seeming contradiction of the wide psychophysical range of discriminable sound levels, the sloping parts of these functions – their dynamic ranges - extend over only 20dB in the auditory nerve and inferior colliculus. Previous studies have, however, demonstrated that, in the presence of noise, firing rate-vs.-sound level functions can shift to the right, preserving the steepest part of the functions at sound levels louder than the background noise and thus preserving sensitivity to higher-intensity tones. This effect has been found in auditory nerve fibres (Coltalupes et al., 1984; Gibson et al 1985), cochlear nucleus (Gibson et al. 1985), IC (Rees and Palmer 1988) and auditory cortex (Philips and Hall, 1986). Although suppression in the cochlea appears to explain this effect to a large extent, Rees and Palmer (1988) found that the effect was greater in the IC than in auditory nerve.

More recently, extending such research into the relationship of adaptation to the dynamic range problem, Dean and colleagues found that neuronal rate-level-functions can adapt not only to ongoing background noise, but to sound level distributions, shifting along the abscissa to include a range of sounds which begins at or close to the most commonly occurring sound levels, and improving neuronal population coding around the most probable levels (Dean et al. 2005). Adaptation thus appears to re-set the dynamic range of rate-vs.-level functions to match current environmental demands. A similar matching process was found first to visual contrast in the retina (Normann & Werblin 1974) and in the striate

cortex (Ohzawa et al. 1985). Adaptation has also been observed with respect to other visual parameters (Brenner et al. 2000) and in other sensory systems (e.g. somatosensory, Maravall et al. 2007). It appears that the simple decline in spike rate, observed in the first ever recordings of sensory neurones (Adrian, 1926), has a functional significance, permitting neurones with limited dynamic ranges to represent the much larger ranges which the environment presents. An outstanding question is whether neurones in the IC can adapt with appropriate speed to cope with the dynamics of sound stimuli, as has been found for visual responses in the fly (Fairhall et al. 2001). It is important to note that other functions of neuronal adaptation have been suggested, not mutually exclusive with those described above. These include minimizing energy expenditure (Laughlin 2001) and separating signals from noise (Benda et al. 2005).

#### **1.4.2 Mechanisms of adaptation**

It is not known which mechanisms drive adaptation in sound level coding in IC. Adaptation may arise through changes in the balance of excitatory and inhibitory inputs to an adapting neurone in the IC, or through changes in the intrinsic excitability of the IC neurone itself. The IC lies at least three synaptic stages beyond the auditory transducers, the cochlear hair cells, and is a site of extensive excitatory and inhibitory synaptic convergence. Some IC neurones also display intrinsic conductances that lead to adaptive responses *in vitro* (Sivaramakrishnan & Oliver 2001; Bal et al. 2002). As discussed above, the IC, and its inputs, are subject to centrifugal influences (Yan et al. 2005; Winer et al. 2005; Lim & Anderson 2007; Bajo et al. 2010). Such processes operate over widely varying timescales; it remains unclear which of them contribute to adaptation observed in the IC *in vivo*, and at what stage in the auditory pathway the adaptation first arises. As part of this thesis, I first characterize the time course of neuronal

adaptation to sound level in the IC, results that have in part previously been reported (Dean et al. 2008). The motivation for assessing the time course was threefold. First, to assess the influence of corticofugal pathways on the time course of the adaptive process; second, the timescale over which the adaptation operates will constrain the usefulness of the adaptive neuronal code and any corticofugal influence on the code, and third, by assessing the time course of the adaptation, insight may be gleaned into which mechanisms are likely to be involved. In support of this last aim, recent studies in the locust have demonstrated that different mechanisms of adaptation lead to significantly different time courses (Hildebrandt et al. 2009).

In addition to gaining mechanistic insights through investigating the time course, the present study tests a specific mechanistic question: is adaptation of IC rate-vs.-level functions generated exclusively within the afferent pathway from cochlear to IC, or does it depend in part or in full on efferent projections from cortex that synapse at or peripherally to IC? I address this question by reversibly deactivating cortex whilst inducing adaptation in the IC.

### **1.5 Summary**

The current thesis aims to advance understanding of auditory adaptation and the auditory corticofugal pathways. In the case of adaptation, it will address the question of how quickly adaptation to distributions of sound levels occurs, aiming to improve understanding of the potential utility of adaptation and to suggest mechanisms which may underlie it. In the case of the corticofugal pathways, this thesis will examine the effect of bilateral cortical deactivation on the responses of collicular neurones. In particular, I address the question of whether corticofugal fibres play a role in generating or otherwise modifying auditory neuronal adaptation.

# 2

## THE CRYOLOOP

---

### **2.1 Introduction**

The aim of using a cryoloop is to inactivate, by cooling, a small area of neuronal tissue around the loop. It is likely that this cooling inactivation results from a variety of processes, including presynaptic mechanisms such as reduced quantal transmitter/vesicle release (Hardingham and Larkman, 1997; Yang et al. 2005) and postsynaptic mechanisms such as depolarization of the postsynaptic membrane resulting from inhibition of ion pumps (Schiff & Somjen 1985). Volgushev and colleagues (2000b), showed that cooling leads to membrane depolarisation and an increase in input resistance in neurons recorded in slices of rat visual cortex. In contrast, Cao and Oertel (2005) showed that in mouse cochlear nucleus slices, reducing the temperature had differential effects on different voltage-sensitive conductances in octopus cells, but, in general, appeared to slow the kinetics of these conductances and lead to hyperpolarisation. Which of these mechanisms dominates cooling inactivation remains a matter of debate (Yang et al. 2005)

Lomber and colleagues (Lomber et al. 1999) defined characteristics of temperature spread and neuronal inactivation for the cryoloop technique in cat cortex. A key finding was that below 24°C, neuronal firing within the area of cortex being cooled was increasingly inhibited, and abolished completely by

20°C. This accords with Yang et al's (2005) observations in brain slices, that FM-32 de-staining, a measure of vesicle release, is strongly inhibited below 24°C. However, Yang and colleagues also observed some inhibition of FM-32 de-staining above 24°C, and, although small in magnitude, this inhibition did not entirely disappear until slices were at 33°C. Recently, Coomber et al. (2011) showed that in guinea pig, cortical field potentials were effectively abolished in all cortical layers cooled to less than 20°C.

However, it is possible that neural activity still occurs even below this temperature. Volgushev and colleagues (2000a), recording in rat slices, found that below 20°C the amplitude of excitatory post-synaptic potentials did not drop off dramatically, but rather showed a gradual decline with temperature. In addition, these authors found that moderate temperatures, such as room temperatures, led to a lower spike threshold and therefore increased stimulus-evoked neural activity. Even as low as 10°C, strong stimulation could evoke neural responses. This is explained by Volgushev et al. (2000b) who showed that cooling operates by depolarization, and therefore that moderate cooling temperatures bring cells closer to threshold and increase spike activity. As a result, cortical cooling is likely to produce an inhibited core of neurones close to the cryoloop, but also a penumbra where cortical excitation is increased in a region which is only moderately cooled (Volgushev et al 2000b). Other complex effects of moderate cooling in this penumbral region might include, for example, an increased temporal summation of postsynaptic shifts resulting from a lengthening of the decay of transient voltage shifts (rat visual cortex slices, layer 2/3; Trevelyan and Jack, 2002).

The problem of facilitation in the penumbra raises an important question: How localised is inactivation of the region of interest when employing the cryoloop technique? Lomber et al. (1999) showed that temperature spread was

limited laterally to distances within 1-2mm of the cryoloop, and did not extend subcortically. Coomber and colleagues (2011) have undertaken the most thorough measurements of cooling extent in smaller animals: using a single cryoloop over guinea pig auditory cortex, they found that cooling to 2°C at the cortical surface led the temperature to drop to 20-24°C within 2.5mm radius of the loop and reduced temperature in the thalamus, midbrain and middle ear by about 4°C, not sufficient to reduce neuronal activity; they confirmed this finding by measuring thallium uptake during cooling (Coomber et al 2011). This relatively localised inactivation provided by the cryoloop permits examination of the functional effects of defined brain areas before, during, and following recovery from cooling (Lomber & Malhotra 2008, Nakamoto et al. 2010). In the current study, by inactivating auditory cortex (AC) through cooling, I aim to inactivate cortical descending projections whilst recording in IC, and thereby to examine their role in neuronal adaptation and the representation of sound level in the IC.

.This chapter focuses on technical aspects of the cryoloop, asking whether the cryoloop calibration data of Lomber et al. (1999) in cat and of Coomber et al. (2011) cooling unilateral AC in guinea pig can be applied to the present study. This question of applicability of results is important not only for the present study, but because the cryoloop is becoming popular as an experimental tool across species (e.g. Nakamoto et al. 2010, Bäuerle et al. 2011, Antunes & Malmierca 2011).

Section 2.2 of this chapter describes the construction of the cryoloop, its operation, and the presentation of sound stimuli over the course of cortical cooling and re-warming. Section 2.3 describes the methods employed in the cooling process, and 2.4 calibration data (in terms of the reported temperature generated by the cryoloop device) with respect to cortical and collicular temperature and

neuronal activity. The central finding is that, for the guinea pig brain, a bilateral cryoloop is effective for cortical deactivation, but cooling temperatures previously employed in cat (Lomber et al 1999) and guinea pig (Nakamoto et al 2008) can, in the case of bilateral cooling loops in the guinea pig at least, lead to direct cooling of lower brain structures in addition to the desired cortical inactivation. This accords with the findings of Coomber et al (2011) using a unilateral cryoloop. I found that by limiting the temperature reduction of the cryoloop, it is possible to deactivate cortex more exclusively, such that any temperature reductions in the midbrain are not of sufficient magnitude to influence suprathreshold neuronal responses directly.

## ***2.2 The cryoloop***

### ***2.2.1 Cryoloop components***

The cryoloop cooling system described below was a modified version of the apparatus described by Lomber et al. (1999); see Figure 2.1. Two 4mm diameter cryoloops were manufactured from hypodermic stainless steel tubing (23 gauge; 0.635 mm outer diameter (O.D.), 0.33mm inner diameter (I.D.)). These were shaped with pliers to conform to the surface of the auditory cortex of an ex-vivo formalin-fixed guinea pig brain. A proprietary micro-thermocouple was silver-soldered to the point of union of the cryoloops. The inlet and outlet to the loops were fit snugly into 0.5 mm ID. Teflon tubing (Zeus Inc., Orangeburg, SC) and the loops attached to grooved plastic connectors fixed to manipulators that permitted movement, controlled by flywheels, of sufficient accuracy in three planes to permit stereotaxic placement. The distance between the loops could also be adjusted, and the manipulator of one loop further allowed for manual adjustment to precise positions, being constructed as an arm with three ball and

socket joints. Finally, the rotation of the connectors with respect to the manipulator could be altered. This degree of freedom was necessary to permit correct alignment of the loop to the contours of the cortex. The loop apparatus was placed anterior to the animal to permit easy loop access to auditory cortex whilst avoiding the IC and cortical electrodes.

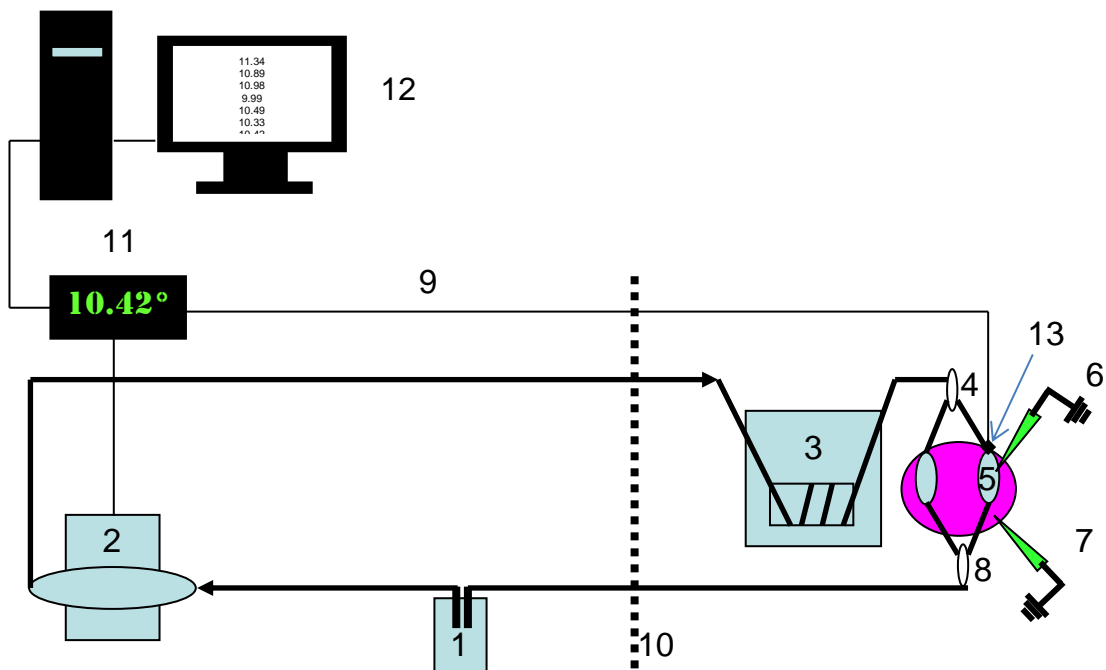


**Figure 2.1 Cryoloop Apparatus.** Thick black lines represent hollow PTFE tubing; thin black lines represent electrical connections. 1: methanol reservoir. 2: pump. 3: Dewar flask containing: spindle around which tubing is wrapped, dry ice pellets, and methanol. 4: Adjustable 3-way valve to split methanol flow. 5: Cryoloop overlying auditory cortex. 6: Electrode recording in right auditory cortex. 7: IC electrode. 8: Valve to reunite flow. 9: BNC cable connecting thermistor to pump control/temperature display console. 10: Wall of sound-attenuating chamber. 11: Pump control unit and temperature display. 12: Computer/monitor recording and displaying the temperature of pump (temperature sampling rate=1Hz). 13: Thermistor recording temperature of the loop.

### **2.2.2 Surgery and cryoloop positioning**

5mm x 5mm craniotomies were made bilaterally over the auditory cortices (Wallace et al, 2000; Wallace M, personal communication). The craniotomy was

extended at its dorsal anterior corner to accommodate the inlet of the cryoloop. These relatively large craniotomies were necessary for accurate cryoloop placement. The dura was removed bilaterally within the craniotomies, and the cryoloops apposed to the brain surface using the stereotaxic manipulator. Loop apposition to cortex was confirmed by visual inspection using a stereo operating microscope. In several experiments, an electrode was placed at right angles to cortex close to the centre of the right loop, its tip positioned just above the cortical surface, and its stereotaxic coordinates noted. Finally, warm agar or petroleum jelly was placed over the craniotomies to protect the brain surface from desiccation (the electrode was retracted during this procedure before being replaced).

### ***2.2.3 Cryoloop operation***

Outside the sound-attenuating chamber, room-temperature methanol was drawn from a 500-ml screw-top flask through 3.0 mm O.D. by 1.5 mm I.D. Teflon tubing (Varian Associates, Walnut Creek, CA; Part cR000020032) which passed through holes in the flask's top drilled for this purpose. It was not necessary to keep more than 100 ml of methanol in the flask, due to its continuous return and minimal evaporation. The pump was a synchronous rotating and reciprocating piston (Lomber et al. 1999; Fluid Metering Inc., Oyster Bay, NY; Model cQSY-Q-1-CSC with cR479 low flow isolation adapter), from which the methanol exited through 1.5-mm O.D. by 0.5-mm I.D. Teflon tubing, 2m in length (Zeus Inc., Orangeburg, SC). This passed into the sound-attenuating chamber, where the methanol flowed through several coils of tubing wrapped around a heavy plastic spindle within a Nalgene Dewar flask containing the coolant mixture of dry ice pellets and methanol (Figure 2.1). The methanol/dry ice mixture cooled the methanol flowing in the tube. The Nalgene Dewar flask was placed as close as

possible to the stereotaxic apparatus to minimise the distance between the coolant fluid and the brain, and hence to reduce warming of the fluid. Upon exiting the flask, the tubing bifurcated at a small-bore 3-way variable connector valve (3-Way Hex, 1.5-mm bore, Kinesis Ltd, St. Neots, UK) and continued as 0.8mm I.D. Teflon tubing (PTFE Tube 0.8 mm × 1.6 mm, Adtech Polymer Engineering, East Stroud, UK) to supply cold methanol to the cryoloops overlying each cortical hemisphere. After passing through the loops apposed to the brain, the methanol flow was brought back together using a second connector valve (as above) and then passed out of the sound-attenuating chamber in 0.8-mm Teflon tubing (as above) to be returned to the reservoir in the screw-top flask.

Cryoloop temperature was monitored by connecting the thermistor via a BNC cable to a pump controller (proprietary manufacture; UCL Department of Neuroscience, Physiology and Pharmacology) outside the sound-attenuating chamber. This controller was used to start and stop the pump as well as to display the recorded temperature. During experimental recordings, the pump speed was altered manually as required to maintain the temperature displayed on the pump controller to within  $\pm 1^{\circ}\text{C}$  of the desired temperature. By such means, loop temperatures as low as  $-10^{\circ}\text{C}$  could be achieved, much lower than those required for effective cooling of the cortex (see below).

### ***2.3 Cryoloop calibration: methods***

Calibration data was gathered from a total of 5 animals weighing 450-650 g. These experiments included recording temperature in AC, in IC during AC cooling, in non-auditory cortex overlying IC, in IC during cooling of non-AC, and in AC during cooling of non-AC. A minimum of 2 animals was used for each of these experiments. These numbers, though small, are appropriate given the small

weight difference between animals and the small variability extant in an inbred colony; similar numbers were used in the data of Coomber and colleagues (2011).

### ***2.3.1 The temperature probe***

In order to measure temperatures at the cortical surface, at various depths below this surface, and within the IC, it was necessary to employ a measurement device of sufficiently small diameter and insulated along its length up to the tip. A modified K-type stainless-steel sheath thermocouple probe of 0.25-mm diameter and 150mm length was used for this purpose (Omega Engineering Ltd, Manchester, UK). For stability, the probe was placed within hard plastic tubing, from which its distal end protruded 1.5 cm. A metal rod was attached to the tubing, to permit connection of this apparatus to the electrode driver. By this means, the thermocouple probe could be advanced from outside the sound-attenuating chamber using the controller of the electrode motor, over either the IC or the AC, with micrometre accuracy of probe placement. The probe was connected to a 2-input K/Logger Recording Thermometer (Omega Engineering Ltd, Manchester, UK) also located outside the sound-attenuating chamber, and this in turn was connected via a USB connection to a PC (running Windows XP) for on-line recording and display of temperature. The temperature of the cryoloop, measured using a thermistor attached to the left cryoloop, was recorded on a separate Windows PC via a serial output from the pump control unit, using a proprietary programme written in the Matlab language (Mathworks, Natick, MA). This script read the serial port input and wrote the data to a Matlab data file, at a rate of 1 Hz. Note that a thermistor, rather than a thermocouple, was used to record the loop temperature, since it was found that a thermocouple attached directly to the loop introduced too much electrical noise and could not be adequately earthed without impairing its function.

### ***2.3.2 Cortical temperature measurement***

The temperature probe was placed in the electrode holder mounted to the electrode driver motor. Probe height was adjusted by advancing the electrode holder on the motor until the probe tip just apposed the cortical surface. The temperature of the loop and the probe were recorded at 1 Hz. Following 1 minute of recording, the pump was switched on and cooling commenced. Once the desired loop temperature had been reached, cooling was allowed to continue for 5-10 minutes. The pump was then switched off and the brain allowed to rewarm for 5-10 minutes. The temperature of the loop and the temperature of the probe were measured continuously during the cycle of cooling and rewarming. The motor driver, which displayed the probe position to within  $\pm 1$  micrometre, was used to advance the probe beneath the cortical surface to the desired depth. This protocol was repeated at a variety of cortical depths for a range of chosen loop temperatures. The aim was to define the temperature at the cryoloop necessary to reduce the temperature in cortical layer VI to a level associated with cortical deactivation; since 2 mm represents layer VI across much of AC (however see Wallace et al. 2000), the thermocline at 2 mm was taken as representing this crucial layer VI thermocline.

### ***2.3.3 IC temperature measurement***

In order to place the temperature probe correctly in IC, the following method was used. First, the location of the IC was verified physiologically by recording neuronal responses to tone and noise stimuli with a glass-coated tungsten electrode (see Chapter 3 for details). The stereotaxic coordinates of the IC were recorded. The electrode was then withdrawn to a position within a few hundred microns of the brain surface, and a length of tungsten wire positioned along the brain surface, such that its tip lay just beneath the electrode, to mark its position visually in addition to the stereotaxic measurements. The electrode was then

removed and replaced on the electrode holder with the temperature probe. The temperature probe was then positioned according to the stereotaxic coordinates of the IC. However, if the electrode marker was at odds with these positions, the probe position was adjusted visually such that its tip was at the end of the tungsten wire. The tungsten wire was then removed, and the probe advanced to the same depth as the electrode had been when IC responses were measured. In this way the probe tip was positioned within the IC. A temperature recording protocol similar to that used in the cortex was then performed for a range of loop temperatures.

#### ***2.3.4 Simultaneous neuronal and temperature measurement***

In a third set of experiments, a broad-band noise search stimulus consisting of 50ms noise bursts at 70dB SPL, separated by 500ms silence, was used to identify single and multi-units along tracks beginning at the surface of AC and extending up to 3 mm below. Both auditory-evoked and spontaneous responses were then recorded over 60-100s in the warm state, 600s post-temperature stabilization in the cool state, and for a further 1200s in the re-warmed state. During this time loop temperature was also recorded, as described above.

#### ***2.3.5 Cooling cortex overlying IC***

It was important to distinguish whether changes in response properties of IC neurones during AC cooling are the result of deactivation of neuronal pathways or, instead, arise due to a direct (and unintentional) cooling effect - the result of brain cooling extending from the site of the cryoloop to subcortical or extra-auditory cortical areas. As described below, IC temperature does appear to fall when AC is cooled bilaterally and unilaterally using the cryoloop method. To control for this possible confounding factor, the temperature to which IC drops when AC is cooled was first measured, as described above. Then, the cryoloop

was positioned on a region of the cortical surface outside the AC, on cortex overlying IC. The cryoloop was used to cool this region of cortex whilst the temperature of the IC was monitored. In this arrangement, the overlying cortex was cooled to achieve the same level of IC cooling as was achieved by cooling the surface of the AC. In this way, IC was cooled to temperatures experienced in IC during typical AC cooling, but whilst AC and its descending pathways were not cooled.

To effect this IC cooling, achieved by placing a single cryoloop on the cortical surface immediately overlying IC, it was important to verify two characteristics of this IC cooling technique. First, to what temperature must the loop be reduced, in this position, to reduce IC temperature to levels similar to those occurring in IC when AC is cooled? Second, when cortex overlying the IC is cooled in this way, is AC itself cooled also? Attempts at measuring the effect of cooling alone (without invoking any descending influences of AC on IC function) would of course be invalid if intra-cortical cooling spreads from the loop to inactivate AC.

To address these questions, three craniotomies were made: a 5 mm diameter craniotomy over the cortex overlying the location of the IC, a 5mm diameter craniotomy over the left (contralateral) AC, and a 2-mm diameter craniotomy over the right AC. This configuration of craniotomies was chosen so that a cryoloop could be placed on cortex overlying IC and a temperature probe could be positioned in the right AC, whilst the overall amount of neuronal tissue exposed – and therefore the baseline temperature of the brain - remained identical to standard cooling experiments.

Following placement of the cryoloop on cortex overlying IC, and electrophysiological identification of the stereotaxic position of the IC, a

temperature probe was placed at the level of the upper border of the IC as described in Section 2.3.3. Loop temperature was then varied between 5°C and 25°C in steps of 5°C, holding each step for 5 minutes, whilst the temperature in the IC probe was recorded. The temperature at the loop necessary to reduce IC temperature to the temperature IC reaches during cooling of bilateral AC was noted. Loop temperature was varied in a range around this point. Thus, a calibration between IC temperature, and temperature of the loop on cortex overlying IC, was effected. The IC temperature probe was then removed and replaced 2mm deep to the surface of the right AC. With the loop still apposed to cortex overlying IC, loop temperature was then again varied in the range 5- 25°C, whilst temperatures in the probe, located in AC, were measured. Finally, the electrode was replaced in IC and neuronal responses were recorded. For the first 8 minutes of the stimulus, the loop, on cortex overlying IC, was held in the warm state. For the next 8 minutes, the cryoloop temperature was reduced enough to cause a reduction in temperature in the IC 5° below the temperature the IC would usually reach when the cryoloops were placed on AC. This additional 5° reduction in temperature was chosen to make the control more stringent - if no change in neuronal responses was observed when cooling IC to 5°C below the temperature it habitually reaches when cortex is cooled to a given temperature, then this would provide good evidence that cooling cortex to this temperature does not alter IC responses by a direct cooling effect. After 8 minutes, the cryoloop apparatus was switched off and the brain allowed to rewarm again, whilst the stimulus ran for another 30 minutes. For some neurones, the stimulus was presented in the warm and rewarm state as well as several different cooled temperatures, with the loop overlying IC held at 5, 10, 15 and 20°C.

## **2.4 Cryoloop calibration data**

### **2.4.1 Loop and cortex temperatures**

The temperature of the cryoloop could be reduced, by increasing pump speed, down to  $-10^{\circ}\text{C}$  over 100-200 s. This required at least 0.5kg of carbon dioxide pellets, and 500mls of methanol, in the methanol ice bath. The carbon dioxide pellets required topping up once in the course of a typical 12-hour experimental recording series. The cryoloop temperature returned to pre-cool values over 200-400 s. The loop could be held reliably within  $\pm 1^{\circ}\text{C}$  of the desired temperature by manually adjusting the speed of pump flow.

A critical question concerns the extent to which cooling itself directly spreads within and beyond the cortex. Studies in cat (Lomber et al 1999) and guinea pig (Nakamoto et al. 2008) employed a cortical surface temperature of  $1-3^{\circ}\text{C}$  in cooling experiments. Coomber and colleagues (2011) found that using a single cryoloop on AC, subcortical structures did undergo a reduction in temperature of  $\sim 4^{\circ}\text{C}$ , including IC. I recorded the temperature throughout the layers of the right AC (Figure 2.2a, b). This was undertaken with both cryoloops in place. Cooling bilaterally, I found that temperatures at the loop used in previous experiments in cat (Lomber et al 1999) result in cooling to a mean temperature of  $7.2^{\circ}\text{C} \pm 1^{\circ}\text{C}$  across the full thickness of the cortex, much cooler than is necessary for cortical inactivation, at least with respect to abolishing the generation of action potentials. This was also cooler than that found in guinea pigs by Coomber et al (2011). Figure 2.2a and b demonstrate that even half a millimetre deep to the deepest extent of cortex, the temperature was still  $< 10^{\circ}\text{C}$ . Thus, though the typically used  $1.5^{\circ}\text{C}$  temperature at the cortical surface is sufficient to inactivate guinea pig cortex, I were impelled to investigate whether this temperature, in my preparation, results in cooling of sub-cortical brain centres to temperatures that can lead to alterations in neuronal responses.

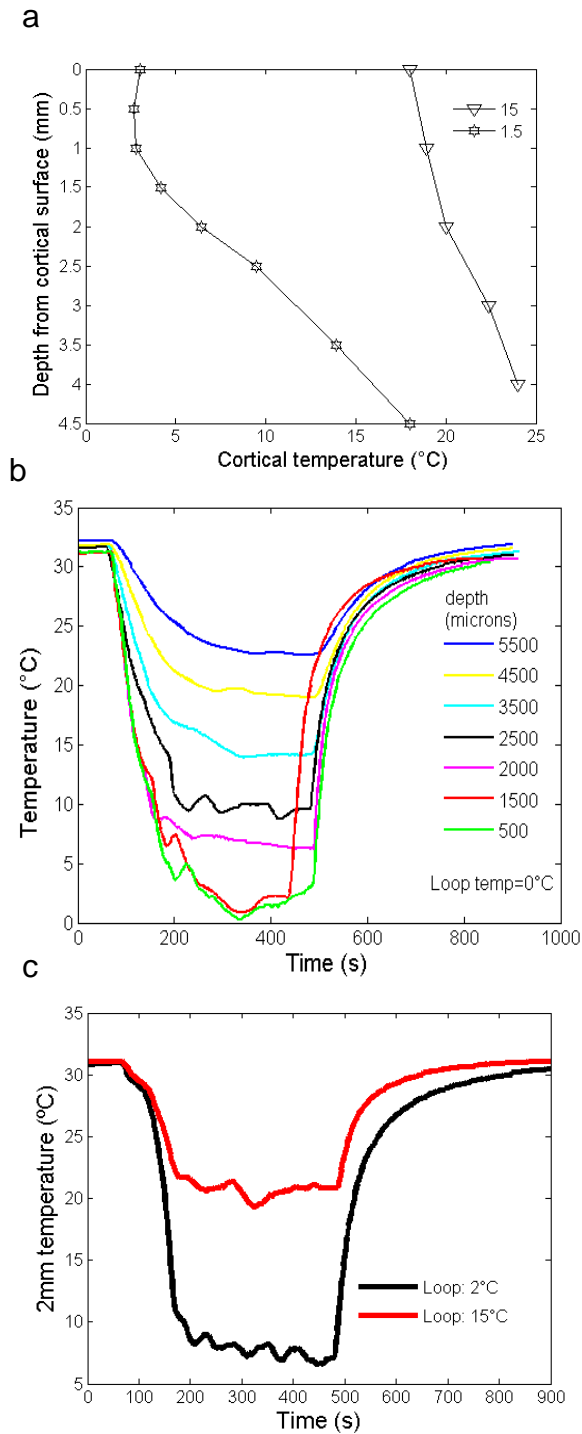


**Figure 2.2 Auditory cortex temperatures during cooling.** a. Thermoclines (temperature gradients). Legend refers to  $15^{\circ}\text{C}$  and  $1.5^{\circ}\text{C}$  loop temperatures. Data averaged from multiple measurements, recorded at a rate of 1 KHz, from one animal, weight = 620g. b. Temperature time course at various cortical depths. c. Temperature changes over time. Cooling loop to  $2^{\circ}\text{C}$  rapidly cooled layer VI to  $7^{\circ}\text{C} \pm 1.5^{\circ}\text{C}$ . Cooling loop to  $15^{\circ}\text{C}$  cooled full-thickness cortex to  $20^{\circ}\text{C} \pm 1^{\circ}\text{C}$ .

The question then arises: what temperature is sufficient to cool and so inactivate the full thickness of the cortex? Assuming that the published data for cessation of neuronal activity below 20°C is correct (Lomber et al. 1999, Coomber et al. 2011; data suggesting this to be appropriate are presented below), it is then necessary to define the loop temperature at which the temperature 2 mm below the cortical surface (i.e. the full thickness of cortex) reaches 20°C. Figure 2.2a, displays the thermocline at 15°C and demonstrates that full thickness cortex is cooled to 20°C when loop temperature is 15°C, suggesting that much higher temperatures than previously thought might be sufficient to cool full thickness cortex and abolish neuronal activity when using bilateral cryoloops. Figure 2.2c shows the difference in temperature change over time in Layer VI of AC (2mm deep) when cooling to 2°C and 15°C. Indeed, I found that cooling the cryoloops to 15°C±1°C resulted in a 2mm depth temperature (mean±SEM) of 20.4°C±0.3°C (n=3 animals, 526g, 560g and 600g). Although it may be the case that the cooling effect in a single cortex was potentiated by having two cryoloops, I found that even cooling with a single cryoloop led to a drop in temperature of only ~5°C across full-thickness of cortex.

#### ***2.4.2 IC temperature during cooling***

The data presented above suggest that, in the guinea pig at least, application of the cryoloop may not cause strictly localised decrease in temperature in the cortex. Does cooling the cortex have a direct cooling effect on the IC? I first made a unilateral craniotomy to admit a single cryoloop over right AC, and recorded temperature across AC during cooling. I then made a second craniotomy over left AC to place the second loop, and repeated the procedure, recording temperature within right AC during bilateral cooling. Figure 2.3 plots the temperature recorded

in the IC for both ipsilateral and bilateral cooling, in a single animal (weight =450g). The starting temperature of the IC is lower in the bilateral condition, likely reflecting the lower overall brain temperature due to the second craniotomy being made to admit the second cryoloop. For both ipsilateral and bilateral cooling, and for all temperatures measured, IC temperature falls as loop temperature is reduced. For unilateral cooling, the temperature drop is  $2.5\pm 1^{\circ}\text{C}$  when loop temperature is  $5^{\circ}\text{C}\pm 1^{\circ}\text{C}$ , which accords with the findings of Coomber and colleagues (2011) of a  $4^{\circ}\text{C}$  drop in IC when loop temperature was  $2^{\circ}\text{C}$ . Cooling bilaterally leads to a greater temperature drop of  $5.5^{\circ}\text{C}\pm 1^{\circ}\text{C}$ . However, Figure 2.3 suggests that during bilateral cooling, by keeping loop temperature between 15 and  $10^{\circ}\text{C}$ , temperature drop in the IC can be reduced to values between 2.6-3.8 $^{\circ}\text{C}$ , corresponding to a minimum IC temperature of  $28.6^{\circ}\text{C}$ . The mean ( $\pm\text{SEM}$ ) temperature in IC when AC was cooled bilaterally to  $15^{\circ}\text{C}$  was  $28.6^{\circ}\text{C}\pm 1.6^{\circ}\text{C}$  (n=2 animals, 620g and 450g). Whether this change is great enough to affect neuronal activity is addressed in Chapter 4.

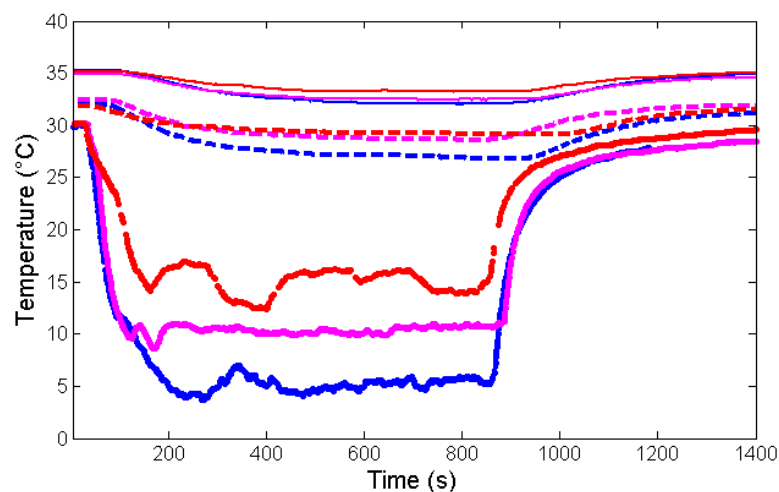


**Figure 2.3 IC/loop temperature change over time during cooling AC.** Lower three traces (thick lines): loop temperature. Middle three traces (dashed): bilateral cryoloops, IC temperature. Upper three traces (solid): ipsilateral cryoloop, IC temperature.

### **2.4.3 Auditory cortex evoked neuronal activity during cooling**

The data presented above imply that loop temperatures should be as warm as possible to avoid cooling IC directly, but suggest that temperatures higher than approximately 15°C are insufficiently cool enough to reduce the deeper layers of cortex to 20°C or lower. The aim is to have as low a temperature as possible without reducing temperature excessively in IC. Figure 2.3 suggests there is little difference in the temperature drop within IC when the temperature of the cryoloop is 10°C compared to 15°C. It is important to determine whether a loop temperature of between 10°C and 15°C - higher than that employed in previous studies – is sufficient to inactivate neurones over the full thickness of guinea pig cortex. It was expected that this would be sufficient, because my measurements showed that at this temperature, cortex was cooled to 20°C, the temperature sufficient to abolish cortical field potentials in Coomber et al's study (2011). Figure 2.4a shows the firing pattern of a typical neurone recorded at a depth of 2100 microns below the surface of auditory cortex, i.e. at the deepest extent of Layer VI. After ~5 minutes of cooling to 10°C, noise-evoked neuronal activity ceases entirely. Five minutes after the pump controlling the flow of coolant is switched off, neuronal activity returns. However, in Figure 2.4b, showing data from a neurone recorded 2400 microns below the surface, several hundred microns deeper than auditory cortex and recorded within the same electrode track as the previous neurone, neuronal activity does not cease completely despite cooling for more than 10 minutes, suggesting that cooling the surface of the cortex to 10°C is sufficient to cool full-thickness cortex but does not inactivate neurones even a small distance below the level of the cortex in this example. This was further tested by cooling the loop to 5°C and recording from the same neurone. Figure 2.4c shows that at this lower temperature, the neurone was indeed

inactivated, suggesting that whilst cooling the cortical surface to 10°C does not inactivate subcortical structures, 5°C at the cortical surface is sufficiently low to do so. These measurements were obtained from an animal weighing 510 g, a representative weight for all experiments (range: 350-700 g). Similar findings were made in several electrode tracks within the AC. An example cortical neurone from a different animal is shown in Figure 2.4d. Having established the principal that, in accord with previously published data, cooling full thickness cortex to 20°C or lower was sufficient for neuronal inactivation, I did not routinely record AC neuronal activity in each experiment.

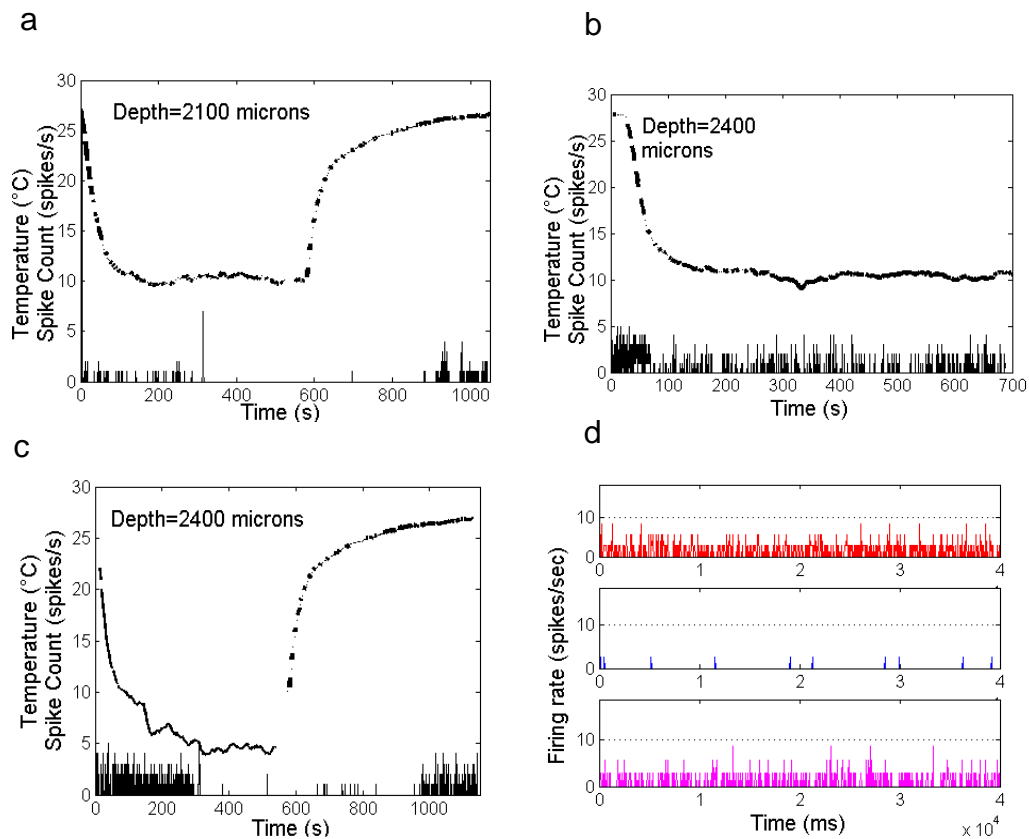


**Figure 2.4 Cortical Inactivation at different loop temperatures. All panels display neuronal responses as peristimulus time histograms (PSTHs; bin width = 50ms). a-c also display temperature on the ordinate. a. A single neurone at a depth of 2100 microns is inactivated by cooling loop to 10°C. b. In the same electrode track, a neurone at a depth of 2400 microns is not inactivated by cooling to 10°C. c. For this neurone, inactivation occurs when cooling to 5°C. Temperature and spike count plotted on ordinate to same scale. d. A cortical neurone in a different animal recorded at a depth of 2000 microns. Top panel: prior to cortical cooling; middle panel: during cooling; bottom panel: 15 minutes after cessation of cooling. Activity driven by broadband noise stimulus.**

#### **2.4.4 Effects of cooling IC without cooling auditory cortex**

As described above, when AC is cooled the IC can also be cooled directly, at least to a small extent. It is possible that this is enough of a temperature drop to affect firing patterns of neurones in the IC, particularly given the data of Yang et al. (2005) suggesting changes in vesicle release in slices even for temperatures of 33°C. In order to examine this possibility, it was necessary to maintain auditory cortex in the warm, active state, to remove any possible effects of blocking

descending corticocollicular neuronal pathways, whilst recording responses of IC cells when cooled to temperatures habitually occurring in IC when auditory cortex is cooled (Figure 2.3).

Figure 2.5a shows the relationship between the temperature at the location of the cryoloop positioned on the (non-auditory) cortical surface overlying IC, and the temperature measured by the probe located within the IC itself. The two temperature traces mirror one another closely, suggesting that IC temperature is influenced by the temperature at the surface of the cortex overlying it, much more than it is influenced by AC temperature (Figure 2.3). The mean $\pm$ SEM temperature difference between IC and overlying cortex is  $10.8^{\circ}\text{C}\pm 1.6^{\circ}\text{C}$ . Cooler cortical temperatures in Figure 2.5a are associated with greater temperature differences between AC and IC.

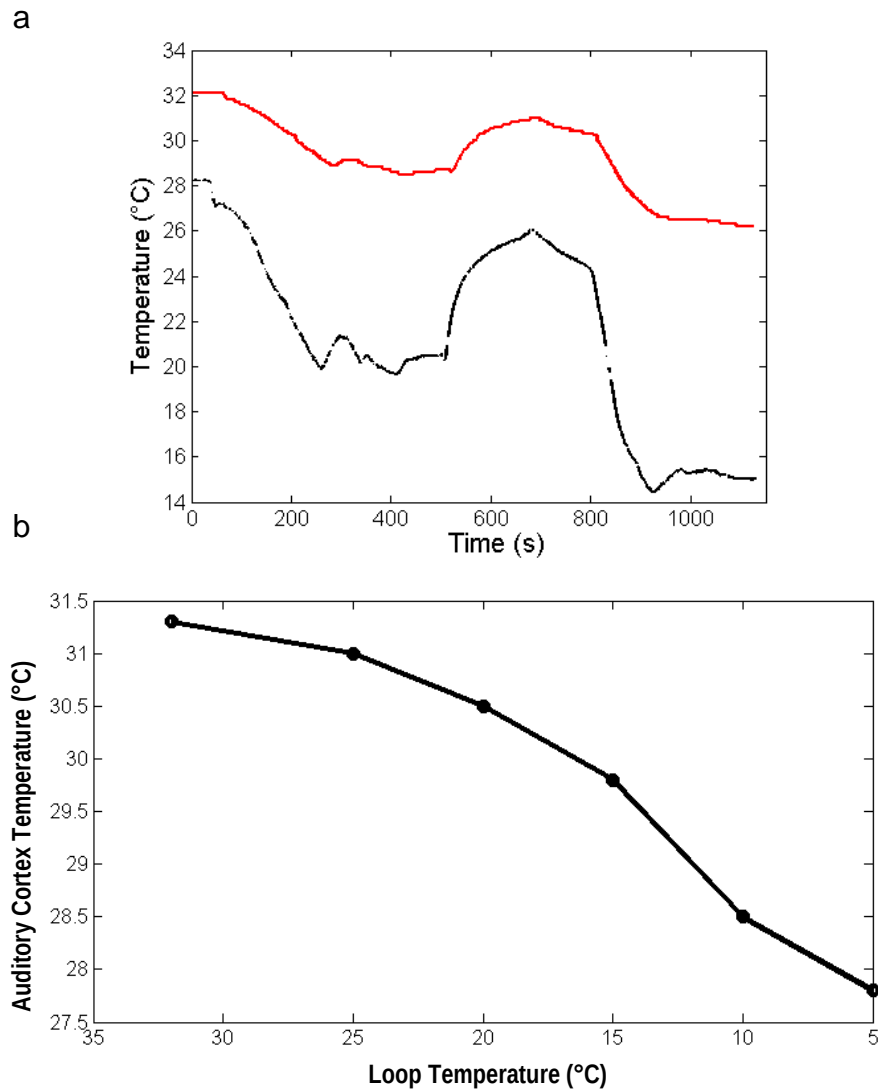


**Figure 2.5 Loop and IC Temperatures.** a. Black trace: temperature at cryoloop during cooling when placed on non-auditory cortex overlying IC. Red trace: IC temperature. Temperature adjusted deliberately up and down to demonstrate relationship between loop and IC temperatures in this position. b. Loop and auditory cortex temperatures. Ipsilateral auditory cortex temperature drops, but not to inactivation temperatures, when cooling loop is on cortex overlying IC, verifying the method of these control experiments and suggesting limited lateral spread of cryoloop cooling.

As shown in Figure 2.5a, the temperature of the loop necessary to reduce IC temperature to 28-29°C - the temperature to which it falls when AC is cooled bilaterally - is around 15°C. Does a temperature drop of this amount in IC result in alterations in neuronal response? In the control experiments described in Chapter 4, the loop overlying IC was cooled to 20°C, 15°C (to mimic the effects of

cooling AC), and, to make the control more stringent, to 10°C and 6°C (see Chapter 4).

Since the aim of this control experiment was to cool IC without inactivating AC, it was important to verify that cooling cortex overlying IC did not lead to appreciable cooling of AC itself. Figure 2.5b illustrates the small drop in temperature measured in deep layers of ipsilateral AC when IC is cooled in this manner. Note that cooling to 15°C at the loop – the temperature necessary to reduce the temperature of the IC by the requisite amount – results only in a 1-2°C change in temperature in the right AC, down to ~29.5°C, and thus well above the inactivation temperature.

Having thus defined the temperature necessary to cool cortex overlying the IC to mimic the effects of AC cortical cooling on IC temperatures, it was then possible to record within IC to investigate whether these moderate decreases in temperature did in fact alter neuronal spike rates. These data are presented in Chapter 4.

## **2.5 Discussion**

A bilateral cryoloop construction, modelled on those previously employed in studies of cortical cooling (e.g. Lomber et al 1999) was constructed to cool auditory cortex bilaterally, and, as Figure 2.2 shows, it did so quickly and reversibly. However, whilst effective, the temperature spread from the cryoloop proved greater in guinea pig brain than that reported in cat, consistent with the data of Coomber et al. (2011). I found in particular that a bilateral cooling cryoloop temperature of 1-3°C lowers sub-cortical temperatures to below the temperature required to inactivate directly neuronal responses, whilst lowering the temperature to 5°C reduces the temperature of the IC to within a few degrees of the known temperature required to inactivate the IC directly. These data are in

accord with those of Coomber et al. (2011) who found a 4°C drop in temperature in subcortical structures, including IC, when cortex was cooled ipsilaterally. The present data suggest that temperature drops an additional 2-3°C when bilateral loops are used. It is therefore important to maintain the surface of the cortex at sufficiently warm temperatures so as not to cool the IC directly. For these reasons, the experimental data reported in the remainder of this thesis are all based on recordings where the cryoloop temperature was held at 12°C±2°C. Although this temperature is well within Lomber and colleagues' complete cooling range in vivo (1999), it is also within the incomplete cooling range in vitro of Volgushev and colleagues (2000a). However, I chose this range because, even at these temperatures, it is still the case that IC can be cooled by several degrees. Chapter 4 presents neuronal recordings made during cooling of the cortex overlying IC, in order deliberately to cool IC, whilst leaving AC intact, to investigate whether there is an effect on neuronal responses of cooling IC to the temperatures it reaches when AC is cooled bilaterally to 12°C±2°C. In general, the conclusion is that the cryoloop is a more parameter-dependent technique than is commonly appreciated, and should be calibrated on at least a species-by-species, if not a laboratory-by-laboratory, basis. In the guinea pig, there is clearly a narrow window of cooling temperatures in which the extent of cooling is sufficient to silence neurones in the cortex completely, whilst avoiding partially silencing or exciting those in the IC due to direct or indirect temperature spread.

# 3

## METHOD OF MEASURING TIME COURSE OF ADAPTATION

---

### ***3.1 Introduction***

Sound stimuli were delivered to anaesthetised adult guinea pigs of body mass 400-700g through headphones in a closed-field sound system, whilst neuronal responses were recorded using extracellular electrodes placed in the right inferior colliculus, as described below.

In the first series of experiments, aimed at assessing the time course of adaptation in the IC, no cryoloop was used. Some of these data were collected, analysed and written up in collaboration with Dr. Isabel Dean and have been previously published (Dean et al 2008). In the second series of experiments, the cryoloop cooling apparatus, described in Chapter 2, was used in conjunction with the switching adaptation stimuli.

### **3.2 Surgery**

Anaesthesia was induced via intraperitoneal injection of urethane (1.0g/kg; 25% solution of NaCl; Sigma-Aldrich, Poole, UK). Analgesia was induced, and supplemented as necessary throughout experiments, with 0.1cc of intramuscular Hypnorm (0.315mg ml<sup>-1</sup> fentanyl citrate and 10mg ml<sup>-1</sup> fluanisone; Janssen-Cilag Ltd., High Wycombe, UK). Atropine sulphate (0.06mg; Animalcare Ltd., York, UK) was administered subcutaneously to reduce bronchial secretions. Lignocaine (0.1ml, 5%) was given at all incision sites prior to incision to effect local anaesthesia. Body temperature, breathing rate, and pedal withdrawal reflexes were monitored to ensure sufficient and stable anaesthesia. Body temperature was maintained by means of a rectal probe and a thermostatically controlled heating blanket. A terminal injection of 1ml Pentoject (sodium pentobarbitone, Animalcare Ltd.) was administered at the end of each experiment.

Incision sites were prepared by shaving over the throat, around the ears, and on top of the head. Ear canals were exposed by sectioning the tragus on each side, and then cleared of debris under microscopic visualisation. A tracheotomy was performed and a tracheal cannula inserted and secured. The animal was then placed in a stereotaxic frame, secured by a bite bar and hollow in-ear speculae permitting visualisation of the tympanic membrane and admitted speakers and tubes for the delivery and sampling of sound. The head was levelled stereotaxically to effect horizontal alignment of the IC laminae. Middle ear pressure was equalised by sealing a high acoustic-impedance cannula into each bulla.

A craniotomy was made (diameter=2-3mm), and the dura removed, to permit access to the right IC through the overlying, intact, cerebral cortex. For experiments using the cryoloop, two further craniotomies (diameter=5mm) were made, one over each auditory cortex, and the dura removed. The location of the

auditory cortex was determined according to the landmarks previously defined (Wallace et al. 2000). For these experiments, a cooling cryoloop, shaped to accommodate the curvature of the cortices, was placed gently against both cortical surfaces without causing tissue deformation (Lomber et al. 1999). Either petroleum jelly or warm 4% agar solution was placed over the craniotomies to prevent desiccation of the cortical surface. A glass-coated tungsten electrode of impedance  $\sim 1.0 \text{ M}\Omega$  (World Precision Instruments, Stevenage, UK) was stereotaxically placed in the brain above the site of the right IC. In several experiments where auditory cortex was exposed, a second electrode was placed at right-angles to the right auditory cortex just above the cortical surface. All experiments were performed in accordance with the United Kingdom Animals (Scientific Procedures) Act of 1986.

### **3.3 Sound delivery**

Stimuli were generated digitally using Tucker Davis Technology's (TDT) Real-Time Processor Visual Design Studio (RPVDS-Ex), interfaced with the Brainware Programme (Jan Schnupp, University of Oxford, UK) used to select stimulus parameters. For the main stimulus used in this study, RPDVS-Ex also interfaced with a Matlab-generated ASCII file containing statistical distributions of sound levels (see below). Following digital generation, stimuli were converted to analogue signals (RP2.1 at 50 kHz sampling rate; TDT), attenuated (PA5; TDT), and amplified (Blueprint A75; Beyerdynamic, Burgess Hill, UK) before being presented to the ears via loudspeaker units (Beyerdynamic DT48 audiological speaker transducers (Beyerdynamic)) fit to custom-made brass tubes that were sealed into the hollow ear speculae. Sound stimuli were delivered to within a few millimetres of the tympanic membranes.

Calibration of the sound system was performed in situ with a probe tube microphone (modified Knowles FG3452; Knowles Electronics Europe, Burgess Hill, UK), precalibrated with respect to the speakers against a high-quality eighth inch Bruel and Kjaer microphone (Type 4136; Bruel and Kjaer, Stevenage, UK); the probe tube was inserted into each ear speculum to within a few millimetres of the tympanic membrane. At the end of surgery, the transfer function of the system was checked to assess the quality of the acoustic coupling.

### ***3.4 Physiological recordings***

Extracellular recordings were made from single neurones in right IC and right auditory cortex (AC). Glass-coated tungsten electrodes (impedance range 0.9-1.1 M $\Omega$ ) were advanced stereotaxically into the IC in a dorsoventral direction, or perpendicularly to the cortical surface over the right auditory cortex, using a motorized manipulator (LN Junior; Luigs and Neumann, Ratingen, Germany). The potential between the electrode and a reference clip on the neck muscles was digitized at 25 kHz, filtered (600-3000Hz), amplified and recorded using TDT System 3 hardware (RX5 Pentusa; TDT) and software (Brainware v 8.11).

### ***3.5 Stimulus design and presentation***

To isolate IC neurones the electrode was advanced through cortex overlying IC whilst bursts of broadband noise were presented diotically (duration=50ms, inter-burst duration=50ms). Stereotaxic coordinates, robust auditory responses, appropriate response latencies, and characteristic laminar progression of best frequencies were used to assess correct electrode placement within the central nucleus of the IC. AC neurones were defined as sound-responsive units in the first 2mm below the surface of primary AC as defined stereotaxically. Once sound-

locked evoked potentials were detected the electrode was advanced in steps of several microns to isolate single neurones. Possible action potentials were isolated from background noise in Brainware based on the positive and negative action potential peak voltages and on the time course of the action potential. Isolation was further assessed both by examining the waveform of potential action potentials on a separate oscilloscope in real time, and by *post-hoc* analysis of autocorrelograms, to check for a refractory period. If isolation decreased during a recording to the point where a single neurone could no longer be clearly discriminated from background noise, the recording was stopped. During cortical cooling, a common observation was that the neurone moved tens of microns away from the electrode. In many cases, this improved isolation; in some cases this led to loss of isolation; where possible, isolation was maintained by retracting the electrode some tens of microns to maintain its relationship to the neurone.

After isolation, two characterizations of the neurone were usually performed. A 'baseline' rate-vs.-level function was obtained by presenting 50ms bursts of white (<~25 kHz) noise, separated by 300ms intervals, at integer sound levels every 5dB from 21 to 85 or 90dB sound pressure level (SPL); levels were presented in random order and each was repeated 10 times. Second, for some neurones, the characteristic frequency (CF) (the frequency at which the lowest sound level evokes a response) of the neurone was determined by manually varying the level and frequency of 50ms pure tones, separated by 300ms intervals, until the frequency was found at which spike rate increased with the lowest threshold. For 23 of 45 (51%) of neurones in the non-cooling time course experiments, CF was also assessed by obtaining a response area (spike rate as a function of frequency and level), extending 2 octaves above and 4 octaves below the manually determined CF at a spacing of 1/10th of an octave over an 80dB

range of levels at 5dB intervals. Here, the CF was again determined as the frequency with the lowest threshold to increase spike rate. Neuronal responses consistent with response characteristics in the central part of the IC, the ICC, were sought.

For the remainder of the experiment a continuous broadband noise stimulus, designed to elicit adaptation, was presented. This stimulus consisted of white noise (<~25 KHz) presented in 40s segments, separated by <0.5 s, for ~10 minutes (but see modification for cryoloop experiments, below). The sound level was set every 50ms to a new value chosen randomly from a defined distribution. Integer decibel values of sound level, spaced every 2dB between 35 and 85dB SPL were used. For a small number of neurones (n=8) the range used was 35-97dB SPL. The sound level distribution consisted of a region of highly probable levels (the stimulus “high probability region”) over either  $51 \pm 6$ dB or  $75 \pm 6$ dB, from which levels were selected with an overall probability of 0.8. The two sound level distributions were alternated in time, such that sound levels were chosen from one distribution for 5s before switching to the other (giving a 10s “switch period”). Thus, over the course of a 10 minute recording, ~60 switch periods were presented. For each of the two sound level distributions, ~40 repeats of every low-probability sound level, and 690 repeats of every high-probability sound level, were presented over the course of a 10 minute recording. The level sequence and noise token were the same for all neurones. For a given sound level distribution, the level sequence differed in each switch period (see Figure 4.1).

### ***3.6 Cryoloop operation with respect to stimulus presentation***

For the cryoloop experiments, two experimental protocols were used. In the ‘continuous’ protocol the baseline cell characterisation stimuli described above were presented in the warm condition only; after this the adaptation stimulus was

presented continuously across cryoloop conditions. Specifically, after ~ 8 minutes of this stimulus in the warm (pre-cooling) condition, the pump was switched on with the stimulus still running. Once the loop temperature had reached the required temperature of  $12^{\circ}\text{C}\pm 1^{\circ}\text{C}$  for 5-7 minutes, another 8 minutes of the stimulus was allowed to run. At this point, ~15 minutes after the pump was switched on, the pump was switched off. For the purpose of analysis, the 'cool condition' was defined as the final 7-8 minutes of the stimulus prior to the pump being switched off. The adaptation stimulus was allowed to continue during the rewarm period. Where possible, after 25 minutes of rewarming, and when the temperature of the loop had come to within a few degrees of the pre-cooled temperature, another 8 minutes of the stimulus was allowed to run. However, in some neurones, isolation began to decrease during this time, so the full 25 minutes was not achieved. For all neurones, the 'rewarm condition', for the purpose of analysis, was defined as the final 8 minutes of the stimulus after the pump was switched off. The full protocol lasted 50 – 60 minutes per neurone.

In the 'discontinuous' protocol, the adaptation stimulus was separated by base-line characterisations in the warm, cool, and rewarm conditions. Both protocols allowed comparison of rate-vs.-level functions and time course of adaptation in the warm, cool, and rewarm conditions. The advantage of the continuous protocol was its simplicity, and the fact that it allowed continuous visualisation of the change in adaptation and firing rate over time with respect to cooling. The discontinuous protocol permitted comparison of the effects of descending projections on adapted and baseline responses. Also, the discontinuous stimulus was used as a control to ensure that effects witnessed in the continuous stimulus were not due to long, continuous, sound presentation, but rather resulted from cryoloop cooling.

### **3.7 Data analysis**

For the cryoloop experiments the analysis was divided into three conditions: warm (final 8 minutes of stimulus prior to pump on); cool (final 8 minutes of stimulus prior to pump off); and rewarm (final 8 minutes prior to end of recording after pump off).

Rate-vs.-level functions were plotted for each of the two level distributions. For the cryoloop experiments, they were also plotted across each of the three cooling conditions, resulting in six rate-vs.-level functions for each neurone for these experiments. These functions were plotted by calculating mean spike count of the neurone during the 50ms epochs corresponding to a given level, taken into account neuronal latency as measured from the 50ms noise bursts used in the collection of the base line rate-vs.-level functions in the warm condition.

For measurement of the time course of adaptation of mean firing rate in each condition, spike rates were averaged across switch periods in the recording for each 50ms time bin following a switch to the 75dB distribution and the 51dB distribution respectively. Single exponential decay constants were fit to this average rate over the 2.5s following the switch, giving a time-constant of the change in firing rate. For the continuous protocol in the cryoloop experiments, the long recording times provided the opportunity to measure how these time-constants changed over the tens of minutes of the stimulus, across different cryoloop conditions. For this analysis, windows of 16-20 switch periods were used to calculate time-constants, and the windows were shifted along by 1 switch-period for each successive fit. For a 60 minute recording, 360 switch half-periods were available for this analysis, allowing 22 time-constants to be measured in rolling windows every 5 s.

For measurement of the time course of adaptation of rate-vs.-level functions, functions were plotted in successive 300ms bins in the 3s following a switch. Root mean square (r.m.s.) differences between each of these 300ms functions and the function fully adapted to the 75dB distribution over the 2s before the switch were calculated. A single exponential decay was fit to the r.m.s data for each neurone, giving a time constant of the change in rate-vs.-level function. Responses during the first switch period of each 40s segment of the switching stimulus were excluded from the above analyses. Finally, long-term changes in neuronal response were analysed by counting the total number of spikes in every 10s switch period, and fitting a single exponential decay to the spike counts over the full duration of the recording. Exponentials in all analyses were accepted if they provided a better fit than a flat line ( $F$  test,  $p < 0.05$  to accept exponential), and passed visual inspection for goodness of fit.

I sought to quantify changes in rate-vs.-level functions during adaptation and cortical cooling. I used two techniques for defining threshold, both with different inadequacies. First, threshold was defined as the sound level associated with a firing rate of 10% of the maximum rate. Whilst this does not always capture threshold in an intuitive sense, this approach is appropriate for many neurones. However, this method can falsely calculate a decreased threshold if total spike rate is decreased. However, this problem was minimized in my data because decreased spike counts were associated with the cool condition, and this condition was also associated with rightward shifts in functions; the direction of inaccuracy of this method is such as to underestimate the amount of rightward shift in the cool condition, since spike rates are lower in this condition, and so the technique will diminish rather than exaggerate results.

The second approach to threshold was designed to extract a “true” threshold: the lowest level associated with a stimulus-driven increase in spike rate. Here threshold was defined as the sound level associated with the second significant increase in firing rate over and above the spontaneous rate. Noise in the functions was dealt with by defining stimulus-driven increases in spike rate as increases followed by at least three more significant successive increases in rate in the level bins louder than that associated with the first significant rise. Saturation was defined as the sound level associated with the first decrease in spike rate after threshold as long as the spike rate one level bin after this point was not significantly greater.

Fisher Information (FI) was analysed in collaboration with Dr. Nicol Harper as described previously (Dean et al. 2005). FI is a measure of neuronal coding accuracy: higher FI reflects higher accuracy of representation of a given sound level. FI can be conceptualised as the square of the slope of the rate-vs.-level function divided by the variance of the spike count (Dayan & Abbott 2001).

# 4

## CORTICAL COOLING AND MIDBRAIN SOUND-EVOKED NEURONAL RESPONSES

---

### ***4.1 Introduction***

The inferior colliculus (IC), the largest structure in the auditory midbrain, is considered an important hub in the auditory pathway, receiving input from auditory centres upstream and downstream of it, and from other, non-auditory, brain regions. IC neurones respond to a range of sound parameters, including frequency, interaural level differences, interaural time delays, and sound intensity, or level. Recently, it has been suggested that neurones within the IC alter their responsiveness, or adapt, when responding to a given distribution of sound levels; this adaptation alters the range of sound levels over which neuronal firing rates change (the dynamic range) towards a range more suited to representation of sound levels around the most probable levels: the accuracy of neuronal coding of

sound level shifts to be maximal at, or around, the most probable sound levels in the distribution (Dean et al. 2005).

The locus in the auditory system where such adaptation is first manifest remains to be determined. It is likely that the IC inherits at least some of its adaptive changes from the initial stage of neuronal processing – the primary auditory nerve fibres that synapse with the sensory hair cells of the cochlea (Wen et al. 2009). However, since the adaptive effects observed in the auditory nerve are insufficient to account for the degree of IC neurone adaptation, and considering that cortical neurones appear to show further modifications in their adaptive code capacity (Watkins and Barbour 2009), the contribution of the IC to adaptive coding for sound level remains to be determined. Are adaptive coding properties engendered within the IC, or does the IC inherit its adaptive coding properties from other centres? If the latter, does the IC potentiate, reduce, or reproduce these adaptive features? This chapter examines an interesting possible contributing factor to the adaptation effects described by Dean et al. (2005, 2008), namely the descending pathways from auditory cortex, discussed in Chapter 1, that send inputs bilaterally to thalamus, IC and, ultimately via multi-synaptic pathways, to the hair cells of the cochlea. There are no direct precedent data suggesting a role for the descending pathways in adaptive coding of sound level. Indirect links are discussed in Section 1.23, and centre on the idea that, during cortical stimulation or inactivation, the greatest and/or most consistent alterations in IC responses occur during the latter part of the stimulus, after adaptation processes are active.

By cooling auditory cortex bilaterally using a cryoloop apparatus, and recording neuronal responses to a stimulus designed to induce adaptation of rate-vs.-level functions to the statistics of sound level, I were able to compare

adaptation in the following three conditions: cortex active, cortex deactivated through cooling, and cortex recovered. A secondary question was whether any changes were specific to adaptation, or whether such changes were also observed for baseline (non-adapted) rate-vs.-level functions. To this end, the influence of cortical cooling on baseline rate-vs.-level functions was examined for a subset of IC neurones. I found that base-line functions do indeed display a wide variety of changes during cortical cooling, but with no clear pattern of effect. By contrast, I observed that rate-vs.-level functions in the adapted state undergo unidirectional changes during cooling, leading, in the majority of neurones, to a shift in sound-evoked threshold to a position well above the mean sound level, suggesting that absence of cortical input greatly impairs the adaptive benefit described by Dean et al. (2005) for the neuronal population within the IC.

The ‘switching stimulus’ I employed also permitted examination of the time course of adaptation, and hence from these experiments I was able also to assess the effects of cooling cortex on the rapidity with which neuronal responses adjust to the range of sound levels in the environment. Data pertaining to these experiments are presented in Chapter 5.

#### ***4.2 Rate-vs.-level functions and the switching stimulus***

Neuronal rate-vs.-level functions were recorded in response to ‘switching stimuli’ before, during, and following recovery from cortical cooling. During the course of the stimulus, sound level was set every 50ms to a new value chosen at random from a defined distribution. The sound-level distribution consisted of a region of highly probable levels (referred to as the stimulus ‘high-probability region’) at either 51 +/- 6 or 75 +/- 6dB SPL, from which levels were selected with an overall probability of 0.8. Sound levels from the rest of the distribution were selected

with an overall probability of 0.2 (Figure 4.1a). These two distributions are henceforward referred to as the 51dB and 75dB stimuli. The 51dB and 75dB stimuli were alternated in time, such that sound levels were chosen from one distribution for 5s (a stimulus ‘half-period’) before switching to the other (Figure 4.1b). Thus, every 5 s, the mean of the high-probability region was changed, thereby changing the mean sound level presented. This stimulus allowed us to examine both the characteristics of rate-vs.-level functions in the fully adapted state (at the end of each 5s half-period), and also the dynamics of adaptation to the mean sound level, as well as the resultant changes in neuronal stimulus-response relationships, over this time course. By combining this stimulus with cryoloop inactivation of the auditory cortex, I examined the extent to which cortical input influences adaptation of IC neurones in the steady state of adaptation (the subject of the current Chapter), and also how cortical inactivation affects the time course of transitions between adaptation states following transitions between sound-level distributions (the subject of Chapter 5).

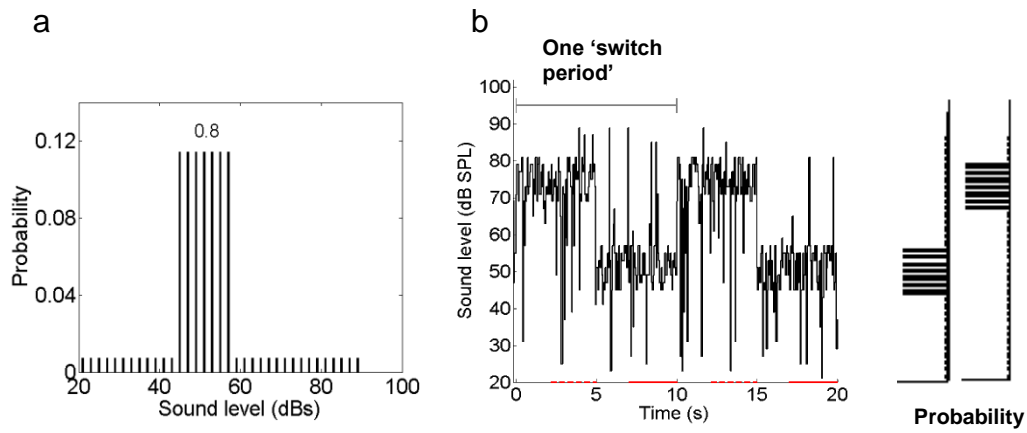


**Figure 4.1 Design of switching stimuli.** A. Distribution of sound levels with high-probability region centred at 51dB SPL (referred to as the “51dB stimulus”). The value 0.8 refers to the probability of a sound level being drawn from the high probability region. b. Sound level over two 10s switch periods, drawn from distributions shown to the right. Mean level changed every 5s when the distribution switched between the 75 and 51dB stimuli; the total range of levels presented remained the same. The red bars on abscissa indicate sampling periods (repeated throughout stimulus) for plotting rate-vs.-level functions from the final 3s of each sound level distribution.

Stimuli were presented in the context of a continuous ‘switching’ paradigm, described in Chapter 3. Consistent with previous work (Dean et al. 2005; Dean et al. 2008), three observations were typically made when comparing baseline to adapted rate-vs.-level functions (Figure 4.2). First, functions shifted along the abscissa when the position of the high-probability region was changed, resulting in shifts in threshold. Second, these shifts often resulted in the threshold lying within the range of sound levels encompassed by the high-probability region. Third, raising the mean sound level often, but not always, resulted in altered slopes, and decreases in firing rates at the maximum sound levels presented, of rate-vs.-level functions (the neurone in Figure 4.2, for example, only shows a decrement in firing rate at the maximum sound levels when adapted to the 75dB stimulus distribution).

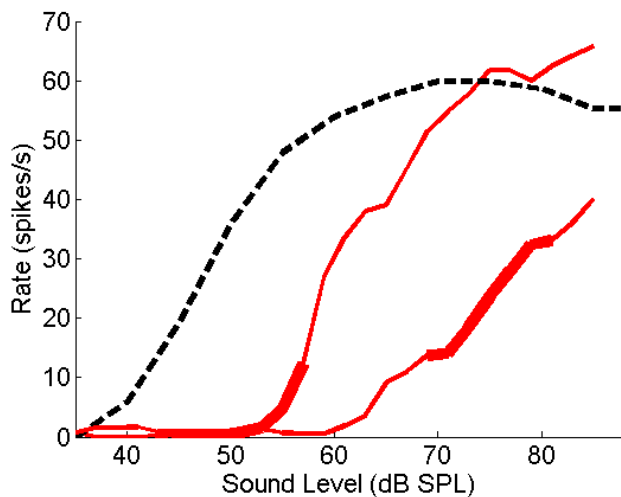


**Figure 4.2 Adaptation and changes in rate-vs.-level function.** Black dotted line: baseline, unadapted function. Red lines: adapted functions. Thick red lines: high-probability regions. Data from a single neurone.

### **4.3 Observations on bilateral AC cooling**

I recorded responses of 94 neurones from 27 guinea pigs with bilateral auditory cortex craniotomies into which the cryoloops were placed. Of these neurones, the responses of 54 were sufficiently well-isolated throughout the three conditions, ‘warm’, ‘cool’, and ‘rewarm’ to warrant analysis. This high rate of neuronal loss of isolation occurred due to a combination of the long recording times necessary and the effects of cooling itself. In many of the recordings lost in the course of an experiment, spike isolation decreased gradually during the cooling condition. In other cases, the isolation increased during cooling and the neurone became tetanic before suddenly ceasing to fire. Both effects are consistent with observations made in the course of any single-neurone recording paradigm and thus are unlikely to have been the result of the cooling technique. However, cooling may have made electrode proximity-induced tetanic firing more likely, since in some cases the brain appeared to retract on the order of tens of microns during cortical cooling. Indeed, in several animals neuronal isolation could reliably be maintained by retracting the electrode 20-50 $\mu$ m during auditory cortical cooling, and extending it once more over the first minute of rewarming. In general, isolating

neurones proved difficult in these experiments, since the bilateral auditory cortex craniotomies rendered the brain less stable than is the case when the skull here is left intact. This situation was not ameliorated by placing agar over the craniotomies, but was slightly improved by venting the *posterior fossa*. A substance that stabilises the brain, but also admits cryoloops and electrodes, would make these bilateral experimental preparations more stable.

Of the 54 isolated neurones, 20 displayed recovery of rate-vs.-level functions such that the function in the ‘rewarm’ condition overlay or lay close to the function in the ‘warm’ condition. In the majority of those that did not recover, the rate-vs.-level functions either remained in the same position during rewarming as during cooling, or else moved further to the right or decreased further in magnitude. However, 3 neurones displayed ‘rebound’ responses, whereby the rate-vs.-level function in the rewarm condition was shifted to left, and/or of greater magnitude, than either the function in the warm, or the cool, conditions.

I also recorded responses of 10 neurones in 2 guinea pigs with a craniotomy made over the left AC, and a craniotomy over the right IC large enough to admit a cryoloop, through which the electrode was advanced. Isolating single-neurone responses was considerably easier in such recordings, likely due to the fact that the brain did not retract noticeably.

#### **4.4 Cooling non-auditory cortex**

Does cooling auditory cortex alter rate-vs.-level functions that are adapted to the switching stimulus? Before addressing this question, it was necessary to control for any direct cooling effects of the cryoloop on the IC. This was particularly important in the light of results presented in Chapter 2, demonstrating that cooling auditory cortex to temperatures necessary for inactivation can lead to a temperature drop of several degrees within the IC itself. Chapter 2 also describes

experiments assessing the temperature drop in IC occurring when the cryoloop is placed not on auditory cortex, but on cortex directly overlying IC. I made use of this cooling effect, largely sparing auditory cortex (see Chapter 2), to cool IC to temperatures which it would typically experience in a standard cryoloop experiment where the cryoloops are placed bilaterally over right and left AC, and – for added stringency of control - to temperatures lower than those it would usually experience. I recorded neuronal responses (n=5; 2 animals) to the switching stimulus at four different cryoloop temperatures: body temperature; 20°C; 15°C; 10°C, and 6°C (Figure 4.3 and 4.4; see Chapter 2).

Figure 4.3 shows the responses of four neurones to the switching stimulus, at different cryoloop temperatures. For these neurones, rate-vs.-level functions largely or completely overlie one another when the brain is warm and when loop temperature is reduced to 10°C. Responses evoked when the cortex was cooled to 10°C are shown for all neurones, since this is the lowest temperature they were recorded at; responses at higher temperatures also overlay the ‘warm’ rate-vs.-level functions, but for clarity, these are not plotted on Figure 4.3*a* and 4.3*b*, but are shown to illustrate the principle in Figure 4.3*c* (20°C) and 4.3*d* (15°C). The ‘rewarm’ condition is also not shown, except in Figure 4.2*a* for the sake of clarity, but in each case, the ‘rewarm’ rate-vs.-level function overlay that recorded in the ‘warm’ and various ‘cool’ conditions.

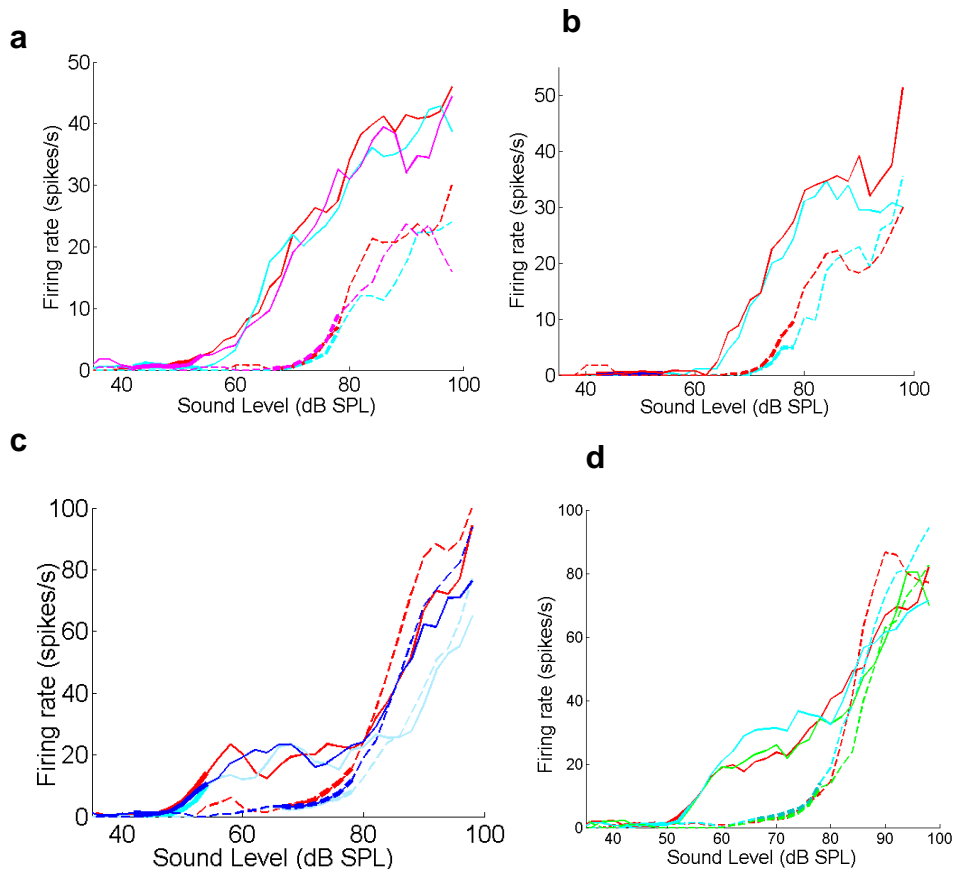


**Figure 4.3 Adapted rate-vs.-level functions in IC; cryoloop placed on cortex overlying IC.** Red=no cooling; blue=20°C; green=15°C; cyan=10°C; magenta=rewarm. a-d display four different neurones from two animals. For all four neurones, functions do not change in form at loop temperatures of 10°C and above. Solid curves: neural responses during presentation of the 51dB stimulus distribution; dashed curves: responses during the 75dB stimulus. Thicker lines on curves represent range of high probability region of stimulus.

Responses of the neurone in Figure 4.3d were also recorded when the cryoloop was cooled to 6°C, shown in Figure 4.4a (black). Here, though there was no change in threshold, firing rates were reduced particularly at higher sound levels. However, the rate-vs.-level function in recovery (magenta), does not return to that of its ‘warm’ form, but remains similar to that evoked under the 6°C temperature reduction. Therefore this decline in spike rate is likely due to factors other than temperature, but may be in part due to temperature effects playing a direct role on neuronal firing rates in IC at 6°C at cortex, i.e. at an IC temperature of 23.5°C (for IC temperature determination, see Chapter 2). The neurone in Figure 4.4b (51dB stimulus) shows a similar pattern, of spike-rate decline at

higher sound levels, which occurs in this neurone during the 10°C cooling condition. This neurone's rate-vs.-level function also fails to recover in the rewarm condition. The responses of this neurone to the 75dB stimulus distribution (4.4c) do not show a similar decline in spike-rate, except during the 'rewarm' condition, suggesting a time-dependent, rather than a temperature-dependent effect.

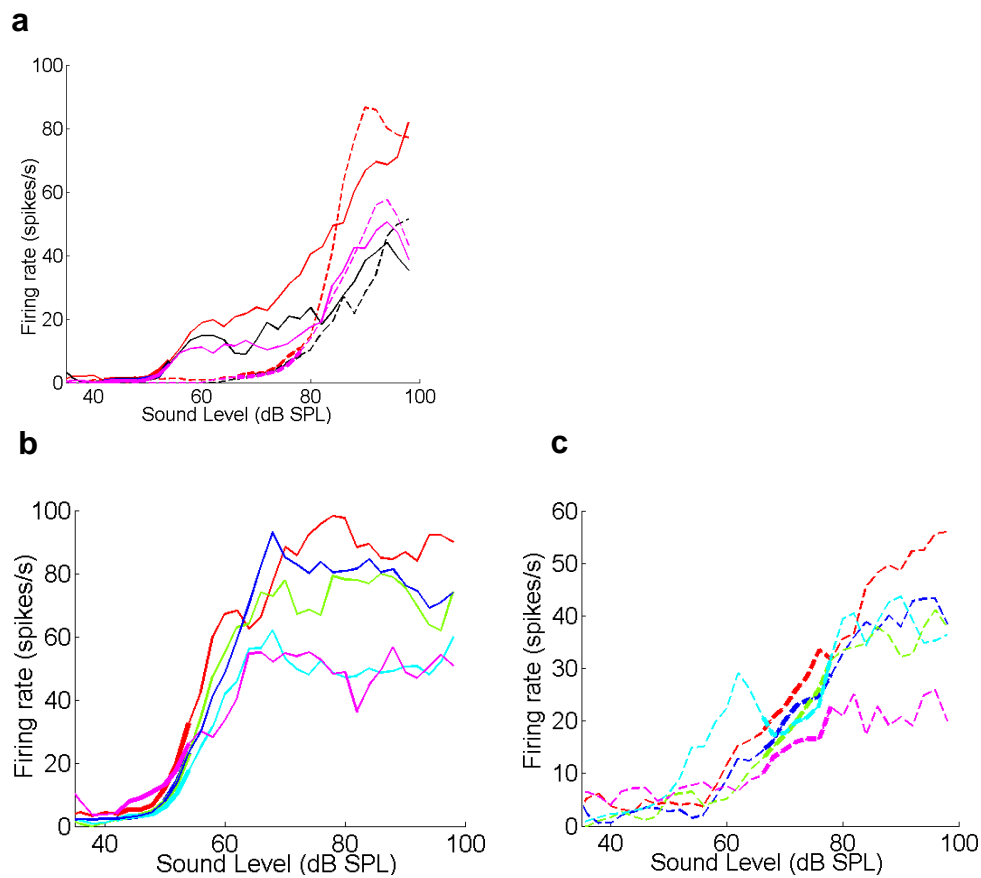


**Figure 4.4 IC Rate-vs.-level functions at different loop temperatures when loop is on cortex overlying IC.** Red=no cooling; blue=20°C; cyan=10°C; black=6°C; magenta=rewarm. Number of neurones =2 in this figure. b and c from same neurone, responses to different stimulus distributions; a – data from a single neurone. Data from 2 animals. Solid curves: neural responses during presentation of the 51dB stimulus distribution; dashed curves: responses during the 75dB stimulus. Thicker lines on curves represent range of high probability region of stimulus.

In summary, across the five neurones recorded from two different animals when IC was cooled via its overlying cortex, rate-vs.-level functions remained largely

unchanged. This observation was made when cortex overlying IC was cooled to a temperature of 20°C, associated with an IC temperature similar to that occurring during bilateral cooling of auditory cortex (see Chapter 2). The same lack of change in rate-vs.-level functions also applies when cortex overlying IC was cooled to 15°C and even 10°C, representing IC temperatures of 27.5°C and 25°C respectively. Therefore, in my experiments, during which auditory cortex is cooled only moderately, any effects on rate-vs.-level functions occurring concomitantly as auditory cortex is cooled are not easily attributable to direct cooling of IC. Nonetheless, I cannot rule out the possibility that some other brain structure is cooled sufficiently by cortical cooling to have a temperature-dependent effect on IC firing rates. For example, recent research suggests that cooling cortex to 2°C leads to circulation of cooled venous blood that has a cooling effect on the cochlear (Shackleton, T, private communication; Coomber et al. 2011). This effect has not, however, been tested at the higher temperature of >10°C; at temperatures of 1-3°C using a unilateral loop appears not to affect neural activity in IC (Coomber et al. 2011).

#### ***4.5 Effects of cortical cooling on adjustments of rate-vs.-level functions***

I analysed the responses of 20 neurones in the IC to the switching stimulus before, during, and after bilateral cooling of the auditory cortex. The question addressed in this chapter is whether the rate-vs.-level functions elicited in response to the two stimulus distributions are altered by cortical inactivation.

As previously reported, and shown in Figure 4.2, rate-vs.-level functions typically displayed three changes during adaptation with intact cortical input: a rightward-shift in threshold along the abscissa, a tendency for the threshold to lie within the range of levels encompassed by the high probability region, and a

reduction in the slope and/or maximum spike rate of rate-vs.-level functions. The changes I observed during cortical cooling, for all but one neurone recorded, reflected a potentiation of these adaptation-associated changes: the rightward shift was increased in certain neurones during cortical cooling, the decrease in slope/maximum spike rate was greater in others, and some displayed increases in both of these changes. In the case of the 51dB stimulus, the cortical-cooling-associated increased rightward shift, where it occurred, always resulted in thresholds adjusting to a position further away from the high-probability distribution. Figures 4.5 to 4.7 classify neurones according to these different types of change in the adaptation of rate-vs.-level functions.

Figure 4.5 shows rate-vs.-level functions that, during cortical cooling, underwent a further rightward shift during cooling, extending the shift associated with adaptation in the ‘warm’ state, with no decreases in maximum spike rate and/or slope, or decreases that were minor in comparison with those in Figure 4.6. The only exception in this group is the neurone in 4.5c, whose rate-vs.-level function for the distribution centred on 75dB does display a reduced slope and maximum spike rate. However, the 51dB stimulus rate-vs.-level function, in 4.5c and in the other neurones in the Figure, undergoes a clear rightward shift in threshold during cortical inactivation. The thresholds of the neurones in Figure 4.5a and b are clearly within the high-probability region of the 51dB stimulus in the cortex-warm condition; in both of these neurones, cortical cooling results in thresholds shifting to lie outside the high-probability region. A similar pattern is observed in Figure 4.5c, in which the threshold lies at the upper edge of the high probability region and is shifted during cooling to a position outside (louder than) the high probability region.

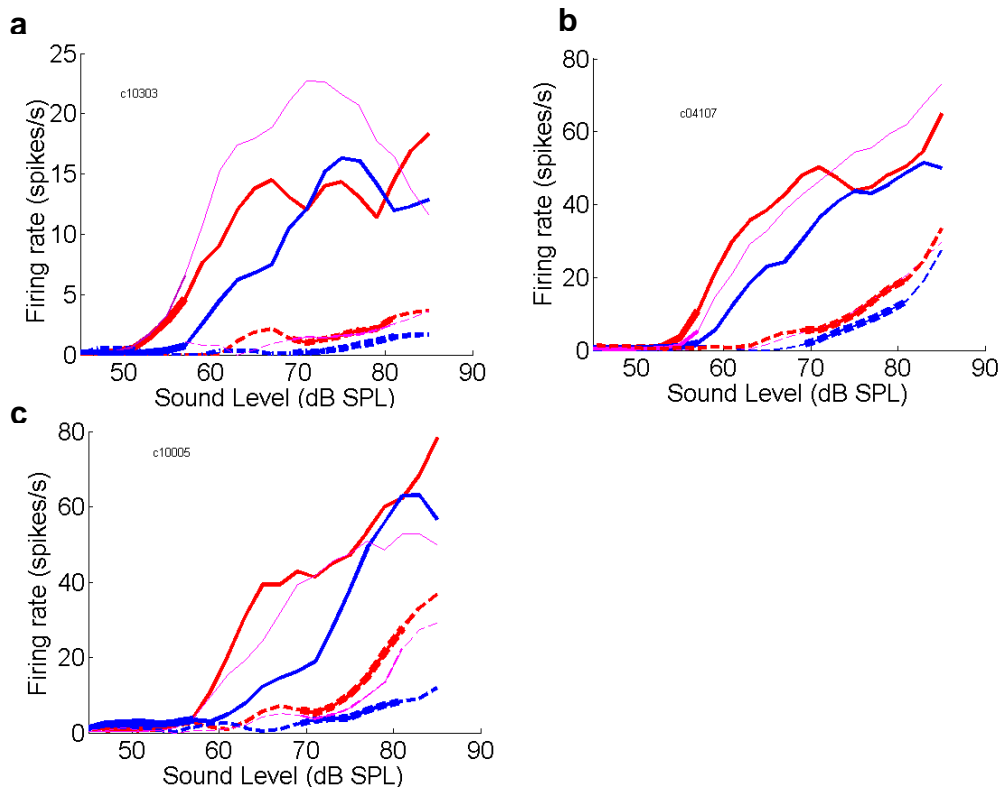


**Figure 4.5 Adapted rate-vs.-level functions during auditory cortex cooling.** Warm (red), cool (blue), rewarm (magenta) conditions. Solid line, responses to 51dB stimulus; dashed line, 75dB stimulus. Thicker lines represent high probability stimulus regions; magenta lines are thin for clarity.

The two neurones in Figure 4.6 display rate-vs.-level functions whose adaptation-associated threshold shifts are similar in both the cortex-warm and cortex-cool conditions. The slope of these neurones' rate-vs.-level functions, however, decreases when cortex is cooled, as do their maximum firing rates. It appears, therefore, that cortical cooling can lead to potentiation of either of the two major effects of adaptation on rate-vs.-level functions, increasing rightward shifts, as for the neurones in Figure 4.5, or further decreasing the slope of functions, as for the neurones in Figure 4.6.

For both neurones in Figure 4.6, especially the neurone whose responses are represented in Figure 4.6a, the initial portion of the curve is not associated with a change in slope during cooling compared to the warm condition, whereas the upper part of the slope is, suggesting a greater effect of cooling on responses

to louder sound levels in these neurones. It is interesting to compare visually the sound level at which the warm versus the cool curves deviate from one another for the two stimulus distributions, particularly in Figure 4.6a. Here, during the 51dB stimulus, this point occurs ~60dB, whereas for the 75dB stimulus, this deviation occurs at ~72dB. This suggests, first, that the effect of the descending fibres is not uniform across sound levels, and second, that this non-uniformity is itself subject to modification according to the adaptation state of the neuron. The shift in sound level associated with cooling across the rate-vs.-level function is quantified in section 4.8.

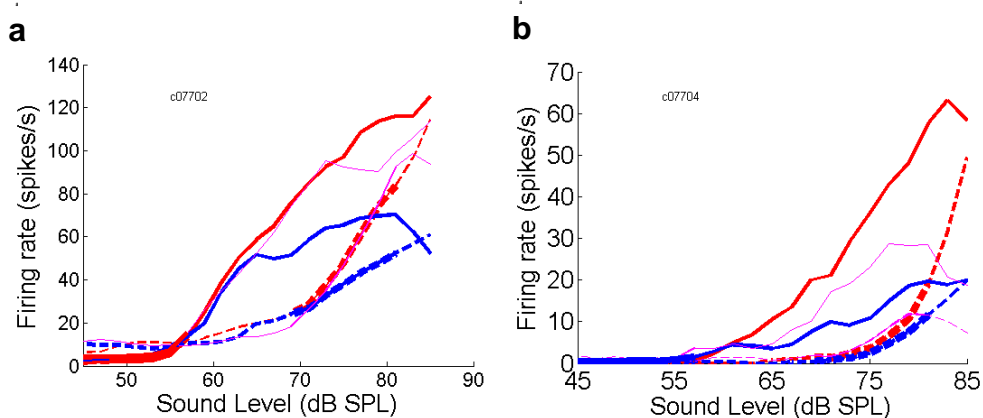


**Figure 4.6 Changes in slope of rate-vs.-level functions during cortical cooling.** a, b display two example neurones. Solid curves: neural responses during presentation of the 51dB stimulus distribution; dashed curves: responses during the 75dB stimulus. Thicker lines on curves represent range of high probability region of stimulus. Red: cortex warm condition; blue: cortex cool condition; magenta: cortex rewarm condition. Magenta lines are thin in both panels for clarity.

A third pattern of change is presented in Figure 4.7. Here, neurones underwent both an increased rightward shift in rate-vs.-level function during cooling, and a decrease in slope/maximum firing rate. The rightward shift tended to be greater in these neurones than in the neurones shown in Figure 4.5.

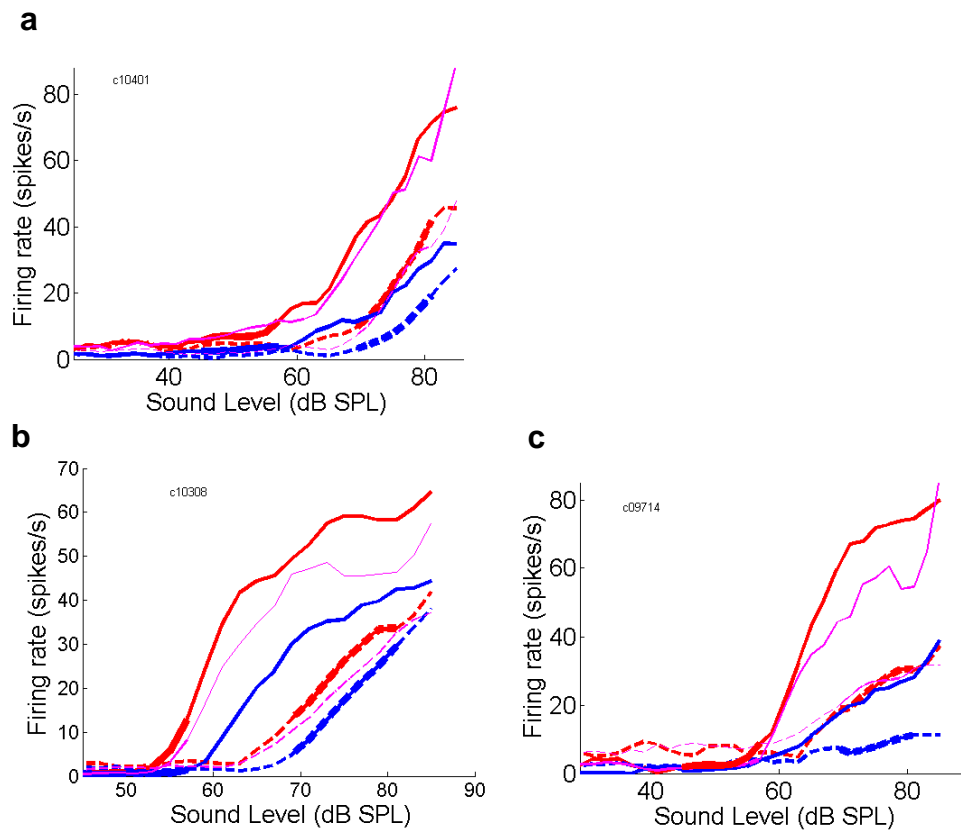


**Figure 4.7: Changes in threshold and slope of rate-vs.-level functions during cortical cooling.** 3 example neurones. Solid curves: neural responses during presentation of the 51dB stimulus distribution; dashed curves: responses during the 75dB stimulus. Thicker lines on curves represent range of high probability region of stimulus. Red: cortex warm condition; blue: cortex cool condition; magenta: cortex rewarm condition. Magenta lines are thin in both panels for clarity.

These changes in rate-vs.-level function again tend to shift the threshold above the high-probability region of the stimulus. Other features of the changes include the observation that a rightward shift is fairly uniform across levels in some neurones, for example 4.7*b*, but in other neurones the shift seems to increase with sound level, as in 4.7*c* (see section 4.8).

Finally, for some neurones the decrease in firing rate across levels was such that during cortical cooling rate-vs.-level functions ceased to change appreciably with sound level (Figure 4.8). As expected, the PSTHs for these neurones across conditions, shown to the right of the rate-vs.-level functions, also

display large decrements in firing rate. These neurones display almost complete cessation of spiking in the absence of cortical input to the IC. Note also the widely different absolute firing rates of the two neurones: the neurone in Figure 4.8c has a low firing rate, and therefore might be expected to show a flattening in rate-vs.-level function, if the effect of cortical cooling was a uniform decrease in responsiveness across the IC. However, the neurone in Figure 4.8a has a much higher firing rate, and the rate-vs.-level function is also depressed almost to a flat line in response to cortical inactivation (3/20 neurones displayed this pattern of almost complete cessation of firing during cooling).

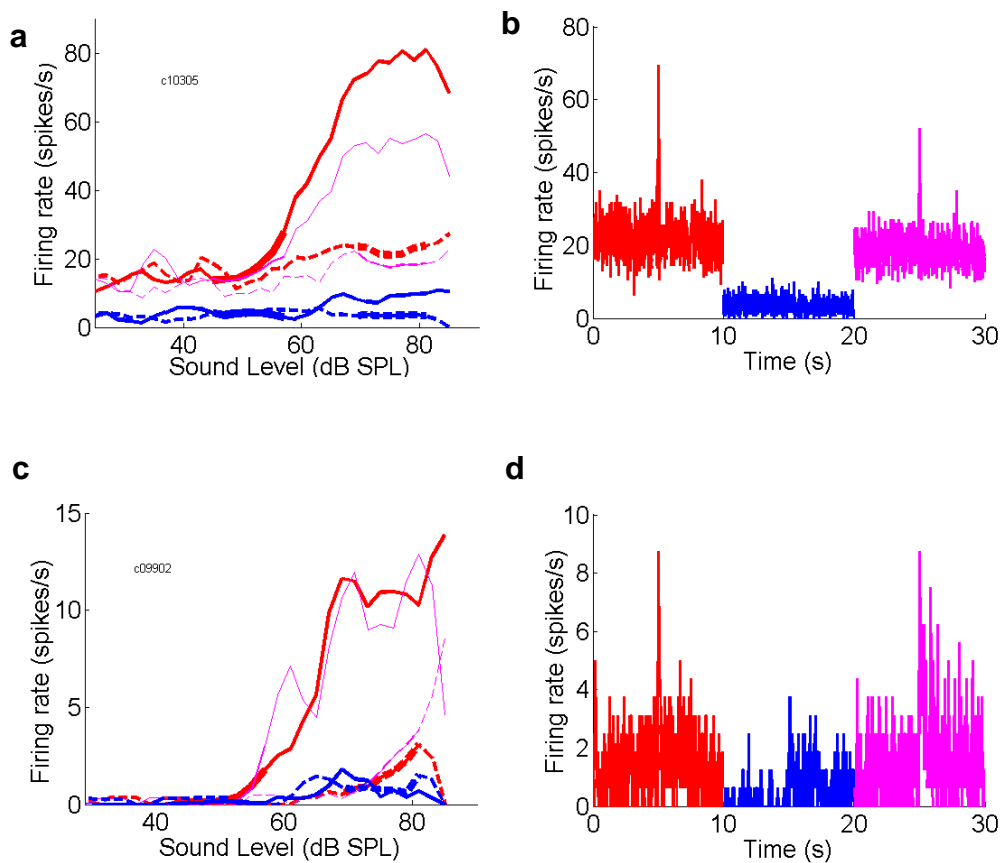


**Figure 4.8** a,c. Rate-vs.-level functions of two neurones showing large decreases in firing rate, and consequent flattening of rate-vs.-level functions, during cortical cooling. b,d. PSTHs of the same neurones; the drop in firing rate of the rate-vs.-level functions is reflected in the drop in firing rate of the PSTH. Note: time-scale on the abscissa of PSTHs is for representational purposes: in each condition, the data for the PSTH was collected during the course of the recording for that condition and averaged over 1 switch period (10 s). See Figure 4.3 for legend explaining rate-vs.-level function curves.

#### **4.6 Baseline rate-vs.-level functions**

I recorded baseline, non-sound-adapted rate-vs.-level functions, also termed silence-adapted functions (Watkins & Barbour 2008) for a subset of neurones. By comparing these with the adapted functions, it was possible to ask if the changes described above reflected general properties of IC neurones without bilateral cortical input, or whether they were an adaptation-specific phenomenon. Fewer neurones were presented with baseline stimuli than the adaptation stimuli. This was because the continuous adaptation protocol precluded recording of baseline responses in the cool condition, and because the question of whether the effects described above are unique to adaptation is secondary, the primary aim of this study being to describe the characteristics of change in the adapted steady-state when cortex is cooled. The baseline rate-vs.-level functions of 18 neurones were recorded in the warm, cool, and rewarm conditions, and in these neurones the discontinuous adaptation protocol was also applied across these conditions. 10 neurones recovered baseline functions in the rewarm condition. Of these, 4 also recovered adapted rate-vs.-level functions.

These neurones are shown in Figure 4.9, where baseline functions (solid lines) are plotted with the switching stimulus functions from the same neurone. For the neurone in 4.9*a*, during cortical cooling, the adapted rate-vs.-level function shifts clearly to the right, particularly at lower sound levels, and less so at higher levels; by contrast, the baseline function does not shift in this way; rather, there appears to be a small shift in the quieter sound levels to the right, and a large shift to the left at higher sound levels. In 4.9*b*, the shifts across conditions appear more similar for functions gathered to basic and adaptation stimuli.

In both 4.9*a* and *b*, it is notable the extent to which the effect of the descending pathways appears to depend upon the adaptation state of the neurone. Compare the effect of cortical cooling on baseline, 51dB, and 75dB functions –

each one appears to alter uniquely. This observation holds also for Figure 4.9c and d. 4.9c shows a similar pattern to 4.9a, where there is no change in baseline functions on cooling, but functions from the 51dB, and particularly the 75dB, stimuli shift to the right during cooling. 4.9d shows another interesting pattern. Here, cooling has a powerful effect on the baseline function, and results in almost complete inhibition in the adapted function.

In summary, for individual neurones, it appears that whereas adapted rate-vs.-level functions tend to shift rightwards during cooling, baseline functions may or may not shift similarly.

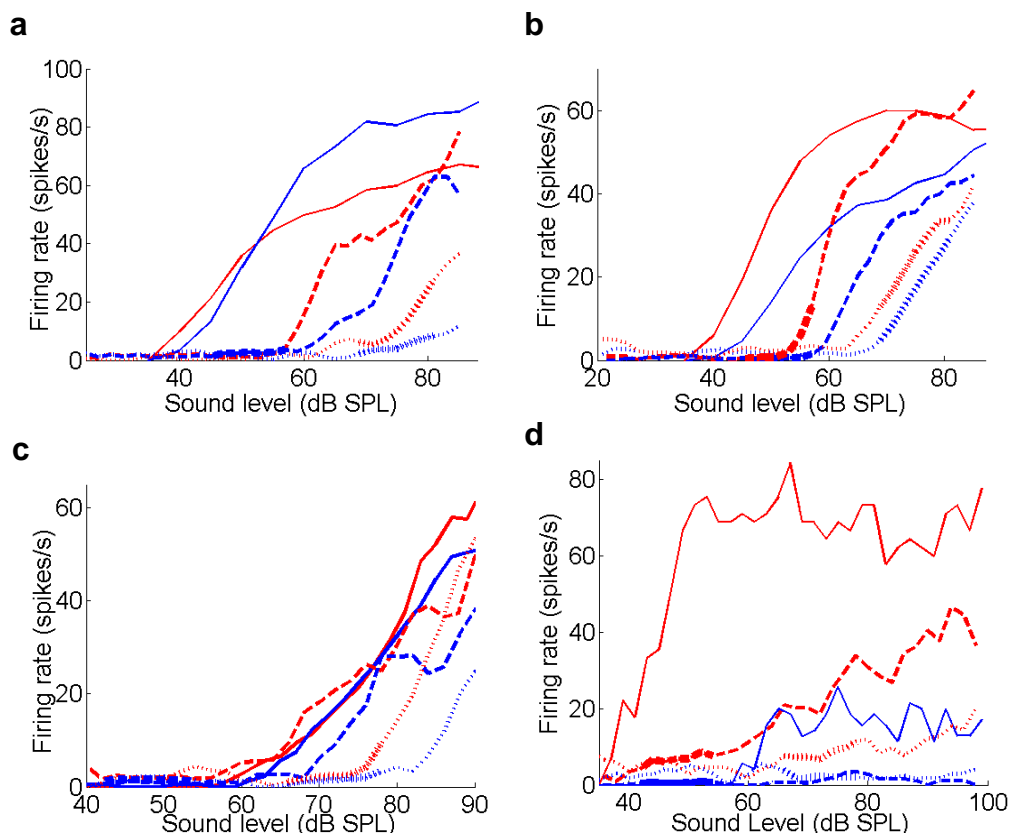


**Figure 4.9 Baseline and adapted functions during cortical inactivation.** Solid lines: baseline (50ms noise bursts separated by 300ms, chosen at random from a flat level distribution.) Long dashes: 51dB stimulus. Short dashes: 75dB stimulus. Red: 'warm'; blue: 'cool'. a-d: example rate-vs.-level functions from four neurones across cooling conditions for different stimuli. a. The effect of cortical cooling is more pronounced when the neurone is adapted. b. The effect of cortical cooling appears similar in adapted and non-adapted states. c. Effect of cooling increases with greater adaptation – no effect on baseline functions, moderate effect at 51dB, and strong effect at 75dB. d. Large effect of cooling even on non-adapted, baseline, functions. See Figure 4.3 legend for further explanation of rate-vs.-level function formatting.

#### 4.7 Recovery of rate-vs.-level functions: adapted and baseline

As described in section 4.1, the majority of adapted rate-vs.-level functions did not recover in the rewarm period. It was interesting that in some cases where adapted functions did not appreciably recover, baseline functions did. Figure 4.10 displays rate-vs.-level functions for warm, cool, and rewarm conditions for the baseline (solid line) and adapted (dashed line) stimuli. In these two examples, recovery was less apparent for adapted rate-vs.-level functions, and more complete for the non-adapted functions. It cannot be the case that this simply reflected more time having elapsed between recovery functions being recorded as responses to the two stimulus types, because baseline functions were collected before the adapted functions.

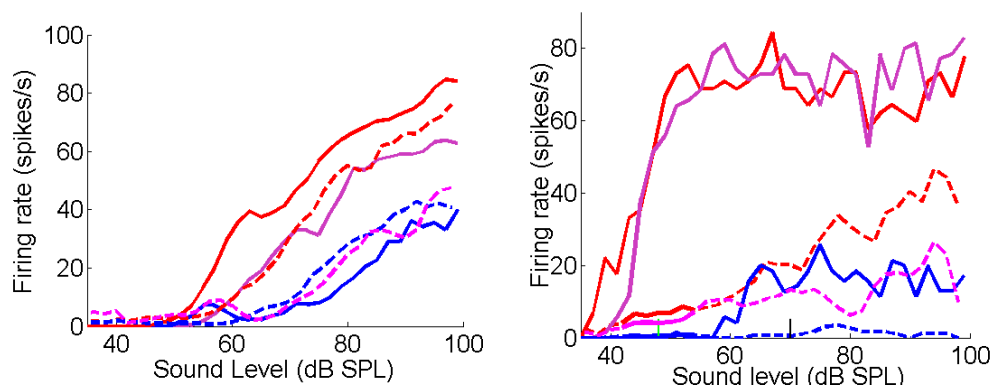


**Figure 4.10** Baseline (solid) and adapted (dashed) rate-vs.-level functions for two example neurones, in the warm (red), cool (blue), and rewarm (magenta) conditions.

For several neurones, rate-vs.-level functions in the ‘cool’ condition shifted to the right relative to ‘warm’, but shifted more leftwards relative to the initial warm, adapted configuration in the rewarm condition (Figure 4.11). These neurones were not included in the population analysis due to the possibility that their initial, warm responses reflect incomplete recovery from the cortical inactivation state following a previous cooling cycle in the same animal.

However, other explanations are possible and warrant future experiments (see Chapter 6).

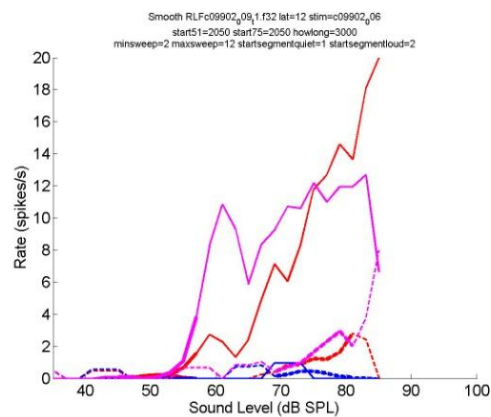


**Figure 4.11** Example of adapted rate-vs.-level functions from a single neurone, displaying recovery with 'rebound'. Solid lines: 51dB stimulus; dashed lines, 75dB stimulus.

## **4.8 Quantification of rate-vs.-level functions**

The aim of this section is to provide an overview of the neuronal population recorded by quantifying some of the changes described above.

### **4.8.1 Threshold, saturation, and other measures**

Figure 4.12 compares thresholds across stimuli for both methods of threshold determination described in Chapter 2. The 51dB stimulus distribution resulted in lower thresholds than the 75dB stimulus distribution in all cryoloop conditions (see Table 4.1).

Method	Significance Determination				10% Determination			
	51dB		75dB		51dB		75dB	
Stimulus	Mean	SD	Mean	SD	Mean	SD	Mean	SD
Thresholds (dB SPL)								
Warm	56.0	6.4	67.8	4.5	60.3	4.6	69.7	6.9
Cool	61.4	9.2	72.2	8.3	63.9	6.2	70.7	7.6
Rewarm	57.1	6.9	68.9	7.5	61.1	4.0	70.0	6.1

**Table 4.1 Neuronal auditory thresholds across conditions, stimuli, and methods.**

The increased threshold for the 75dB stimulus compared to the 51dB stimulus was significant across the population for all cryoloop conditions, for both methods of threshold determination. For the significance determination method, the difference in thresholds between stimuli was statistically significant as follows: warm,  $p < 0.0005$ ; cool,  $p = 0.0113$ ; rewarm,  $p < 0.0005$ . For the 10% method, the significance levels were: warm,  $p < 0.0005$ ; cool,  $p = 0.0031$ ; rewarm,  $p < 0.0005$  ( $n = 20$  neurones; Student's paired t-test). The difference between 51dB and 75dB thresholds was not significantly changed by cortical cooling (t-test of warm 75dB-51dB differences versus cool differences:  $p = 0.1608$ ).

The two methods resulted in thresholds not significantly different, across the two methods, for the 51dB stimulus, cooled condition, but for the 51dB stimulus, warm and rewarm conditions, the 10% method produced significantly greater thresholds (paired t-test: warm/51,  $p = 0.0014$ ; cool/51,  $p = 0.0844$ ; rewarm/51,  $p = 0.0014$ ). This relationship is displayed in the scatter-plot of Figure 4.12C. For the 75dB stimulus, the two methods produced similar thresholds across

all conditions (warm,  $p= 0.6846$ ; cool,  $p=0.5756$ ; rewarm,  $p= 0.6069$ ). In summary, thresholds were significantly greater for the 75dB stimulus compared to the 51dB stimulus, across all three cryoloop conditions. This was the case for both determination methods.

For subsequent analysis, comparing threshold shifts across cryoloop conditions, the significance threshold determination method is used, because the thresholds produced by the 10% method were generally higher and appeared less consonant with visual impressions of rate-vs.-level function thresholds.

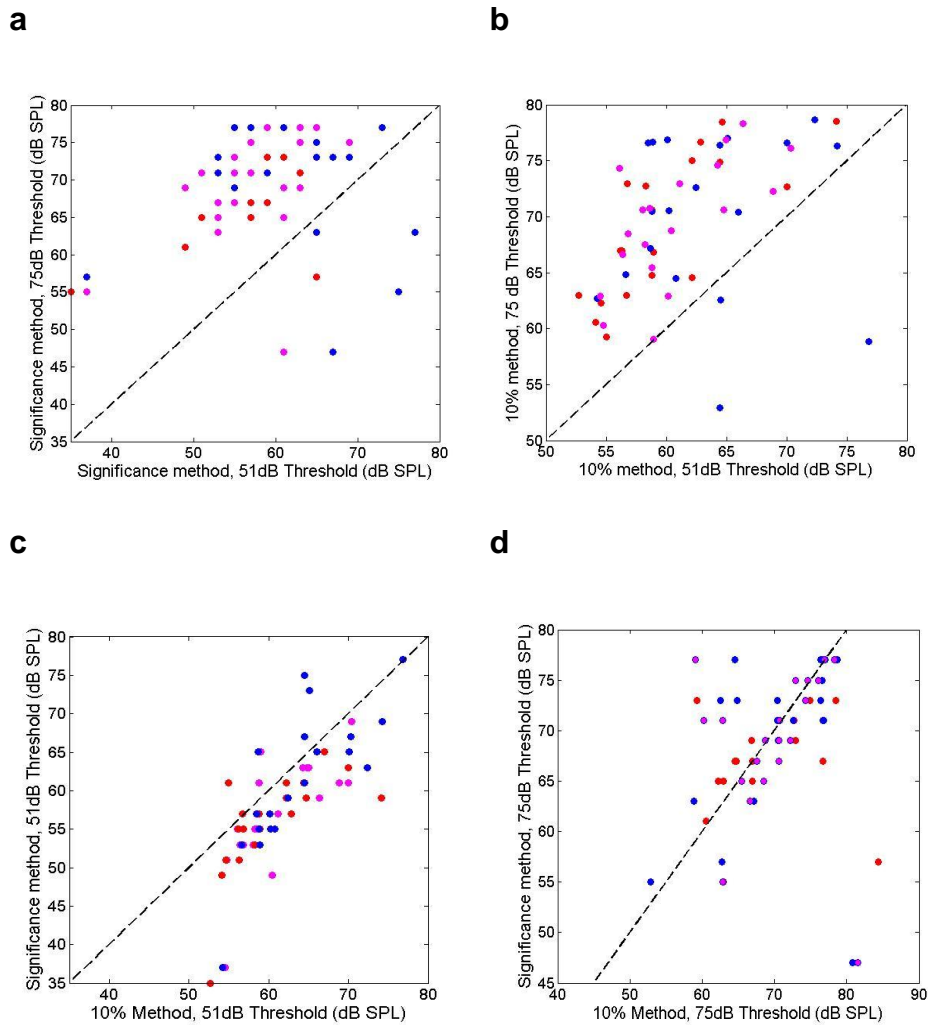


**Figure 4.12 Threshold measures.** Colours represent one of three cortical temperature states, warm (red), cool (blue) or rewarm (magenta). Each point represents data from a single IC neurone in a single cortical cooling state, so that each neurone provides 3 data points (one red, one blue, one magenta) for each graph. a. Significance method; thresholds tend to lie above unity, reflecting higher thresholds for the 75dB stimulus. b. 10% determination method: again, thresholds are higher for the 75dB stimulus. c,d. Comparison of methods for 51dB (c) and 75dB (d) stimuli. The methods produce similar thresholds over the population but can result in different thresholds for individual neurones, with 10% thresholds tending towards higher values.

Across the population of neurones, for the 51dB stimulus, 16/20 (80%) neurones increased threshold during cortical inactivation, 1 (5%) decreased threshold and 3 (15%) underwent no change in threshold (Figure 4.13). For the 75dB stimulus, 15/20 neurones (75%) increased threshold, 2 neurones (10%) decreased threshold and 3 neurones (15%) underwent no change in threshold.

Though the population size is small, it seems reasonable to make two general observations: first, the vast majority of neurones tend to increase threshold when cortex is cooled; second, this increase occurs in similar proportions across the population for both stimulus distributions.

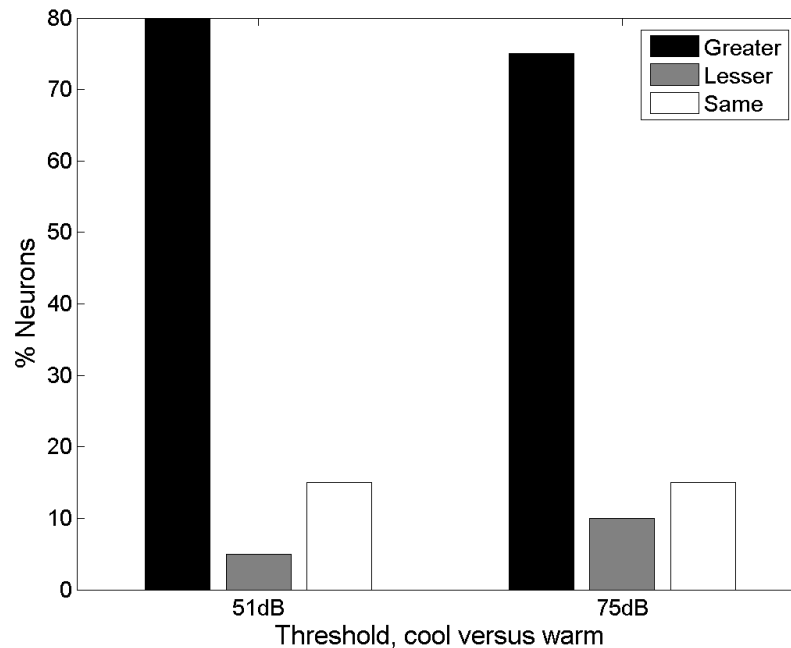


**Figure 4.13 Direction of threshold shift during cooling across population.** 'Greater': threshold in cool condition higher than in warm condition. 'Lesser': threshold lower in cool condition; 'same': no change in threshold between conditions.

How much do thresholds change? For the 51dB stimulus, the maximum rightward shift during the 'cool' condition was 18dB; the minimum rightward shift was 2dB (i.e. the smallest change resolvable with the switching stimulus). The maximum leftward shift was -4dB. The mean shift across the population was 5.4dB (n=20; 25% quartile, 1.5dB; 75% quartile, 12.5dB). For the 75dB stimulus, the maximum rightward shift was 12dB, the minimum, 2dB, and the mean 4.21dB, with quartiles of -1.5dB and 7.5dB. Overall, then, the 51dB stimulus distribution had the largest rightward shift, and the greatest mean, but a t-test revealed no significant difference between the threshold changes (rather than the

absolute thresholds) on cooling when the two distributions are compared ( $p=0.73$ ). Across the population, warm thresholds were significantly lower than cool thresholds for both the 51dB stimulus distribution ( $p= 0.00019$ ), and the 75dB stimulus distribution ( $p= 0.0095$ , paired t-test,  $n=20$ ).

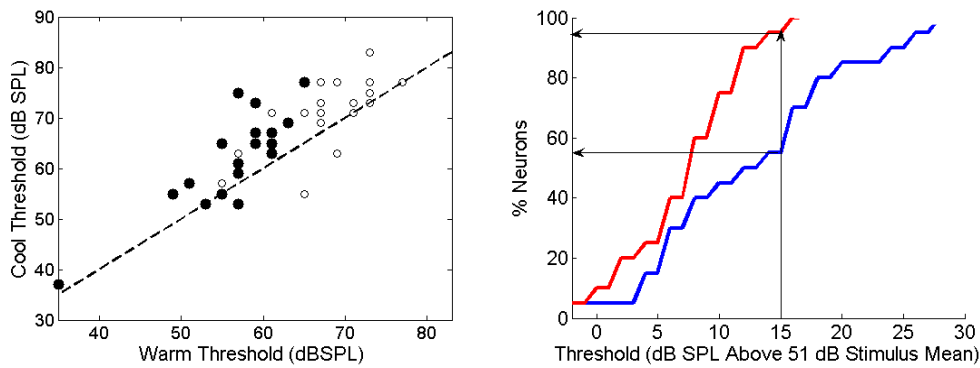


**Figure 4.14 Threshold changes during cooling.** a. Cool thresholds are greater than warm thresholds. Filled circles: 51dB stimulus. Open circles: 75dB stimulus. b. Almost all neurones have thresholds within 15dB of the stimulus mean in the warm condition; however in the cool condition, just over half of neurones have thresholds within 15dB of the stimulus mean.

Figure 4.14a displays this relationship for both stimuli: the cool thresholds lie above the line of unity in most cases. It seems clear from the above results that, during cooling, thresholds shift rightwards, across the population. What effect could such a shift have on sound level representation? As discussed in Section 4.1, one effect of adaptation may be to raise thresholds towards, or just above, the mean sound level. Figure 4.14b suggests that almost all neurones in the warm condition, when adapted, have threshold within 15dB of the mean of the high probability region of the stimulus. However, during cortical cooling, this picture changes, such that just over half of neurones, in the cortex-cooled state, have thresholds within 15dB of this mean (Figure 4.14b). This would imply that rate-vs.-level functions in the cooled condition adjust less effectively to the mean sound level in the environment, in that they would be unable to respond to levels surrounding the mean.

Given these shifts in threshold, saturation points might also be expected to alter. However, not all cells' rate-vs.-level functions saturated, resulting in too few data points across the population to perform a similar assessment as with threshold. Nonetheless saturation does appear to be affected by cortical inactivation. Figure 4.15a shows the percentage of cells saturating, for each cryoloop condition. Here, a neurone was said to saturate if its maximum firing rate did not occur at the highest sound level presented. Data in Figure 4.15a suggest that more cells in the cooled condition reached saturation, compared to the warm condition. Considering that rate-vs.-level functions shifted to the right, this is perhaps unexpected. Rather, a rightward shift would tend to push saturation point to levels beyond the maximum level presented. The fact that this was not the case suggests that in addition to a rightward shift along the abscissa, rate-vs.-level functions in the cooled condition were also compressed, with a smaller dynamic range of outputs. This possibility is also examined in Figure 4.15.

To quantify the rate-vs.-level function with respect to dynamic range, two measures were used. First, output dynamic range was defined as the difference in spike rate between the spike rates at 10% and 90% of maximum. Second, input dynamic range was defined as the range of levels between the two levels associated with the 10% and 90% spike rates (Mulders et al. 2008). As shown in Figure 4.15b-e, both input and output dynamic ranges were significantly reduced in the cooled condition, for both stimulus distributions. This suggests that, in the cool condition, neurones respond to a more limited range of sound levels, and do so with a smaller variation in spike rate.

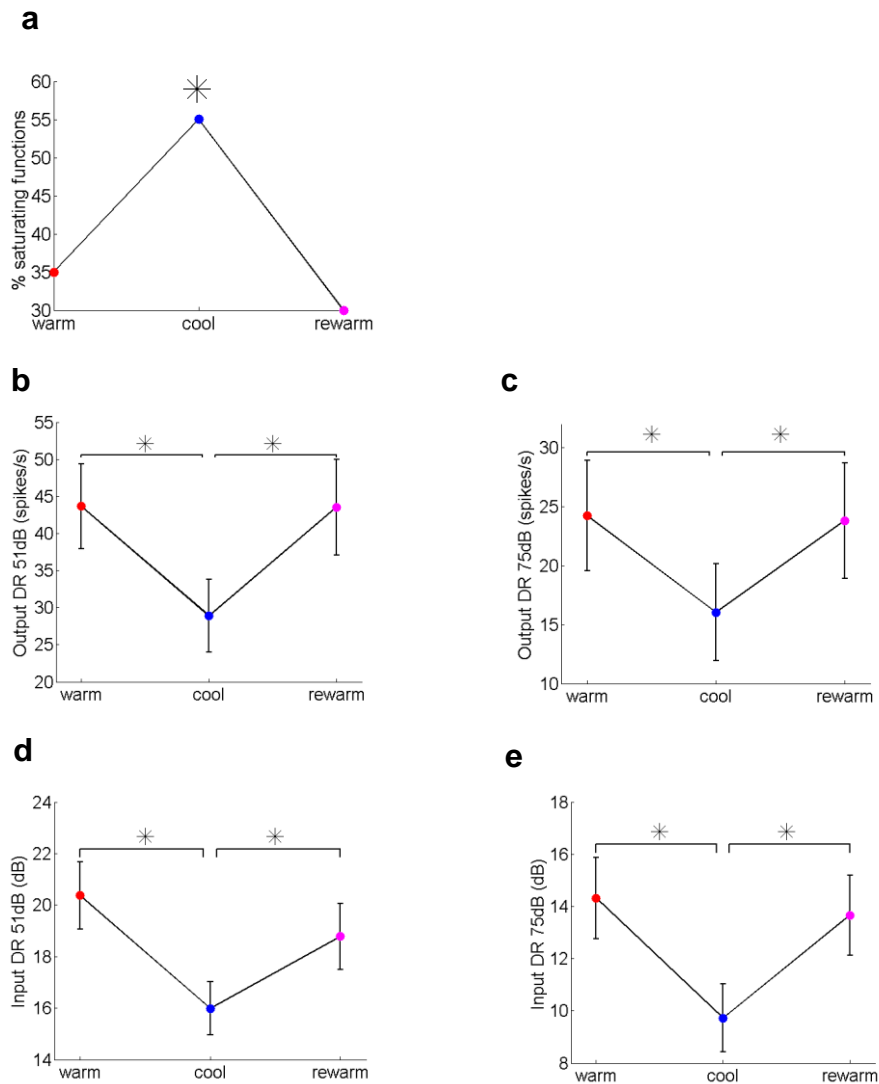


**Figure 4.15 Saturation, Input and Output Dynamic Range.** a. More neurones had saturating rate-vs.-level functions in the cooled condition. b-e. Both output dynamic range and input dynamic range decreased during cortical cooling.

### 4.8.2 Assessing suprathreshold alterations

As discussed above, threshold is altered by cortical inactivation. However, rate-vs.-level function shifts during cooling suggest that cortical inactivation may have effects at higher sound levels different from the effects seen at threshold levels. It is important also to examine the shifts in level at other points in the rate-vs.-level function. A simple way of addressing this point is to ask whether threshold shifts represent the greatest change across the rate-vs.-level function. In Figure 4.18a, threshold in the warm condition is plotted as a function of the sound level associated with the greatest rightward shift in the rate-vs.-level function

curve when cortex is cooled. If the points lay along the line of unity, this would suggest that threshold is indeed the point on the curve undergoing maximum rightward shift during cortical cooling. However, the points lie above this line, indicating that, for most neurones, the maximum rightward-shift in the rate-vs.-level functions occurs above threshold. Note that for some rate-vs.-level functions it was not possible to measure points of maximum shift because the firing rates in the cool conditions dropped to near zero across levels, and these neurones were excluded from this analysis (n=3).

These data suggest that cooling-induced shifts in rate-vs.-level function are not uniform across levels, even within a given adaptation state. To quantify this change across the whole function, and so assess cortical effects across the function, the dB shift along the abscissa between warm and cool functions was measured for each level. Beginning at the warm threshold level, the firing rate at each dB in the warm condition was measured. The shift was then measured as the distance, in dB, to the point associated with the same firing rate on the cool rate-vs.-level function. This was achieved by interpolating within the cool function to measure the sound level associated with the equivalent firing rate at that decibel level on the warm function. From this analysis, dB-shift-versus-dB functions were produced (Figure 4.16). In effect, this analysis measures the extra decibel input into the auditory system which is required to achieve an equivalent IC neural output in the cool state as is achieved at each decibel level in the warm state.

Due to the high thresholds of rate-vs.-level functions plotted from responses gathered in the cool condition to the 75dB stimulus, it was only possible to perform this analysis for the responses to 51dB stimulus. In 4/20 neurones during the 51dB stimulus, complexities in rate-vs.-level-functions, and the tendency for cool functions to saturate at dB levels of lower magnitude, meant

that this analysis did not lead to clearly interpretable graphs. For the remaining 16/20 neurones at 51dB, visual representation of this analysis appeared to fall into three groups. For group one, level shift increased monotonically with level, such that the greatest shifts in level were at the highest levels. These are shown, in Figure 4.16*a* and *b*, and the relevant rate-vs.-level functions in 4.16*c* and *d* (6/16 neurones). For group two, level shift was non-monotonic, peaking before falling off at higher levels (4.16*e* and *f*; 8/16 neurones). For group three, the greatest level shift was around threshold, and level shifts tended to decrease with increasing sound level (Figure 4.17; 2/16 neurones).

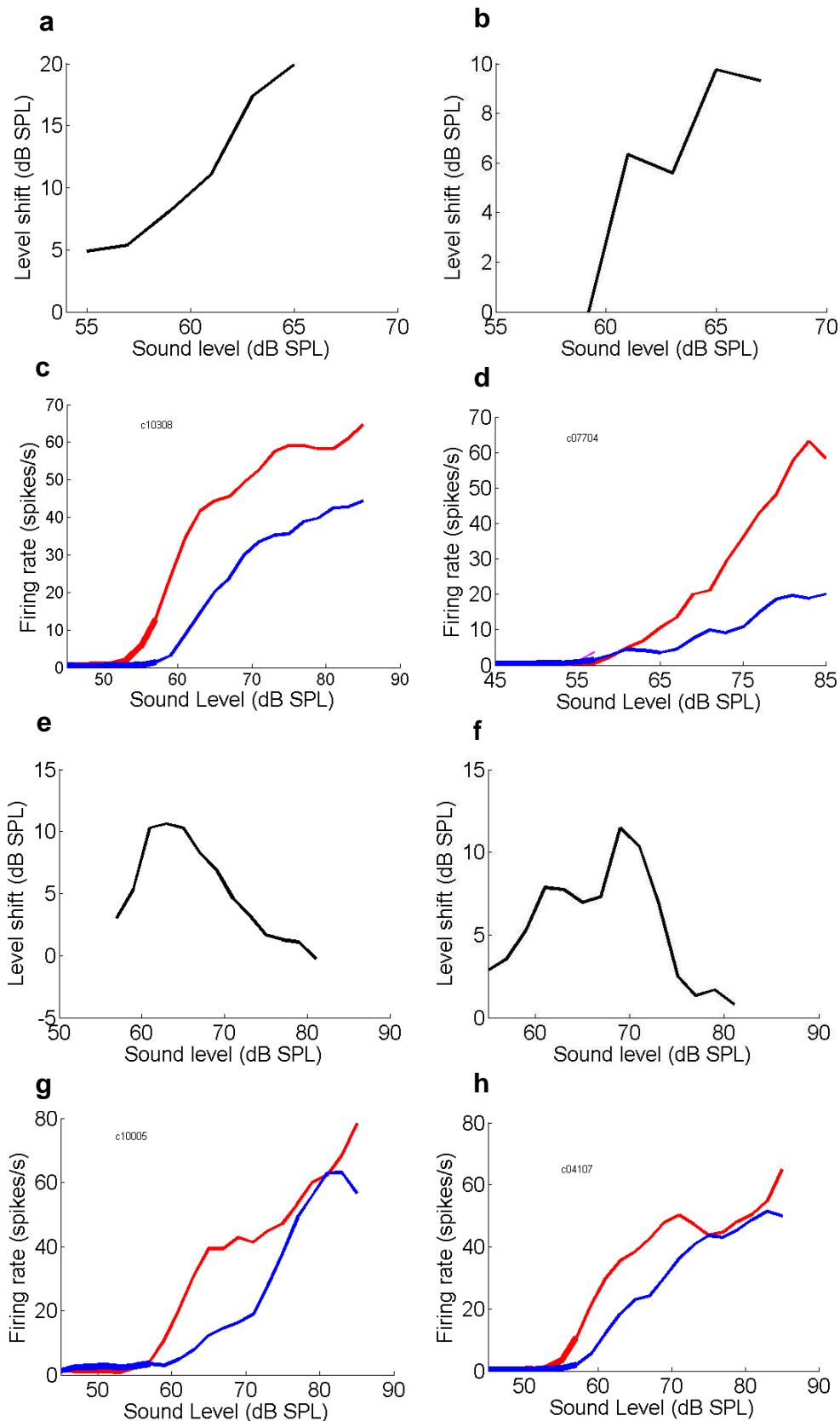


**Figure 4.16 Level shift by level.** a,b. Shift in sound level required after cortical cooling to maintain given spike rate output from individual IC neurones at each sound level in warm condition. Monotonic functions. c,d. 51dB stimulus rate-vs.-level functions associated with the dB-shift-versus-dB functions in a,b. e,f. Non-monotonic level shift functions. g,h. Rate-vs.-level functions associated with the dB-shift-versus-dB functions in e,f. . Red functions – warm; blue functions – cool. All functions shown are derived from 51dB stimulus.

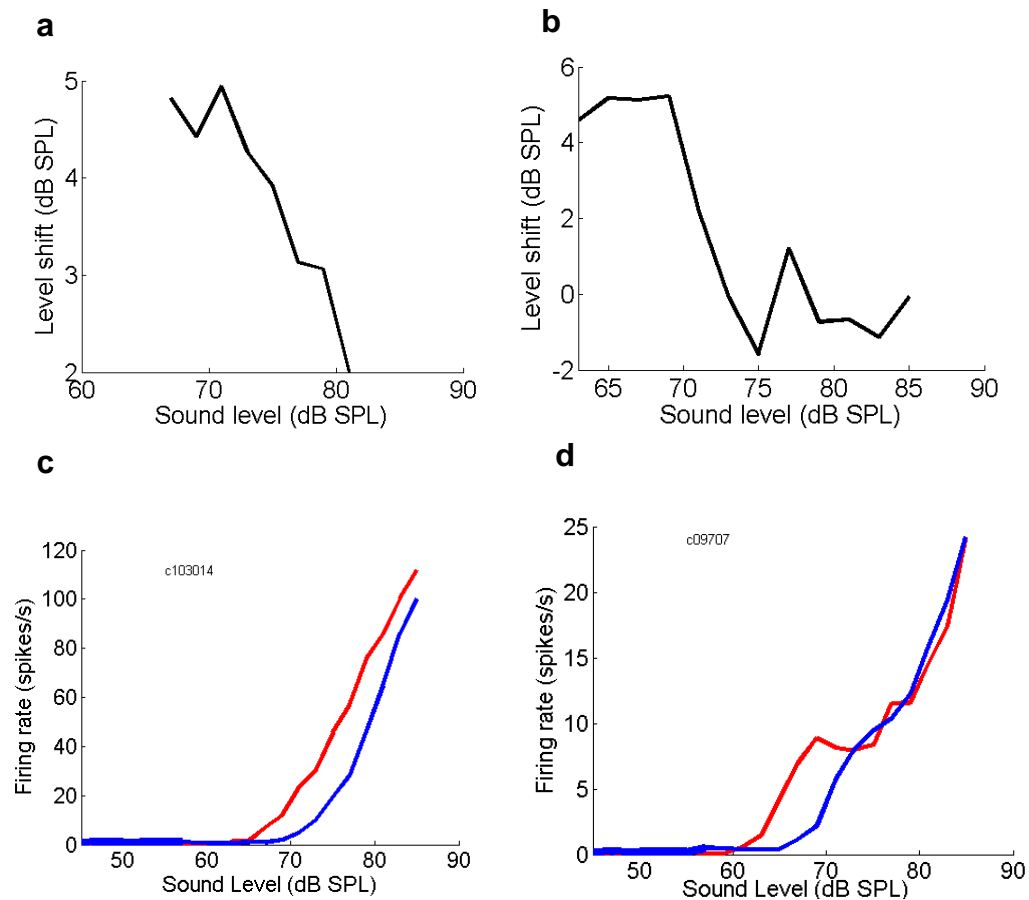


**Figure 4.17 Level shift by level.** a,b. Decreasing functions in individual IC neurons. d, rate-vs.-level-function of neurone in a; d, rate-vs.-level-function of neurone in d. All data from 51dB stimuli.

Are the effects of descending pathways independent of the adaptation state (i.e. whether adapted to 51dB or 75dB stimulus) of the neurone? Comparing the effects of cortical cooling on adapted rate-vs.-level functions visually suggests that descending pathways may exert differential effects on the responses to the two different stimulus distributions. If on the other hand they exert similar effects on the responses at the two stimulus distributions, the mean level shifts associated with cortical cooling at 51dB should be correlated with the shifts at 75dB. Figure 4.18b and c indicate however that there is no correlation of either the mean or

maximum changes comparing the two different distributions ( $R=0.04, p=0.898$  and  $R=0.257, p=0.474$  respectively; corrcoeff covariance test, Matlab, The Mathworks), suggesting that different adaptation states of the neurone are associated with differential effects of the descending pathways.

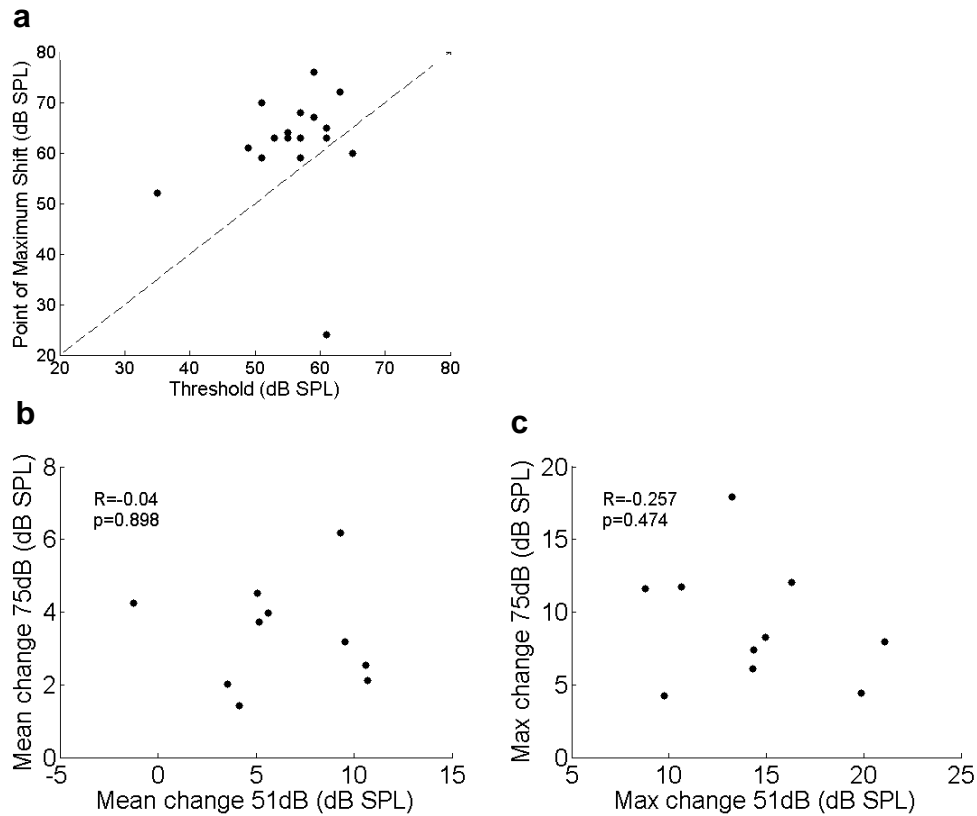


**Figure 4.18 Mean and maximum changes across the population.** a. The sound level associated with the maximum rate-vs.-level function shift is usually greater than the threshold level. b,c. There is no correlation between the two level distributions of either the mean (b) or maximum (c) amount of dB change comparing 'warm' and 'cool' functions.

From these data, it appears that the descending pathways have neurone-specific, level-specific, and adaptation-state specific effects; cooling cortex tends to potentiate the effects observed as a result of adaptation. One important effect of adaptation, not yet examined, is that it is associated with improved coding by the neuronal population around the mean sound level. The penultimate section of this chapter thus asks whether deactivation of the descending pathways also alters

adaptation-associated changes in the accuracy with which neurones code sound level.

#### ***4.9 Coding measures of rate-vs.-level function shift***

It has previously been shown that adjustments of rate-vs.-level functions to sound level distributions improve the coding of those distributions particularly around the mean, both by single neurones and across the population (Dean et al, 2005). Does cortical cooling affect this process of stimulus-driven improvement in sound-level representation? To address this question, Fisher Information (FI), which can be used to measure neuronal coding accuracy, was calculated for single neurones and for the population. In a previous study, Dean et al (2005) found that the peak FI often shifts to lie close to the high-probability region of the relevant stimulus distribution. This study, as in the present case, used more than one stimulus distribution. However, unlike the present study, all distributions in Dean et al. (2005) were presented separately with respect to each other, over blocks of ~5 minutes. The switching paradigm used here, whereby the stimulus distributions are contiguous in time and switch every 5 s, was not employed. A second study by Dean et al (2008) used the switching stimulus employed here, but did not measure FI. Thus an important and unknown question, apart from the effects of the descending pathways, is whether the switching stimulus leads to changes in FI in a manner similar to that reported for a non-switching stimulus (Dean et al 2005).

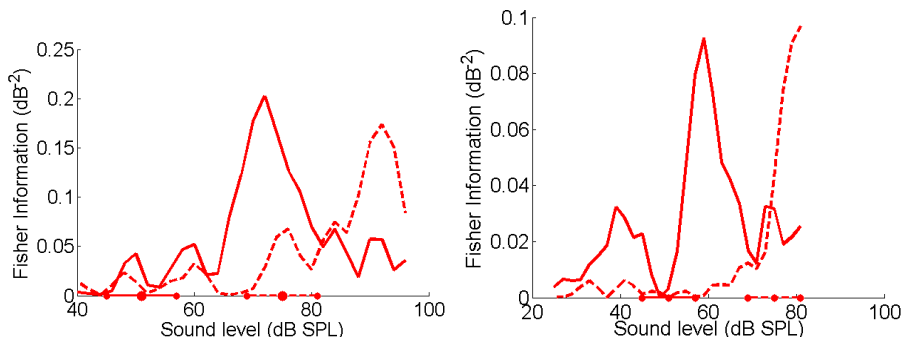


**Figure 4.19 FI and the switching stimulus.** Fisher information plotted against sound level for two IC neurones. Solid lines represent FI corresponding to the 51dB stimulus distribution, whilst dashed lines represent that for the 75dB stimulus distribution. Rate-vs.-level functions shift to the right when mean sound level is increased.

The two neurones in Figure 4.19 show clear alterations in FI, in the expected directions, when their responses adapt to the two sound level distributions. In both cases, the peak of the FI alters to a position louder than the mean sound level. As with the non-switching stimulus employed by Dean et al. (2005), the switching stimulus is associated with changes in sound-level representation leading to alterations in level coding accuracy. Note that in both neurones of Figure 4.19, the maximum FI shifts rightwards when mean sound level is increased; this is consistent with previous findings of improved coding of level around the most commonly occurring sound level associated with adaptation (Dean et al. 2005). Does cortical cooling alter these coding changes?

Figure 4.20*a-c* shows data from three neurones in the warm, cool, and rewarm conditions for the 51dB stimulus. The neurone in the top left panel displays a clear rightward shift in peak FI from ~65dB, during the 51dB stimulus in the warm condition, to ~78dB during the 51dB stimulus in the cool condition. Similar shifts in peak FI are shown for the other two neurones in Figure 4.20 suggesting that for these cells, corticofugal input is important in keeping the most accurately represented level – the peak of the FI – at a lower sound level, i.e. closer to the most commonly occurring levels, than occurs without the input..

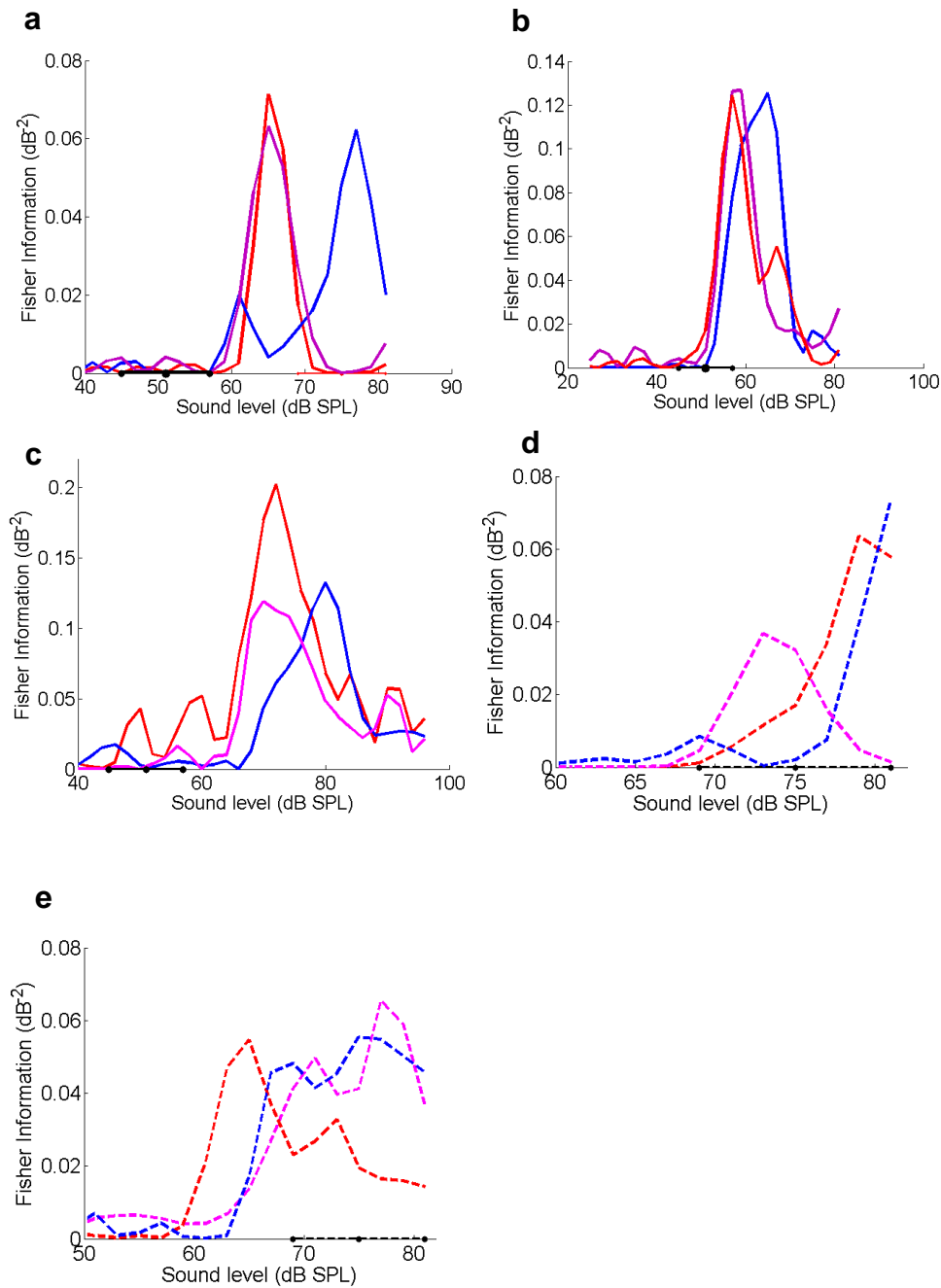


**Figure 4.20 FI of rate-vs.-level functions in single neurones.** a-c. 51dB stimulus. a. Large shift in maximum FI during cooling, with complete recovery during rewarm period. b. Smaller shift, complete recovery. c. Partial recovery. d-e. 75dB stimulus distribution. d. Small shift in maximum FI during cooling, with rebound pattern recovery during rewarm period. e. Small shift, no recovery. Bars on the abscissa represent stimulus high probability range centred at either 51dB (a-c) or 75dB (d-e).

Figure 4.20d-e contains FI plots for the 75dB stimulus. By comparison to Figure 4.20a-c, these plots shift little with cooling. It is likely that, for many of these neurones, a greater shift would be observed if responses had been recorded

at higher sound levels, since often the FI appears not yet to have reached its maximum at the highest sound levels presented (Figure 4.20d).

Not all neurones display shifts in FI. It is therefore important to ask how these changes operate on a population level. Figure 4.21 presents the population FI for the two stimulus distributions. Note that in the warm condition, for the 51dB stimulus distribution, the peak of the population FI lies at the upper edge of the stimulus high-probability region, meaning that coding accuracy increases over most of the high-probability region. By contrast, for the cool condition, the majority of the high-probability region lies under a part of the FI curve that has not yet increased from its lowest values. Again, this points to a cortical role in refining IC coding according to the mean sound level of the stimulus. A similar, but less pronounced, effect is seen for the 75dB stimulus: here, there is a rightward shift when cortex is cooled, but the peak of the function does not clearly shift – it appears that the peak lies beyond the range of sound levels presented, at least for the cool condition.

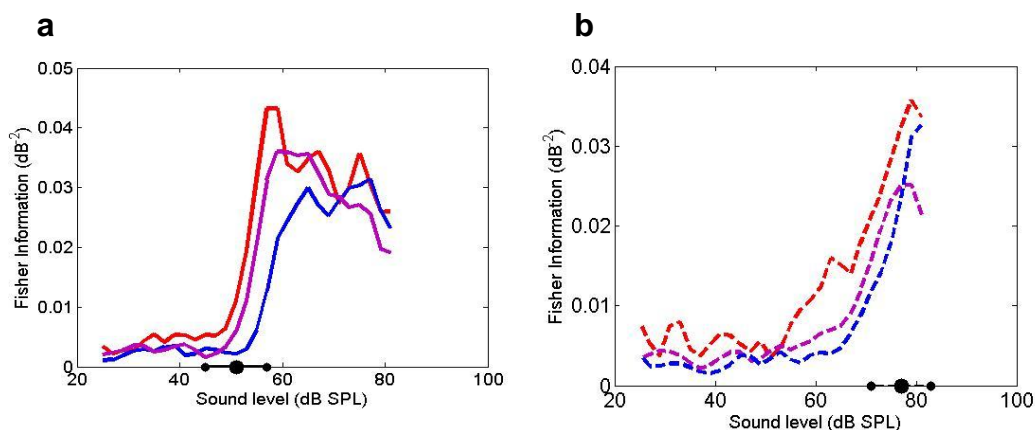


**Figure 4.21 Population FI.** a. 51dB stimulus distribution. b. 75dB stimulus distribution. Note the rightward shift in a, and in particular, the loss of coding over the high-probability region. Red – cortex warm condition; magenta – cortex rewarm condition; blue – cortex cooled condition. Dotted lines: 51dB stimulus; dashed lines: 75dB stimulus.

These FI data support the rate-vs.-level function data in suggesting a role for the descending pathways in improving the effects of adaptation on neuronal

representation of sound level. Compared to when cortex is active, when cortical descending pathways are inactivated, coding accuracy is reduced over the commonly presented sound levels, both for individual neurones and for the population.

#### **4.10 Unilateral cooling**

One question arising from the results presented above is the extent to which bilateral cortical cooling contributed to the shifts in rate-vs.-level functions, and the consequent changes in coding. Would ipsilateral or contralateral cooling alone have produced such results? The results presented below are not intended as a definitive answer to this question, but rather are preliminary data recorded in order to suggest future directions for fruitful investigation.

##### **4.10.1 Contralateral cooling**

Data presented above suggest that there is no effect on rate-vs.-level functions of cooling non-auditory cortex directly overlying IC. Use was made of this finding in the contralateral cooling experiments. Cryoloops were arranged such that one lay over left (contralateral) auditory cortex, and one lay over the cortex overlying the right IC. It was possible thus to record neurones in the warm condition, then, in the cortex overlying IC cooled condition, and then to alter the flow to the AC loop and record the neurone in the contralateral-AC cooled condition. This arrangement permitted a further test of the IC-cooling control, whilst also examining the effect of contralateral cooling. As shown in Figure 4.22, rate-vs.-level functions in these different conditions shifted clearly in 1/3 neurones (4.22*b*), and only in the contralateral-cortex cooled condition. For the other two neurones, 4.22*c* and 4.22*d*, neither cooling over IC, nor over contralateral AC, had any effect on rate-vs.-level functions.

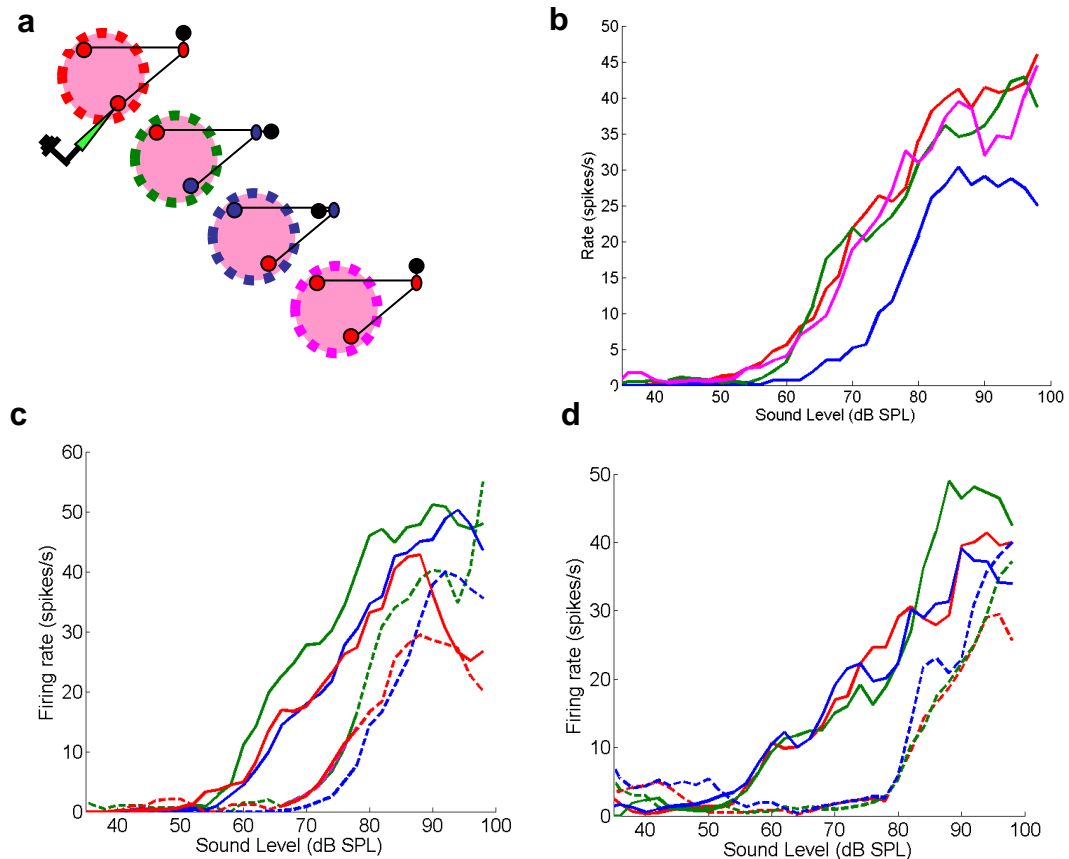


**Figure 4.22 Contralateral AC cooling compared to cooling cortex over IC.** *a.* The four cooling conditions. Large pink circles represent the brain. Dashed circles around the pink circles correspond to colours of relevant warm/cool condition and graphs colours in b-d, i.e. red=no cooling, green=cortex overlying IC cooled, blue=contralateral AC cooling, magenta=recovery. Small filled coloured circles within the brain represent cryoloops in different conditions (red = warm, blue = cool) and in different positions – cortical location represented by upper circle, IC represented by lower circle in each brain. Small black lines represent PTFE tubing carrying coolant. Coloured circle outside the brain represents three-way valve where cryoloop coolant was split into two streams. Black oblong attached to this circle represents position of valve, which when shifted altered the coolant flow to different loops (middle two conditions) or cut off flow altogether (top and bottom condition, warm and rewarm). Of three neurones isolated (b-d), one showed a distinct rightward shift in rate-vs.-level function in response to the 51dB stimulus during contralateral cooling (b). For this neurone, no other conditions lead to changes in rate-vs.-level function. In c, there was no rightward shift in any condition during the 51dB stimulus, but at 75dB only the contralateral IC cooling condition showed an effect – ipsilateral cortex cooling had no effect on rate-vs.-level functions. In d, neither ipsi nor contralateral cooling had an appreciable effect on rate-vs.-level functions at either stimulus distribution.

#### 4.10.2 Ipsilateral cooling

For ipsilateral cooling experiments, loops were placed as for the bilateral experiments, since technical considerations prevented a repeat of the experiments described above for contralateral cooling. This arrangement also permitted

ipsilateral versus contralateral effects to be examined (see below). Results of ipsilateral cooling on three neurones are presented in Figure 4.23. Effects are generally small, and only one of the cells undergoes a rightward shift in rate-vs.-level function (4.23c). Unusually, there is a boosting of spike rate during cooling in the neurone in 4.23d, though no change in threshold is apparent.

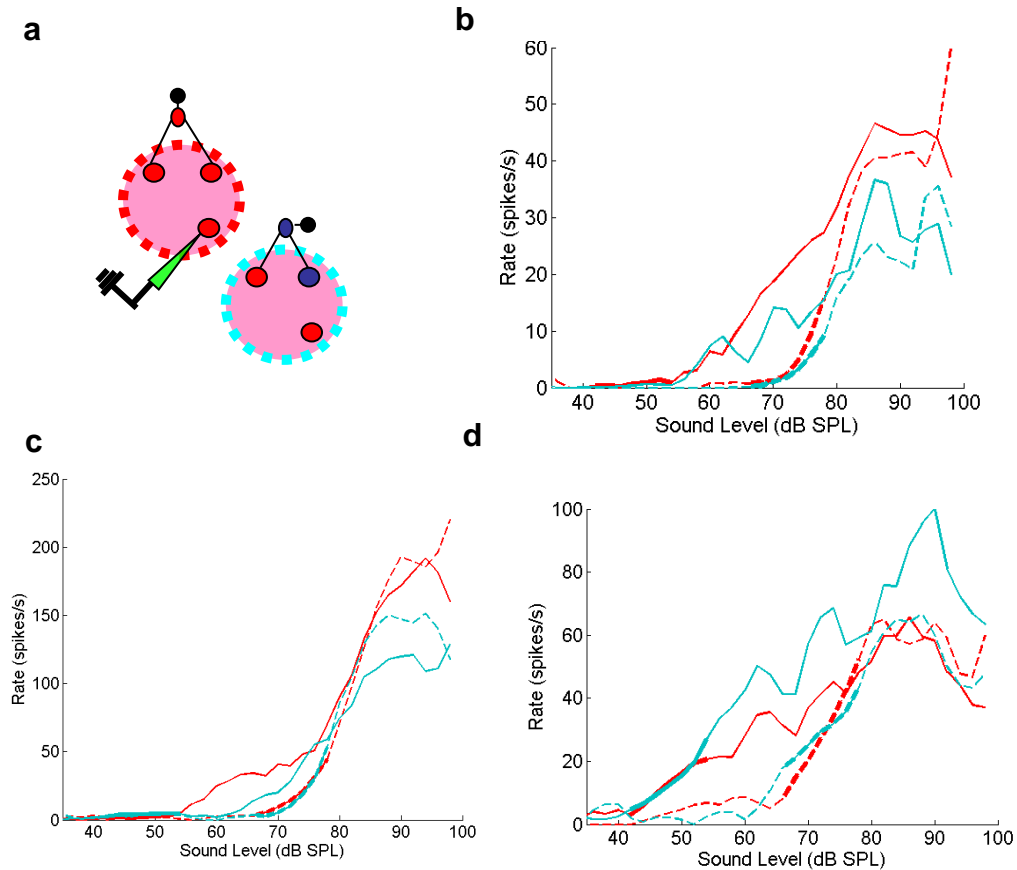


**Figure 4.23 Ipsilateral AC cooling.** **a.** The cryoloop arrangement. Large pink circles represent the brain. Dashed circles around the pink circles correspond to colours of relevant warm/cool conditions and graphs colours in b-d: red=no cooling, light blue=ipsilateral AC cooling only. Smaller filled coloured circles within the brain represent brain locations in different conditions (red = warm, blue = cool). Small black lines represent PTFE tubing carrying coolant to cryoloops. Coloured circle outside the brain represents three-way valve where cryoloop coolant was split into two streams. Black oblong attached to this circle represents position of valve, which when shifted altered the coolant flow to different loops (lower dashed circle in a) or cut off flow (upper dashed circled in a). **b-c.** Rate-vs.-level functions for 3 different neurones. Red=cortex warm condition, light blue = ipsilateral auditory cortex cool condition, contralateral cortex warm condition. Solid lines = 51dB stimulus; dashed lines = 75dB stimulus. **b.** For this neurone, there is a decrease in spike rate, but no change in threshold during cortical cooling during both 51dB and 75dB stimuli. **c.** For the neurone in c, there is a rightward shift in the 51dB rate-vs.-level function during ipsilateral cortical cooling. **d.** For this neurone, whilst there is no change in threshold, there is an increased spike rate at most sound levels during cooling.

### **4.10.3 *Ipsi- and contralateral cooling comparisons***

The bilateral placement of cryoloops, one on each AC, allowed recording of IC neurones during ipsilateral and contralateral inactivation. The ideal experiment would be to randomise ipsi-, contra-, and bilateral conditions and repeat all three, with periods of recovery in between, for each neurone. However, this would take a prohibitively long time. As a compromise, I chose the sequence ipsi-, then rewarm, then contra, then rewarm. It was thus possible to examine two out of the three cooling configurations, as shown in Figure 4.24. These data appear to suggest that ipsilateral cooling exerts less effect than contralateral cooling in the neurones recorded: in each case, contralateral cooling results in a large decrease in spike rate. However, a major caveat here is that the conditions were not randomised, so that the effects may be attributed to length of time of cooling rather than the particular condition.

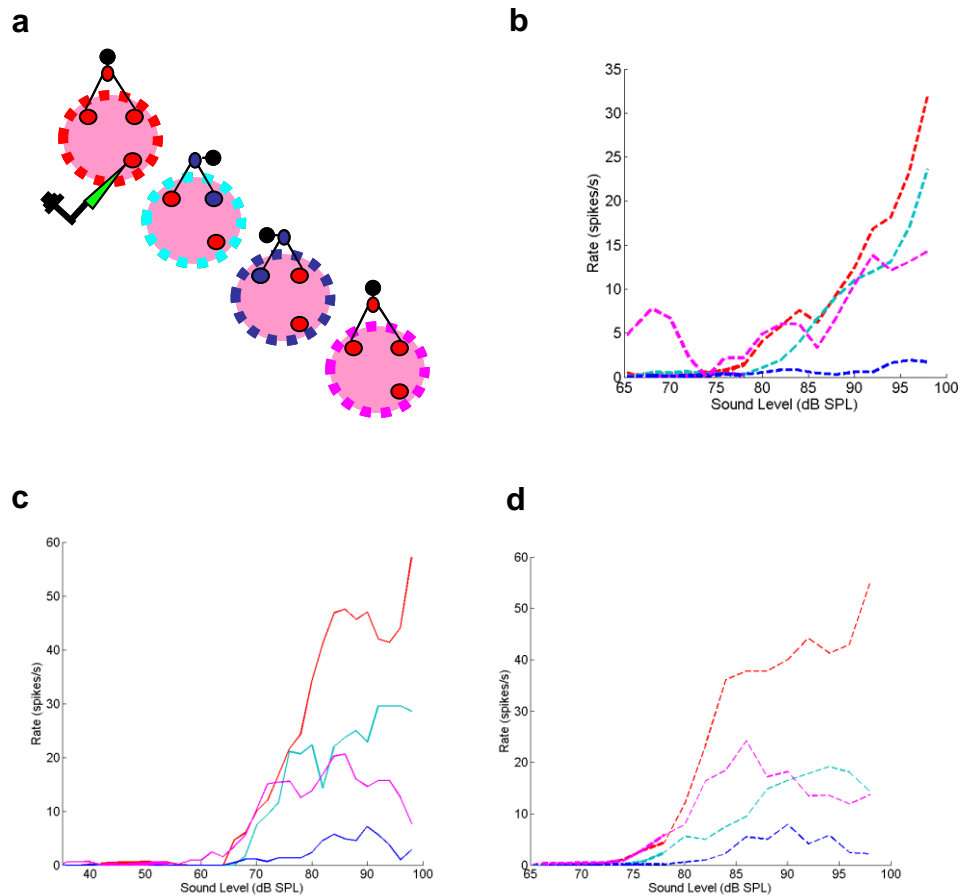


**Figure 4.24 Ipsi- and contralateral AC cooling.** a. The cryoloop arrangement. Large pink circles represent the brain. Dashed circles around the pink circles correspond to colours of relevant warm/cool conditions and graphs colours in b-d: red=no cooling, light blue=ipsilateral AC cooling only, dark blue=contralateral AC cooling only, magenta=rewarm. Smaller filled coloured circles within the brain represent brain locations in different conditions (red = warm, blue = cool). Small black lines represent PTFE tubing carrying coolant to cryoloops. Coloured circle outside the brain represents three-way valve where cryoloop coolant was split into two streams. Black oblong attached to this circle represents position of valve, which when shifted altered the coolant flow to different loops. b-c. Rate-vs-level functions for 3 different neurones. Red=cortex warm condition, light blue=ipsilateral auditory cortex cool condition, contralateral cortex warm condition, dark blue, contralateral auditory cortex cool, ipsilateral auditory cortex warm condition. Solid lines = 51dB stimulus; dashed lines = 75dB stimulus. b. 75dB stimulus, striking shift and flattening of rate-vs-level function during contralateral cooling only, with little change during ipsilateral cooling. c and d show less dramatic, but still obvious, examples of the same effect, where contralateral cooling has more effect than ipsilateral cooling on both 51dB stimulus responses (c) and 75dB responses (d).

#### 4.11 Summary

Rate-vs.-level functions were examined in response to two stimulus distributions, across three cooling conditions. The primary finding was that bilateral cortical

cooling evokes clear changes in rate-vs.-level functions, which may be interpreted as potentiating the changes occurring during adaptation. Closer analysis of these changes suggests that cortical inactivation results in changes in sound level representation that are dependent on the sound level itself, on the individual neurone, on the adaptation state of the neurone, and the particular side of the cortex that is inactivated. The changes in rate-vs.-level function I observe also have implications for neuronal coding of sound level. In individual cells, the peak Fisher Information shifts to lie further away from the mean sound level when cortex is cooled. Across the population, too, for the 51dB stimulus distribution, the boost in coding accuracy adaptation confers over the highly probable levels is diminished when cortex is cooled. Cortex, according to these results, is an important contributor to the usefulness of adaptation to sound level statistics in the midbrain. Preliminary results concerning the laterality of cortical effects cannot yet be interpreted, but suggest that further investigations comparing differential ipsi and contralateral AC contributions to the effects observed would be of interest.

# 5

## COOLING EFFECTS ON ADAPTATION TIME COURSE

---

### **5.1 Introduction**

This chapter unites the two main themes of this thesis, examining first the time course of adaptation in the IC, and then the effects of cortical inactivation upon it. Knowledge of the time course of adaptation, in the absence of any cortical manipulation, is important for understanding potential roles and mechanisms of adaptation. These time course data, with cortex active, were collected and analysed prior to the cryoloop experiments, in a collaboration between the current author and Dr. Isabel Dean, and have in part been published previously (Dean et al. 2008). These data are presented below. The major finding of these studies is that adaptation in the IC is relatively rapid, with an average decay time-constant of 159.7ms. This chapter then goes on to examine the effects of cortical cooling on the magnitude and time course of adaptation in IC neurones. Cooling cortex does alter adaptation responses to the switching stimulus, decreasing spike-rates across the population in the cooled condition. Cooling cortex was associated with alterations of the time course of adaptation in individual neurones, increasing the speed in some cells and decreasing the speed in others. Across the population

recorded, overall there was a significant decrease in the rapidity of adaptation during cortical cooling.

## **5.2 Stimuli and recordings**

Two sets of experiments were performed. In the first, responses were recorded from 45 inferior colliculus (IC) neurones in 18 guinea pigs, to approximately 10 minutes of diotic, broadband noise. In the second, the same stimulus was presented with the cryoloop *in situ*, and was repeated prior to cooling, during cooling, and following recovery from cooling, or was presented continuously for ~1 hour in total during which conditions were varied. For these experiments, 94 neurones, from 27 guinea pigs, were isolated and 20 of these neurones were used for analysis of the time course discussed below. Others were not included because the adaptation time course in the rewarm condition was significantly different from the time course in the warm condition, suggesting that factors other than the direct effect of cortical cooling might have been responsible, in these excluded neurones, for any changes observed during cortical cooling.

## **5.3 Time course without cortical cooling**

### **5.3.1 Rapid, asymmetrical adaptation**

Earlier work employed a stimulus that allowed only a low-resolution measure of the adaptation time course (Dean *et al.*, 2005). Do IC neurones adapt to sound level statistics rapidly, over a faster time scale than could previously be assessed? Here, by switching repeatedly between sound level distributions, I was able to assess in detail the time course over which neuronal responses adapt from one level distribution to another. I was able also to assess the extent to which this time course was affected by cortical inactivation.

Similarly to experiments described in previous chapters, here I recorded neural responses to a ‘switching’ stimulus consisting of continuous broadband noise whose sound level was selected every 50s from one of two underlying sound level probability distributions. Every 5 s, this distribution ‘switched’ between a distribution centred on 51dB and a distribution centred on 75dB. Adaptation of the neuronal response over the 5s half-period (Figure 5.1a) was apparent when the firing rate of each neurone was averaged over multiple cycles of the switching stimulus (Figure 5.1b, 5.3a-c). Upon switching to the 75dB stimulus, firing rate increased sharply, and then gradually decreased to reach an approximately steady-state for the remainder of the 75dB stimulus. Switching to the 51dB stimulus usually elicited a sudden reduction in firing rate; in some cases, the rate partially recovered to reach a steady-state during the course of the 51dB stimulus. Only 1 of the 45 neurones recorded in the time course experiments, and none of the 94 recorded for the cryoloop experiments, showed neither of these adaptive effects; this one neurone showed a sharp increase in firing rate following the switch to the 75dB stimulus, and a sharp decrease after switching to the 51dB stimulus, but no adaptation of firing rate during either 5s half-period (data not shown; see Chapter 2). Across all adapting neurones, the adaptation occurring during the 75dB stimulus led to a mean reduction in firing rate of  $58\pm 17\%$  (mean $\pm$ SD, n=44 neurones; firing rate in first 50ms of 75dB half-period compared to that in final 1s).

In order to quantify the time course of adaptation, I fit single exponentials to the mean firing rate following the switch between sound level distributions (Fig. 5.1b, c). For the 75dB stimulus, the fit was significant for 98% (44/45) of neurones (see Chapter 3). The median time constant of adaptation to the 75dB stimulus across these adapting neurones was 159.7ms (25-75% quartiles 73.7-

203.9ms, n=44). The time constant of adaptation during the 75dB stimulus was negatively correlated with the depth of adaptation (Spearman's rank correlation coefficient  $r_s = -0.48$ ,  $p = 0.001$ ;  $n = 44$ ), indicating that rapidly-adapting neurones underwent larger changes in their firing rates than more slowly-adapting neurones.

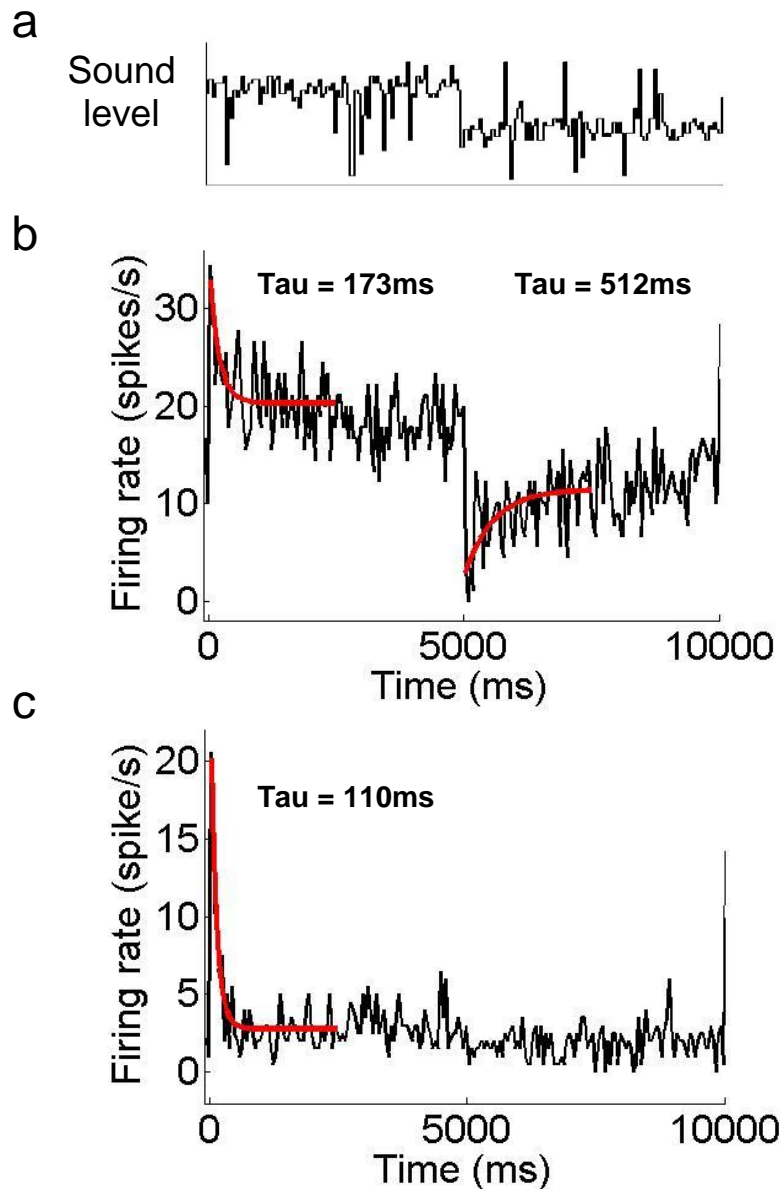


**Figure 5.1 Time course of adaptation of mean firing rates during the adaptation switching stimulus.** a. representation of sound levels over one switch period: 75dB stimulus distribution switched to the 51dB stimulus distribution after 5 s. b, c. mean firing rate against time, averaged over many cycles of the switching stimulus indicated in a, for two neurones. The red curves show single exponential fits to firing rate after switch in sound level distribution; time constants are shown.

Adaptation of mean firing rate to the 51dB stimulus is evident in Figure 5.1b, although many neurones did not show obvious adaptation of mean firing rates following the switch to this stimulus (Fig. 5.1c). Rate-vs.-level functions for such neurones, however, did adapt to the 51dB stimulus. This apparent paradox was expected, since one effect of the adaptation is to shift the neuronal threshold towards the most commonly-occurring levels, and, therefore, sound levels within the high-probability region of the 51dB stimulus usually lay at or below threshold in both states of adaptation. Thus, both immediately after the switch to this stimulus, and a few seconds later, the most probable levels evoked few spikes. This results in little change in average rate over time, despite the adjustment of the rate-vs.-level function over less probable levels, because the average rate is dominated by the responses to the most commonly-occurring levels. Single exponentials could be fit to mean firing rates for 12/45 neurones during the 51dB half-period. The median time constant of adaptation to the 51dB stimulus was 331.8ms (25-75% quartiles 187.3-523.1ms, n=12). There was an asymmetry in the time course of adaptation between the two sound level distributions: adaptation to the 51dB stimulus was significantly slower than that to the 75dB stimulus ( $p < 0.01$ , paired t-test; mean increase in time constant 88%; Fig. 5.2).

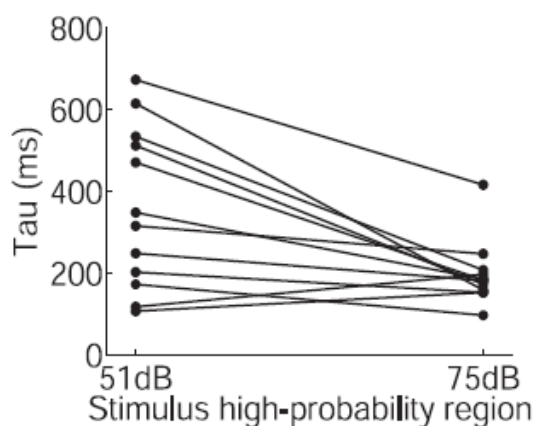


**Figure 5.2** Time course of adaptation to the 51dB and 75dB stimulus distributions.

### **5.3.2 The time course of adaptation and stimulus time scales**

The results above indicate that adaptation time course differs between the two directions of change in mean level. In order to examine whether adaptation time course also depends on time scales within the stimulus, the period of the switch between sound level distributions was varied between 5 and 20 s. This did not significantly alter the time course of adaptation to the 75dB stimulus across the population of neurones tested (two-way ANOVA,  $p < 0.0005$  for effect of neurone,  $p = 0.2$  for effect of switch period;  $n = 16$  neurones). Further, varying the length of time sound remained at any given level (the 'epoch'), between 25 and 200ms, also had no effect on adaptation time course across the neuronal population (two-way ANOVA,  $p < 0.005$  for effect of neurone,  $p = 0.1$  for effect of epoch;  $n = 14$  neurones). These results indicate that the time course of adaptation to the sound level statistics of the stimulus is not dependent on the two time-scales within it.

## **5.4 Time course of adaptation during cortical cooling**

### **5.4.1 Adaptation of mean spike rates**

Is the time course described above affected by cortical cooling? I addressed this question by presenting the switching stimulus before, during, and after cortical cooling whilst recording in IC. In the 'warm' condition, the adaptation profile of neurones was similar to that described above. As expected, upon switching to the 75dB stimulus, neurones' firing rates increased sharply and then gradually decreased to reach an approximately steady state; switching to the 51dB stimulus tended to elicit a sudden reduction in firing rate. Cortical cooling, in some neurones, had little effect on this adaptation pattern overall, but was associated with a small change in firing rate. For other neurones, cooling was associated with

larger reductions in spike rate, and for these neurones little firing-rate adaptation was apparent during either the 51dB or the 75dB stimulus distribution (Figure 5.3d). Across the population, removing bilateral cortical input appears to decrease firing rate during the adaptation stimulus, for both distributions (n=20; see Table 5.1). Note that the low firing rates reflect the nature of the stimulus: the firing rates are dominated by responses to the most commonly occurring levels, i.e. the high probability region; since rate-vs.-level functions adapt such that part or all of the high probability region lies at, or below, threshold, spike rates are necessarily low, and drop further during cortical cooling, usually resulting in a greater proportion of the high probability region lying below threshold, as the rate-vs.-level functions shift further to the right.

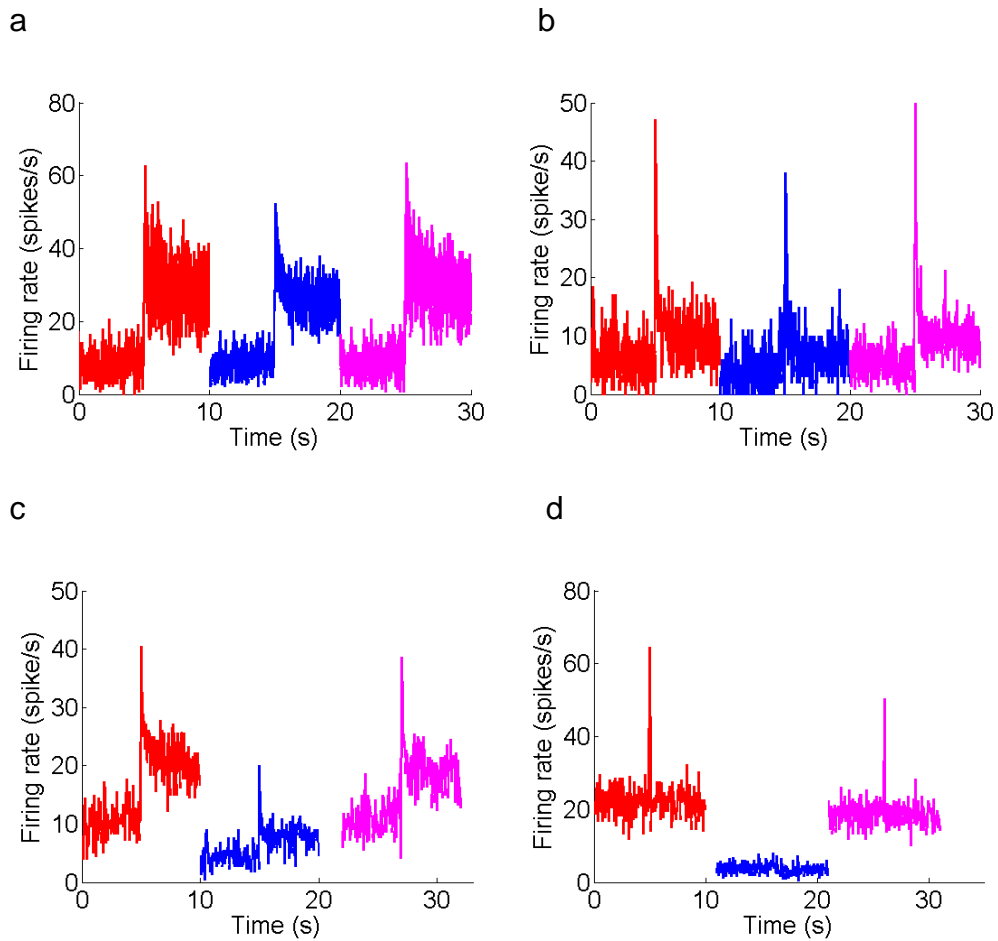


**Figure 5.3 Adaptation to the 51dB and 75dB stimulus distributions across cooling conditions.** Four different neurones shown. Red: warm; Blue: cool; Magenta: rewarm. Time axis does not reflect actual experimental protocol but rather shows responses averaged across switch-periods, and separated by cryolop condition. Thus 3 10s PSTHs are shown for each neuron, corresponding to the three stimulus conditions. Firing rates over the course of the adaptation stimulus changed little during cooling (a), moderately (b and c), or in some cases were completely inhibited (d).

Initial rate	WARM		COOL		REWARM	
	51	75	51	75	51	75
Mean	6.11	34.68	2.15	21.63	5.77	34.62
STD	7.724	27.459	2.429	23.265	6.2614	24.735
p-value vs. cool (vs. rewarm)	0.0223 (0.5821)	0.0021 (0.9839)			0.0070	0.0030

Adapted rate	WARM		COOL		REWARM	
	51	75	51	75	51	75
Mean	6.9777	13.8512	3.8714	8.2743	5.9822	13.8378
STD	6.9162	12.5888	3.2968	9.5441	5.4228	13.4063
p-value vs. cool (vs. rewarm)	0.0325 (0.3178)	0.0010 (0.9916)			0.0413	0.0076

% Adaptation	WARM		COOL		REWARM	
	51	75	51	75	51	75
% Adaptation of firing rates averaged across population	114.2	60.1	180	61.7	103.7	60.0
STD	99.599	16.3876	100.3204	17.3799	186.1503	19.5068
p-value vs. cool (vs. rewarm)	0.1495 (0.5208)	0.5089 (0.5708)			0.9708	0.6490

**Table 5.1 Initial and adapted firing rates following switches to the 51dB and 75dB stimulus distributions, across cooling conditions.**

Across all recovered neurones, adaptation occurring during the 75dB stimulus in the warm condition led to a mean reduction in firing rate of 60.1%±16% (mean±SD, n=20 neurones; firing rate over first 100ms of 75dB half-period compared with that in final 1s). This is similar to that measured in experiments prior to the cryoloop being employed (n=44; mean=58%±17%), suggesting that the population used for the cryoloop analysis is characteristic of the IC in general. It also implies that the methodological differences between these experiments, including cortical craniotomies and placement of cryoloops in the cooling experiments, did not affect the magnitude of adaptation.

Paired t-tests were used to compare ‘warm’ *versus* ‘cool’ conditions, both for initial and steady-state firing rates following a switch to a different distribution. The initial firing rate was defined as the rate over the first two time bins, i.e. 100ms, after a switch to the 75dB stimulus, averaged across switches. Steady-state firing rate was defined as the average rate in the last 1s of the stimulus. The majority (16/20) of neurones underwent a significant reduction in initial spike rate during cooling, 2/20 a significant increase, and 2/20 displayed no change. This contrasts with the steady state firing rate, for which 9/20 neurones displayed a decreased firing rate in the ‘cool’ versus the ‘warm’ condition, 6/20 no change, and 5/20 a significantly greater response. Note that the initial firing rate does not correspond to an onset firing rate, usually defined as the initial response to sounds from silence, but rather reflects the initial response to a new stimulus distribution after a switch from a previous distribution.

Changes in firing rate were averaged across the population to assess the effects of cortical cooling. As shown in Table 5.1 and Figure 5.4, firing rates immediately following a switch, across the population, for both 51dB and 75dB stimuli, are significantly reduced in the ‘cool’ condition compared to the ‘warm’ (51dB:  $p=0.022$ ; 75dB:  $p=0.0021$ ) and ‘rewarm’ conditions ( $p=0.0070$  and  $0.0030$ ) but are not significantly different comparing the ‘warm’ and ‘rewarm’ conditions. The same pattern of change is observed across steady-state spike rates. However, the amount of spike-rate adaptation, i.e. the adapted firing rate, relative to the initial rate, over the course of the 75dB stimulus, is similar across conditions, with response reductions (mean $\pm$ STD) of  $60\% \pm 16\%$  (warm),  $61.7\% \pm 17\%$  (cool), and  $60.1\% \pm 19\%$  (rewarm). These response reductions across three conditions were not significantly different from one another.

As expected from data presented in section 5.3.1 above, there was a tendency for firing rates to increase over the course of the 51dB stimulus. Even though, following a switch to the 51dB stimulus, a mean change of 114% and 180% was observed for the warm and cool conditions respectively, large standard errors resulted in a lack of significant difference between these conditions for this change. In summary, cortical inactivation consistently led to a reduction in overall firing rate, but was associated with preserved adaptation depth relative to these rates: adaptation continues to operate both with cortex active and with cortex inactive.

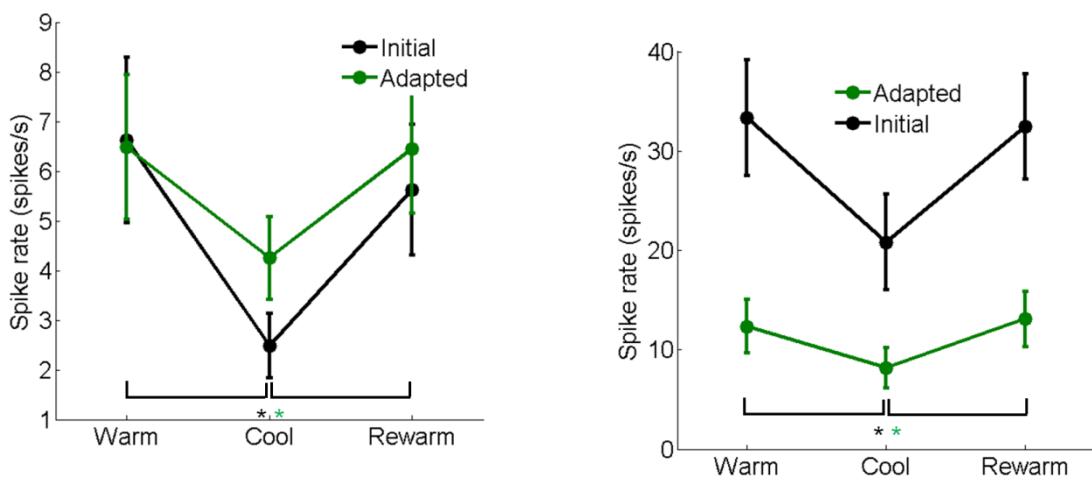


**Figure 5.4 Changes in firing rates across population for 51dB (left) and 75dB (right) stimulus distributions.** Stars denote significant differences between warm/rewarm and cool conditions. The colour of the star indicates initial firing rates or adapted rates.

#### **5.4.2 Time constants of adaptation during cortical cooling**

Single exponential time constants were fit to firing rates as described in Section 5.2. Examples of tau (time constant) fits in warm and cool conditions are shown in Figure 5.5a-c. 19/20 fits were significant in the warm condition; 14/20 were

significant for the cool condition. This difference likely reflects a decline in the responses of some neurones in the cooled condition, which, as for the example neurone shown in Figure 5.3*d*, led to a loss of the characteristic sharp increase, and subsequent decrease, of firing rates following a switch to the 75dB stimulus. Only these 14 neurones are subsequently analysed. With regards to the 51dB stimulus, there were no significant fits in the cool condition, reflecting the greater rightward shift in rate-vs.-level function associated with cooling.

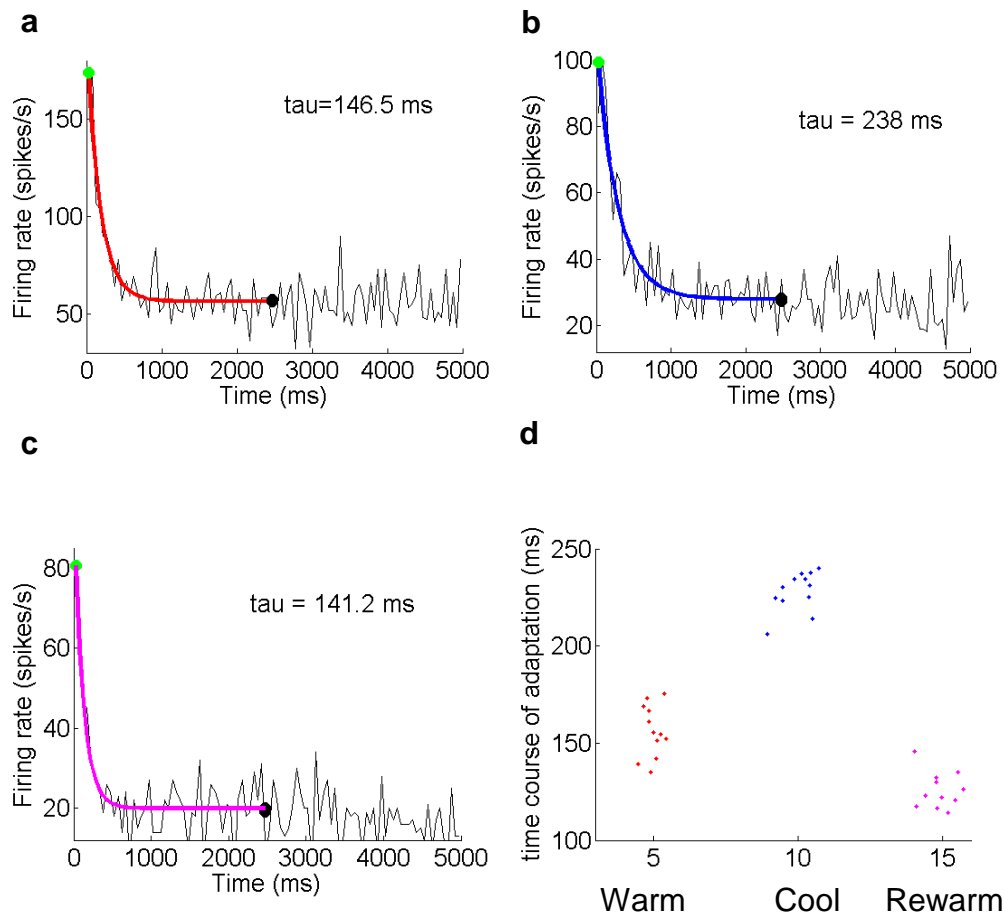


**Figure 5.5 Time constants fit to average firing rates following switch to 75dB.** a-c, average firing rates plotted in black, with the single exponential fit overlain in red (a, warm), blue (b, cool) or magenta (c, rewarm), and the tau value for the condition displayed. In d, each dot represents a time-constant derived from a randomly selected subset of 2/3 of switch half-periods. For ease of visualisation, these values are plotted against the mean of the half-period numbers selected, to separate the points within conditions, and, to separate the conditions, an arbitrary value was added for each condition. In this neuron, time constants were significantly greater in the cool condition compare to the warm and rewarm conditions. In some neurones, this pattern was reversed, and the time constant was less in the cool condition. For this neuron, the rewarm condition appeared to ‘overshoot’ in recovery: time constants become lower, and the time course therefore faster, in the rewarm compared to the warm condition. In 5.5d the variation in x-axis position of the dots within conditions reflects the mean value of the particular repeats chosen for the analysis, for ease of visualisation.

Figure 5.6 presents time-constants across conditions for the neural population, both in absolute terms (5.8a) and in terms of percentage change from the ‘warm’ condition for each neurone (5.8b). The time course of adaptation displays a wide degree of variation with respect to changes during cooling. The greatest change

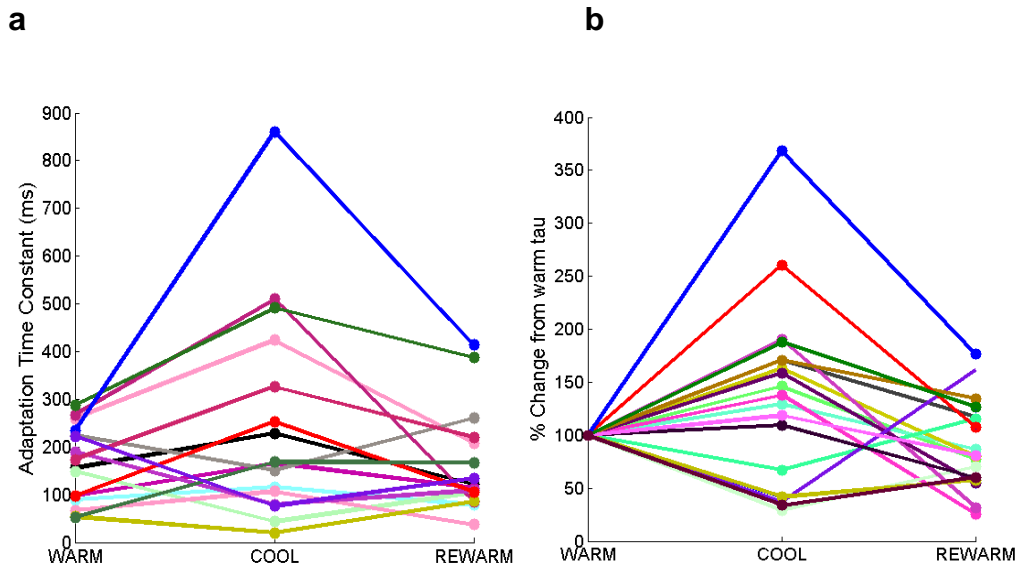
resulted in almost a four-fold increase of the tau, from 233ms to 860ms in one neurone. These data reflect the tendency for tau values to increase with cooling.

Figure 5.6 also shows that time-constants in the cooled condition, across the population, occupied a greater spread of values, consistent with the two-sample F-test result for variance (see above).

Time constants were fit to firing rates averaged from multiple switch half-periods. To determine whether the time-constants changed significantly in different cooling conditions for individual neurones, twelve time-constants were generated for each neurone, by selecting, at random, twelve different subsets of 2/3 of the switch half-periods from which to average time-constants (jackknife resampling; Figure 5.5*d*). By this method a significant increase in tau with cooling was found for 9/14 neurones, a significant decrease in time-constant for 3/14 neurones, and no significant change for 2/14 neurones.

	Mean (ms)	Std (ms)	p-value compared to warm	p-value compared to cool
Warm	157.1300	77.942	NaN	0.009
Cool	326.48	261.44	0.009	NaN
Rewarm	176.62	119.85	0.665	0.028

**Table 5.2 Time constants of adaptation following a switch to the 75dB stimulus, across cooling conditions; n= 14 neurones.**



**Figure 5.6 Changes in time-constant following switches to the 75dB stimulus in warm, cool, and rewarm conditions.** a, adaptation time constants across conditions; b, the same time constants replotted relative to the warm time constant in each neurone.

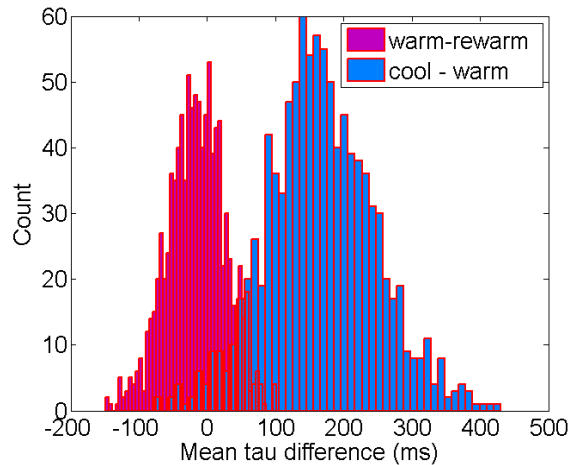


**Figure 5.7 Time constants of adaptation following a switch to the 75dB stimulus.** Tau values were calculated for individual neurones by selecting a different 2/3 subset of switch periods many times (bootstrap method). Individual neurone warm taus were subtracted from the cool tau of that neurone for each particular 2/3 subset. The figure displays a histogram of tau values resulting from these multiple samples, for all neurones in the population. For the distribution in red, rewarm taus were subtracted from warm taus. Note that the distribution's mean is just below 0, suggesting that warm and rewarm conditions are associated with similar values of time constant. For the distribution in blue, warm taus were subtracted from cool taus. Here, the mean of the distribution is 180ms, suggesting that across the population cooling is associated with a 180ms increase in time constant.

To test whether changes in tau were significantly different across conditions, a bootstrap resampling with replacement was applied to the data to create distributions of values for comparison. Figure 5.7 shows the resulting values. The blue histogram reflects the ‘cool’ tau values minus the ‘warm’ tau values. The centre of this distribution is around 180ms, and this therefore is the mean increase in adaptation time constant that resulted from cortical deactivation – an increase of greater than 200% compared to the ‘warm’ population tau value (see Table 5.2). The time constant values in the ‘cool’ condition were significantly greater than those in the ‘warm’ condition ( $p=0.009$ ; paired t-test). Similarly, ‘rewarm’ taus were smaller than ‘cool’ taus ( $p=0.028$ ). However, ‘warm’ and ‘rewarm’ taus were not significantly different from one another when analysed by the bootstrap method (paired t-test;  $p=0.665$ ). A 2-sample right-tailed F-test (cool vs. warm taus) for variance was highly significant: taus in the cool condition have a greater variance than in the warm condition ( $p<0.005$ ).

The time constant of adaptation during the 75dB stimulus was not negatively correlated with the depth of adaptation in the ‘warm’ condition (Spearman’s rank correlation coefficient  $r_s = -0.3196$ ,  $p = 0.281$ ;  $n = 14$ ), suggesting, perhaps, that more data is required for this correlation to reach significance (it was found to be significant in the experiments prior to those using the cryoloop; see section 5.3 and discussion). Interestingly, this correlation did become significant for the population when cortex was cooled (Spearman’s rank correlation coefficient  $r_s = -0.6386$ ,  $p = 0.0188$ ;  $n = 14$ ; Figure 5.8), but again this correlation dropped below significance in the rewarm condition (Spearman’s rank correlation coefficient  $r_s = -0.4339$ ,  $p=0.0931$ ).

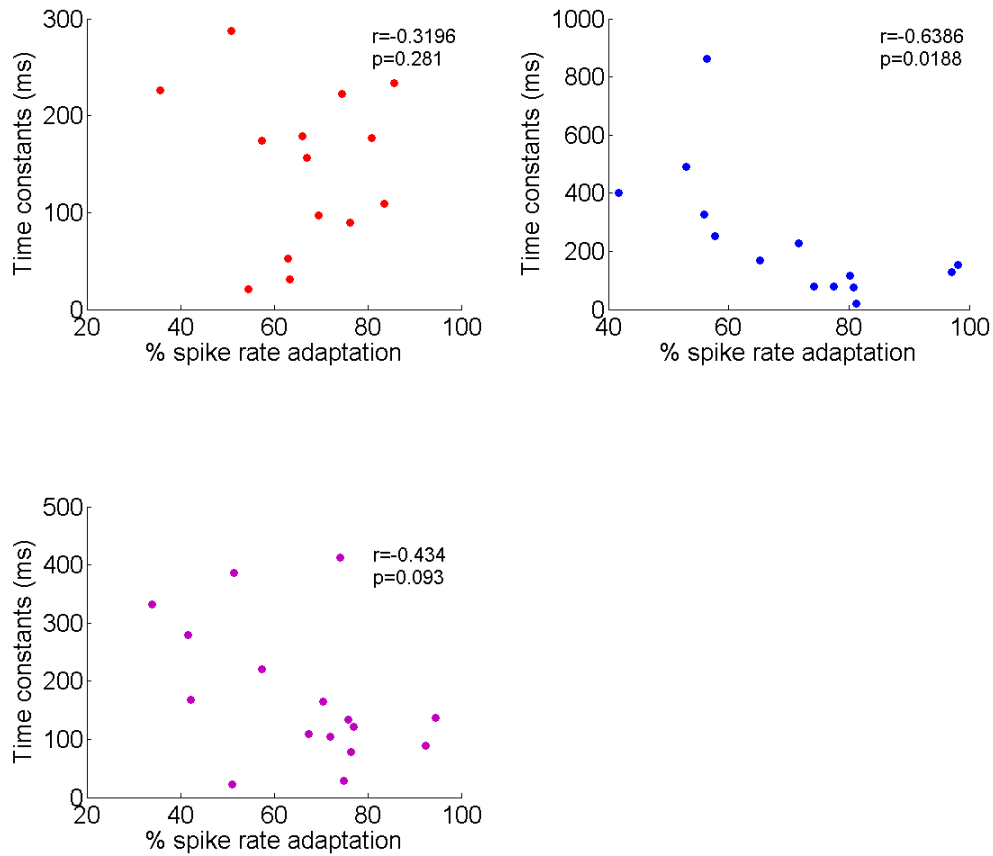


**Figure 5.8 Time constants and spike rate adaptation across conditions.** Red, blue, magenta=warm, cool, rewarm, conditions. Correlation coefficients and p-values shown. Time-constants were negatively correlated with depth of adaptation in the cool condition only.

It was possible, for a few neurones in which the adaptation stimulus was presented continuously and spike-rate variability was low, to assess the change in time-constants by sampling the data in overlapping windows during the stimulus as conditions changed. This was achieved by taking moving windows of blocks of switch-periods and calculating the time-constant values for each window, then shifting the window one switch period. Data from two neurones are shown in Figure 5.9.

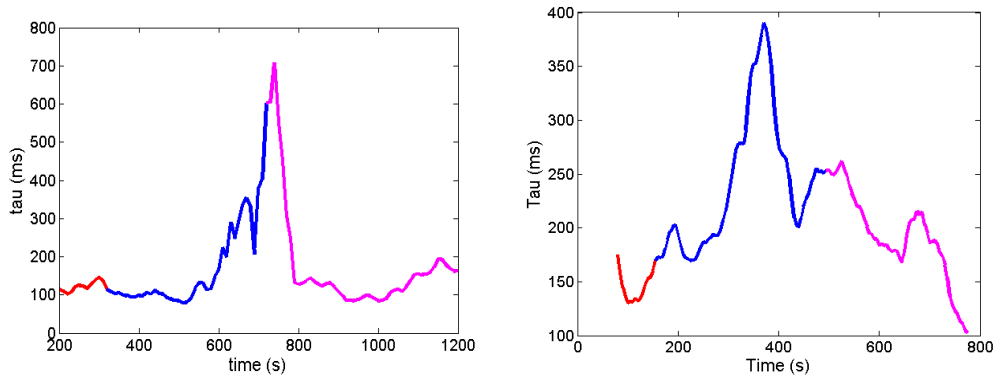


**Figure 5.9 Adaptation speed ( $\tau$ ) alterations over the course of the cooling cycle, for two neurones. Time constants averaged over 16 switch periods**

For the neurone on the left, the  $\tau$  value appears to follow the course of the cooling and warming cycles, increasing during cooling and decreasing during rewarming. However, the  $\tau$  of the neurone on the right reaches a peak and declines during cooling, suggesting that another process governs the changes in time constant in addition to cortical cooling.

A final observation concerns an apparent correlation between the magnitude of the ‘warm’  $\tau$ , and the magnitude of the change in  $\tau$  on cooling. This relationship is only apparent when correlating the absolute change, irrespective of its sign. As Figure 5.11 indicates, it appears that the greater the ‘warm’  $\tau$ , the greater the absolute magnitude of change likely to occur during cooling.

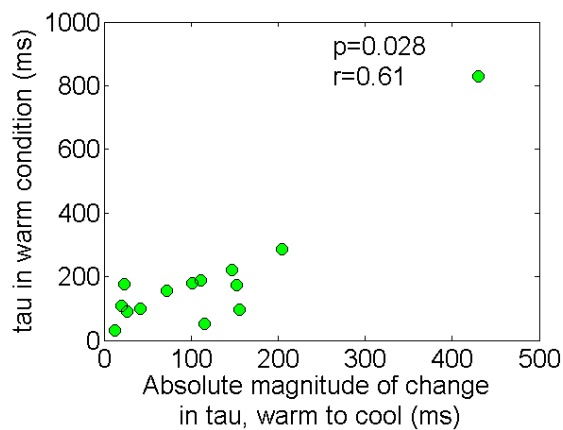


**Figure 5.10 Correlation between time-constants in warm condition and magnitude of change in time constant between warm and cool conditions.**

### **5.4.3 Adjustments of rate-vs.-level functions over time**

How does adaptation of a neurone's mean firing rate over time correspond to the time course of changes in its representation of sound level, i.e. its input-output function? To examine this, rate-vs.-level functions were constructed from responses during successive, 300ms-duration intervals following the switch between sound-level distributions. By comparing these 300ms rate-vs.-level functions to the functions constructed from responses immediately preceding the switch (calculated over the final 3s of each stimulus), the transformation in the representation of sound level could be visualised as adaptation proceeded (Fig. 5.11). In a 10 minute recording, over the first 300ms there were approximately 40 repeats of every sound level in the high probability region, but only 3 repeats in the low probability regions. Thus, accurate construction of rate-vs.-level functions over 300ms intervals could only be performed for sound levels drawn from the high-probability region of each stimulus, except for a few neurones with low intrinsic spiking variability and long recording durations. The time course of adaptation of mean firing rate was reflected in the evolution of rate-vs.-level functions over successive 300ms intervals. Figure 5.11 illustrates that neuronal rate-vs.-level functions reached their final form rapidly following the switch to the 75dB stimulus. The time constants of the change in mean firing rate for the neurones in Figures 5.11*a, b, c* and *d* were 20.6ms, 152.4ms, 224.4ms and 152.0ms respectively and their rate-vs.-level functions had completely (Fig. 5.11*a*) or largely (Fig. 5.11*b,d*) reached their final form by the end of the second interval (i.e. within 600ms of the switch).

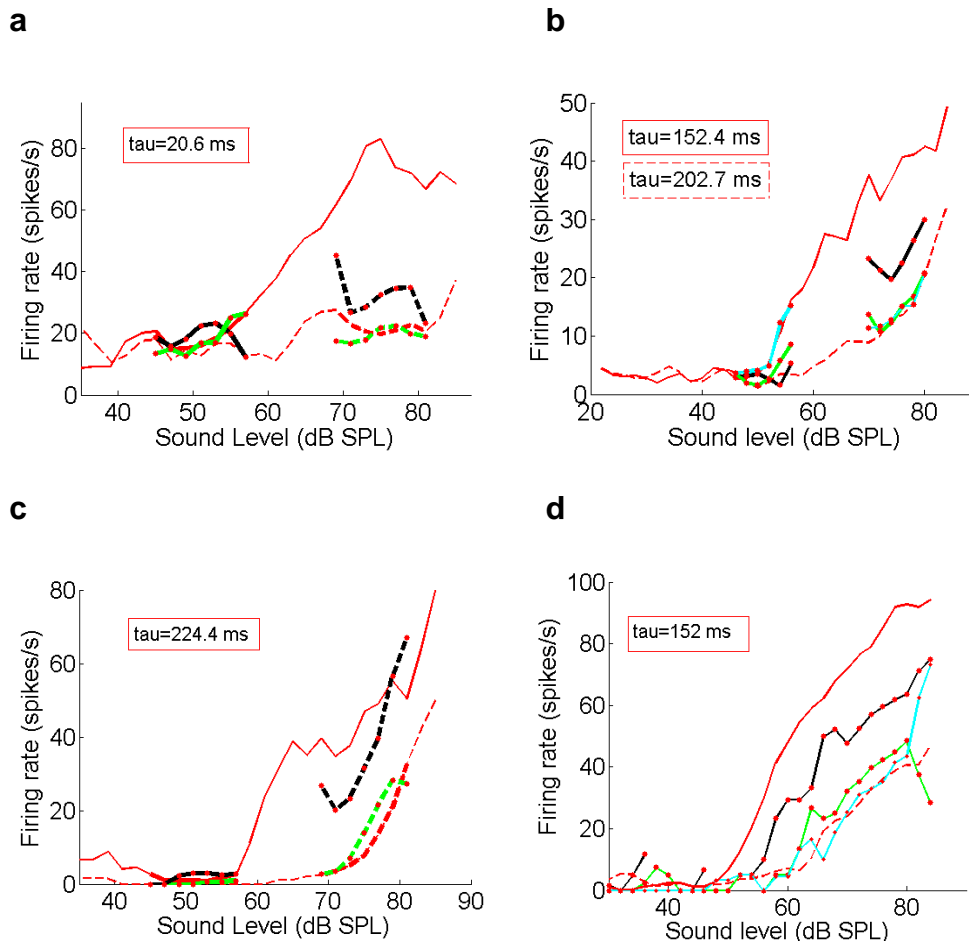


**Figure 5.11 Rate-vs.-level function adjustments between two adapted states.** *a–d*. Each panel shows rate-vs.-level functions of one neurone obtained during the final 3s of the 51dB (red solid line) and 75dB (red dashed line) half-periods of the switching stimulus. Rate-vs.-level functions are also shown for the first (black lines, red symbols), second (green lines, red symbols), and third (cyan lines and red symbols) 300ms time bins after the switch between sound level distributions. For most neurones, 300ms functions were plotted for the stimulus high-probability regions only, because less probable levels were presented too few times. For the neurone in *d*, which showed little spike-rate variability, a sufficient number of switch periods was presented to plot responses over the full range of levels; for clarity, in this neurone only adaptation to the 75dB stimulus is shown. Time constants from single exponential fits to mean firing rate are shown (red box: 75dB stimulus; dashed red box: 51dB stimulus, where fit).

Although it is more difficult to visualise changes in rate-vs.-level functions over the most probable levels of the 51dB stimulus, for the neurone shown in Figure 5.11b (time constant during 51dB stimulus=202.7ms) this function reached its final position within the third 300ms interval following the switch. For some neurones that were recorded for long durations, rate-vs.-level functions could be

constructed over both high- and low-probability regions, as illustrated in Figure 5.11*d*; adaptation over the full range of levels occurred in register with adaptation over the stimulus high-probability region.

Adjustments of rate-vs.-level functions over time were also assessed during cortical cooling. Are changes in time constants of firing-rate adaptation between cooling conditions reflected in the evolution of rate-vs.-level functions in these conditions? Figure 5.12*a* shows the response of a neurone whose time constant decreased during cortical cooling. Here solid lines represent the firing-rates across sound levels in response to the 51dB stimulus, and dashed lines the rates across the 75dB stimulus. Compare the first 300ms-rate-vs.-level functions in the ‘warm’ versus the ‘cool’ conditions. In the ‘warm’ condition, this function (black dashed line with red dots) has begun to adjust towards the final, fully-adapted position associated with the 75dB stimulus, but part of the function, especially across the loud sound levels, remains close to the 51dB stimulus distribution. By contrast, in the ‘cool’ condition, where the time-constant of adaptation was faster, the first 300ms-rate-vs-level function (black dashed line with blue dots) has largely reached its final form. Compare also the second 300ms rate-vs.-level functions between conditions. In the ‘warm’ condition (green dashed line, red dots), this function has largely, but not completely, reached its final form, whereas in the cool condition (green dashed line, blue dots), this function has completely reached its final form. The opposite pattern is observed in the neurone whose responses are represented in Figure 5.12*b*. Here, in the warm condition, where the fully adapted function for the 51dB stimulus is shifted to the left, the rate-vs.-level function is adjusted more rapidly than in the cool condition. These two neurones, then, suggest that during cortical cooling, the evolution in the rate-vs.-level function reflects the time constant of the change in firing rate, as

it does in the warm condition. Therefore, changes in time-constants between cooling conditions would be expected to affect the rapidity with which the rate-vs.-level functions adjust between adapted states in response to changes in sound-level distributions.

To confirm that changes in mean firing rate are related to changes in rate-vs.-level functions, a single exponential was fit to the root mean square (r.m.s) differences between each of the 300ms functions and the function from the final portion of the half-period (see Chapter 3), for the neuronal population in experiments without the cryoloop. This fit was significant for 28/44 neurones. The resulting time constants of change in rate-vs.-level functions were highly correlated with the time constants of adaptation of mean firing rate (Spearman's rank correlation coefficient  $r_s=0.8$ ,  $p < 0.0001$ ;  $n=28$ ).

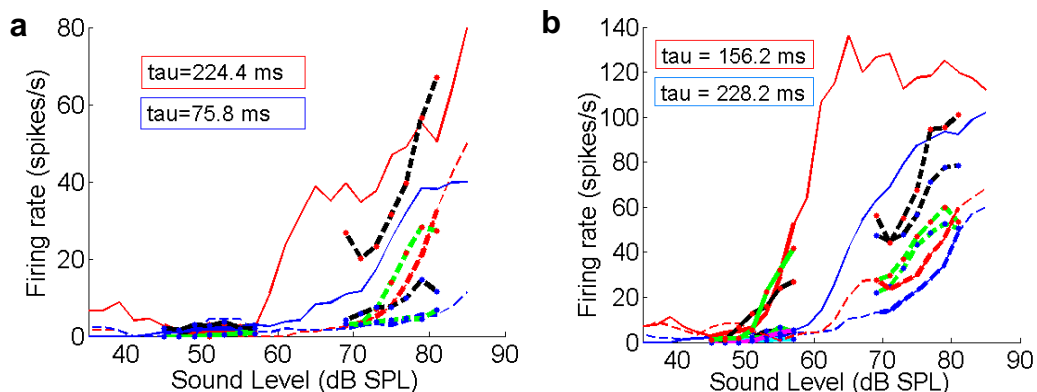


**Figure 5.12 Time course of adjustments of rate-vs.-level function in warm and cool conditions.** Functions constructed over the full range of levels represent steady state for the 51dB (solid lines) and 75dB (dashed lines) stimuli, in both 'warm' (red) and 'cool' (blue) conditions. Red markers on lines indicate rate-vs.-level functions in the 'warm' condition; blue markers, the 'cool'. Black dashed line: 1<sup>st</sup> 300ms rate-vs.-level function; green dashed line: 2<sup>nd</sup> 300ms rate-vs.-level function. a. A single neurone whose time constant decreased during the cortex-cool condition; b. A single neurone whose time constant increased during the cortex-cool condition. Time constants of adaptation of mean firing rate following a switch to the 75dB distribution shown in red ('warm') and blue ('cool') text boxes.

#### 5.4.4 Adaptation time constants vary with neuronal characteristic frequency (CF)

Previous studies have demonstrated that the time course of spike rate adaptation of auditory nerve fibres (ANFs) during pure tone bursts is related to neuronal CF

(Crumling and Saunders, 2007; Westerman and Smith, 1985). A similar relationship was observed in the adaptation to sound level statistics examined here. Figure 5.13 shows adaptation time-constants for the 75dB stimulus as a function of CF in the ‘warm’ condition. The median CF was 1198 Hz (range 100-11000 Hz; n = 40). Adaptation time constants were negatively correlated with CF (Spearman’s rank correlation coefficient  $r_s = -0.5$ ,  $p < 0.001$ ,  $n = 40$ ). Thus, neurones with higher CFs tend to adapt to the new level distribution more rapidly than those with lower CFs.

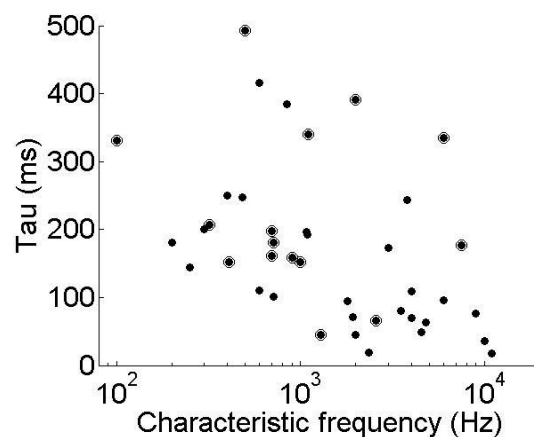


**Figure 5.13** Time course of adaptation is related to neuronal CF. Time constant of adaptation of mean firing rate during the 75dB stimulus is shown as a function of neuronal CF (n=40; all recordings made in warm condition). The circled points indicate neurones for which a slow component of adaptation could also be measured.  $r_s$ , Spearman’s rank correlation coefficient.

#### ***5.4.5 A slow component of adaptation is apparent in some neurones***

In addition to the adaptation occurring during each cycle of the switching stimulus, the responses of some neurones also displayed a slower adaptation, occurring over the course of many switching cycles (Figure 5.14). I analysed this long-term adaptation for all neurones from responses recorded to the standard switching stimulus (i.e. 10s switch period, 50ms epoch) in the ‘warm’ conditions (for experiments carried out prior to cryoloop experiments). The slow adaptation

was apparent in 36% (16/45) of neurones. Fit with a single exponential, the median time constant of the slow adaptation was 12.3s (25-75% quartiles 8.0-26.6 s, n = 16 neurones). There was no significant relation between the time course of the slow adaptation and that of the rapid adaptation (Spearman's rank correlation coefficient  $r_s=-0.17$ ,  $p=0.5$ ) or neuronal CF ( $r_s=-0.03$ ,  $p=0.9$ ). This slow adaptation resulted in a median decrease in average firing rate of 37% (25-75% quartiles 26-40%, n=16) over the first 5 minutes of recording (comparing rates at 0-10s to those at 270-300s of recording). The depth of the slow adaptation was not correlated with that of the fast adaptation ( $r_s=-0.06$ ,  $p=0.83$ ).

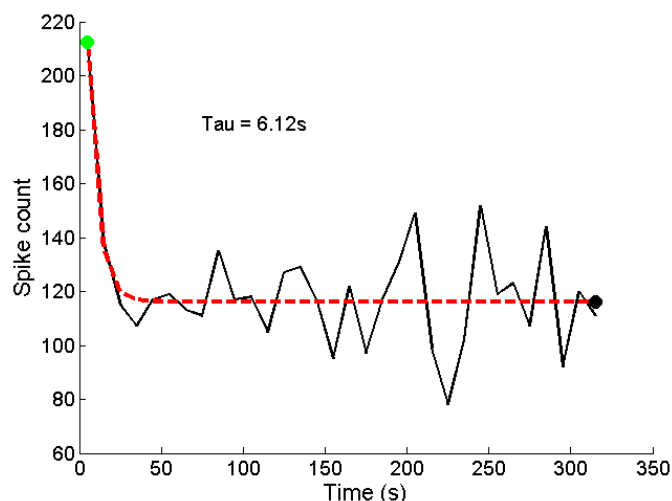


**Figure 5.14 Long term adaptation.** Spike count over 5s switch period from one neurone during first 5 minutes of recording. The dashed red curve shows single exponential fit to spike counts ( $\tau=6.12$  s).

## 5.5 Discussion

By recording neuronal responses to a switching stimulus, and averaging spike rates over many switches, I was able to quantify how rapidly IC neurones adapt to novel sound level distributions. Consistent with previous work in barrel cortex (Maravall et al. 2007), there was a close correspondence between adjustments in mean spike rate and adjustments in input-output function. This time course was rapid, permitting neurones to adjust rate-vs.-level functions to new environments

in under a fifth of a second. Unlike adaptation in the blow-fly visual system (Fairhall et al. 2001), it seemed that temporal characteristics of the stimulus did not influence the time course of the neuronal adaptation. However, two physiological factors did influence the time course. First, neuronal characteristic frequency was related to the rapidity of adaptation. Second, removing descending, cortical inputs to the IC, as well as cortical inputs to more peripheral and central sites, led to a doubling of adaptation time constants across the population. Without cortex, the neuronal population appears more sluggish at adapting to novel sound environments.

# 6

## DISCUSSION

---

### **6.1 Introduction**

This thesis has described a series of experiments testing the hypothesis that the auditory corticofugal system plays a role in the generation or modulation of midbrain neuronal adaptation to sound level statistics, employing a cryoloop to cool and reversibly deactivate auditory cortex. As a preliminary control, I measured temperatures within cortex and IC during cooling, and found that the cooling effect spread further than previously reported in the cat (Lomber et al. 1999), a finding consistent with recent data in the guinea pig (Coomber et al 2011). This finding has important implications for future studies using the cryoloop bilaterally, and was critical to my bilateral AC cooling experiments in showing that a relatively warm 10°C-14°C was sufficient to cool cortex without excessively cooling IC.

Through cortical cooling, I deactivated cortex whilst recording IC single unit responses to a stimulus that switched every 5s between two different sound level distributions. I found changes both to the time course of adaptation and to the input-output functions of adapting neurones. Without cortex, mean adaptation time course almost doubled across the population, rendering IC slower at adapting to new sound level distributions. Moreover, rate-vs.-level functions shifted to

higher sound levels during cortical cooling, leading to mal-adapted input-output relationships such that neurones often failed to respond to sound levels around the mean. These results suggest that adaptation is a property generated by the ascending auditory pathways, but that cortex plays a role in modulating adaptation to make the process useful in the representation of sound level across different environments.

## **6.2 Cryoloop apparatus**

I constructed a cryoloop apparatus as described by Lomber and colleagues (1999), with the modification that it was suitable for placement of two cryoloops, one on each auditory cortex. I used temperature probes to record temperatures at the cryoloop and at various brain sites, including auditory cortex at multiple depths, IC, and cortex overlying IC. I expected that, similar to cat data, cooling to a few degrees above zero would have little or no cooling effect on subcortical structures. However, unlike in the cat, it appears that in the guinea pig there is no sharp drop-off of cooling effect a few mm deep to the cryoloop, but rather, the loop effect spreads continuously downwards into neuronal tissue, the temperature increasing with depth. During bilateral cooling, the temperature drop is even greater. This last finding adds to the work of Coomber et al. (2011) who measured temperatures in guinea pig brain using a single cryoloop.

I placed an insulated thermocouple probe in IC itself and found that IC is cooled by up to 6°C during bilateral cooling to 5°C at the cortical surface. This drop was sufficient to reduce IC temperature to within 2°C of the temperature at which, according to Lomber and colleagues (1999), neuronal spiking is affected. I was concerned that this was too small a margin of error, and risked confounding my results by a direct or blood-supply mediated cooling effect on IC. Therefore, it was important to determine the warmest temperature possible to cool the surface

of auditory cortex such that layers V and VI would be inactivated with minimal IC cooling. By placing the thermocouple probe at a depth consistent with layer VI of auditory cortex, I defined the temperature at the loop necessary to cool layer VI to 20°C, the temperature necessary for cessation of neuronal spiking activity. This temperature was  $12^{\circ}\text{C}\pm 1^{\circ}\text{C}$  – much warmer than the  $1.5^{\circ}\text{C}$  normally considered necessary based on the work of Lomber and colleagues in cat (Lomber et al. 1999). I found that even at this relatively warm temperature, IC temperature decreases by up to  $3^{\circ}\text{C}$ . Although my data on IC cooling accord well with the extent of cooling found by Coomber and colleagues (2011), in their study a loop temperature of  $2^{\circ}\text{C}$  was necessary to reduce temperature 2mm deep to the cortical surface to  $15\text{-}20^{\circ}\text{C}$ . The main difference between our studies is not, however, in the AC thermocline: in both the work of Coomber and colleagues and in the present study, the temperature drop across the 2.5mm of cortex was  $5\text{-}10^{\circ}\text{C}$ . Rather, the difference arises from the loop temperature-cortical surface temperature differential: in the work of Coomber and colleagues, it appears that a loop temperature of  $2^{\circ}\text{C}$  was necessary to reduce cortical surface temperature to  $10\text{-}15^{\circ}\text{C}$ ; in my data, cortical surface temperature dropped to within  $1\text{-}2^{\circ}\text{C}$  of loop temperature. Further experiments and discussion between laboratories will be important in resolving the cause of this difference.

Is a temperature decrease of the magnitude I discovered in IC sufficient to affect neuronal responses? The data of Lomber and colleagues suggest that this will not affect neuronal firing *in vivo* (Lomber et al. 1999), and the data of Coomber and colleagues (2011), using thallium uptake as a measure of neuronal responses, also suggest that a drop of  $4^{\circ}\text{C}$  in IC has no effect on neuronal responses. However, data from hippocampal slices suggest that even mild temperature drops result in small decreases in vesicular release (Schiff & Somjen

1985). It was therefore necessary to record neuronal responses in IC to ensure that this thermocline did not alter neuronal firing in my experiments. To this end, I cooled IC by cooling non-auditory cortex overlying IC. I verified that cooling of this cortical area did not spread appreciably to auditory cortex, and recorded IC neuronal responses when IC was cooled to various temperatures, including the temperature it would characteristically reach when cooling cortex to 10-13°C. I found that IC responses were unchanged during direct IC cooling, until the temperature of the loop cooling cortex overlying IC was reduced to 6°C; even then, I saw only changes in spike rate but no change in parameters I routinely observed changing when I cooled auditory cortex, such as threshold changes or alterations in the slope of rate-vs.-level functions. In summary, then, these control experiments defined the temperature window that permits cooling deactivation of the auditory cortex without functionally important cooling of IC.

However, despite these attempts to control for direct cooling effects, the possibility remains that cooling cortex led to cooling of venous blood which may have gone on to cool structures more peripheral than IC, such as cochlear itself. This possibility is suggested by Coomber and colleagues (2011) who found a 5°C temperature drop in venous blood at the tentorium when cooling AC to 2°C. Although the effect of cooling may have been less in my study due to the warmer temperature I employed, it is difficult to draw firm conclusions given that I used two cryoloops, possibly potentiating the effect. Any future experiments should consider using suitably placed temperature probes, similar to those used by Coomber et al (2011), to account for this possibility.

Although I strove to limit the temperature reduction as much as possible with the aim of avoiding confounding cooling effects spreading beyond cortex, this effort may have inadvertently led to another confounding effect: the drawback

of my relatively moderate cooling paradigm is that, as suggested by the studies of Volgushev and colleagues (2000a; 2000b), moderate cooling can result in incomplete neural silencing. It is therefore possible that I did not cool auditory cortex sufficiently to entirely abolish neural spikes. A further problem is that a moderately cooled brain area is likely to show increases, not decreases in excitability, and, by maintaining cortex at a temperature close to this range, it is likely that I induced increased cortical excitability close or even within auditory cortex. Therefore, in interpreting myself, it should be borne in mind that the effects observed may be due entirely to cooling, to a mixture of cortical cooling and excitation, or entirely to cortical excitation. Further work should explore this possibility by recording in multiple auditory sites during bilateral cooling.

### **6.3 General observations during cortical cooling**

The cryoloop experiments involved making two large craniotomies over the auditory cortices, as well as a small craniotomy over the cortex overlying IC. The effect of this surgery was to render the guinea pig brain prone to breathing-related movements, which could be reduced but not eliminated by venting the *posterior fossa* of cerebrospinal fluid. In addition, cooling cortex led in most cases to a retraction of the brain towards the recording electrode. These conditions rendered recording neurones for the hour required by my experiments a challenge, and future experiments should improve brain stabilisation by the use of a firmer substance than solidified agar or petroleum jelly.

## **6.4 Effects of cortical cooling on rate-vs.-level functions**

### **6.4.1 Cooling-associated threshold shifts**

During adaptation to sound level distributions, rate-vs.-level functions typically shift along the abscissa such that thresholds tend to lie close to the mean level. These adapted neuronal thresholds increased significantly during cooling for both the 51dB and 75dB stimulus distributions. For the 51dB stimulus, the mean increase was 5.4dB, but several neurones showed much greater shifts than this, one neurone having a threshold shift of 18dB during cortical cooling. The mean shift for the 75dB stimulus was 4.2dB; there was no significant difference, across the population, in the amount of shift between the two stimulus distributions. Previous data from Sun and colleagues (1996) in the big brown bat found a different pattern, whereby IC rate-vs.-level functions shifted to the right during cortical excitation, and to the left during cortical inhibition. However, Sun et al.'s stimuli were only 4ms in duration and therefore minimized adaptation effects. Although comparison across species may not be valid, this data is consistent with the notion that the rightward shifts I observed in rate-vs.-level function may have depended on the adaptation state of the neuron, and that, in a non-adapted state, a different pattern may have emerged. The baseline rate-vs.-level function data support this idea: I observed that baseline functions did not consistently shift rightwards during cortical cooling even if, in the same neuron, the adapted functions did shift to the right. Thus, taking Sun et al.'s data in comparison with this observation, I conclude that the adaptation state of the neuron, and thus the stimulus duration, is a variable upon which the corticofugal modulatory effect depends. This is to some extent consistent with recent data: Antunes and Malmierca (2011), recording auditory responses in guinea pig MGB, found that cortical deactivation led to baseline tuning curve alterations which were correlated with the degree of stimulus specific adaptation a given neurone underwent.

What are the effects of threshold shifts of adapted rate-vs.-level functions? Over 90% of neurones in the warm condition, when adapted, have threshold within 15dB of the mean. However, during cortical cooling, this picture changes, such that only 55% of neurones, in the cortex-cooled state, have thresholds within 15dB of the mean. Thus, cortical activity is associated with adapted thresholds that lie closer to the mean stimulus level than when cortex is inactive. The activity of corticofugal pathways thus appears to be to decrease adapted thresholds across the IC, limiting adaptation to enable the population to respond to sound levels closer to the mean level, whilst preserving the beneficial effects of adaptation on neural coding.

#### ***6.4.2 Cooling-associated modulation of levels louder than threshold***

Although a few neurones displayed a uniform rightward-shift in input-output function across levels, for most, the degree of change was not homogenous across levels. Plotting functions of amount of level change against sound level, I observed three general patterns: a monotonically increasing shift in level during cooling with increasing level; a non-monotonic, peaked function where the maximum level shift occurred at intermediate levels; and finally a class of neurones whose rate-vs.-level functions changed most at or close to threshold during cooling.

No previous studies have examined the effects of bilateral activation or inactivation of auditory cortex on sound-level representation in the IC (or indeed in any subcortical structure). However, previous work in rat IC has demonstrated irregular and complex changes in rate-vs.-level functions associated with ipsilateral cortical inactivation, with no clear relationship between sound level and degree of level change and with no measurement of recovery (Popelár et al. 2003).

More consistent with my results are observations in cat thalamus during cortical excitation. He and colleagues (1997) identified three classes of neurones whose spike-rate alterations during cortical manipulation depend on sound level. Low-intensity effective neurones displayed the greatest increase in spike-rate at low sound levels during global ipsilateral auditory cortical electrical stimulation, with little facilitation at high levels, whereas high-intensity effective neurones displayed the opposite pattern. The final class showed complex changes. Those neurones described in the present study whose change in rate-vs.-level functions monotonically increase with level during cooling may well serve as inputs to thalamic neurones of He et al's high-intensity effective type. The peaked level-change functions in my data may correspond to He et al's complex neurones. I also observed some neurones in which threshold levels, or those just above threshold, appeared to be the greatest point of change across the function, which would best correspond to He and colleagues' low-intensity effective neurones.

Despite this interesting correspondence between deactivation here and He and colleague's stimulation data, it might, however, be more appropriate to view these changes as a continuum with arbitrary divisions rather than claiming distinct sub-classes of neurones. The current sample size was 20, He and colleague's 18; and these small numbers might artificially suggest sub-groups. Indeed, it appeared from my limited sample that there was a continuum of levels associated with maximum shifts in level on cooling. This would suggest that corticofugal inputs can potentially boost sound levels selectively across the entire neuronal dynamic range. Such level-specific amplification at the midbrain may be one mechanism whereby cortex can select signals of any given mean level from a noisy environment. Data from de Boer and Thornton are consistent with a role for

corticofugal assistance with discriminating speech in noise (de Boer and Thornton, 2008).

### **6.4.3 Saturation and dynamic range**

I observed that more neurones displayed saturating rate-vs.-level functions during cortical cooling than when cortex was active (55% versus 35% of neurones). A previous study suggests that ipsilateral cortical ablation can be associated with changes in monotonicity of neuronal response, but the few example neurones presented in that study show changes from saturated to monotonic responses when tetrodotoxin was applied to auditory cortex (Popelár et al. 2003).

In addition to these changes in saturation, cortical inactivation was associated with greater adaptation-associated declines in rate-vs.-level function slopes and firing rates. This resulted in decreased input dynamic range of adapted rate-vs.-level functions. The range of firing rates neurones employed in representing sound levels, the output dynamic range, was also compressed. Thus, I made two central observations regarding rate-vs.-level functions: first, when cortex is inactive, the adaptation observed in IC fails to adjust neuronal dynamic range to lie as close to the mean sound level as when cortex is active, and second, this mal-adjusted dynamic range is decreased. The tendency for threshold to increase due to adaptation of responses, and the decrement in dynamic range attendant on this adaptation, both seem to be properties of adaptation inherent to the ascending neuronal pathways. The action of the cortex leads to two modifications of these two parameters. First, corticofugal activity may limit adaptive rightward shifts in dynamic range; in other words, dynamic range is relatively left shifted, towards the mean sound level in the environment, by corticofugal activity. Second, the descending pathways appear to counteract

adaptation-associated decrements in dynamic range, thereby increasing the dynamic range, which adaptation has a tendency to reduce in any given adaptation state. It appears that without cortex, adaptation in the IC would lead to severe restrictions on neuronal responsiveness to the acoustic environment, resulting in high thresholds and small dynamic ranges. However, my results suggest that cortical activity transforms the functional effects of adaptation, refining what would otherwise be a simple loss of sensitivity around mean levels into a process for the expansion of neuronal dynamic range and the moment-to-moment maintenance of sensitivity to commonly occurring sounds.

#### ***6.4.4 Adaptation state and rate-vs.-level function shift on cooling***

I found no significant difference in the extent of rate-vs.-level function threshold shift during cooling when comparing the 51dB and 75dB distributions, suggesting that, across the population, cortical inactivation does not lead to changes in the extent to which rate-vs.-level function can alter between stimulus distributions. However, for individual neurones I observed clear differences in shifts across stimulus distributions, with individual neurones displaying large shifts in function at the 51dB distribution, and little change at the 75dB stimulus distribution, and vice-versa.

I also observed that non-adapted, or onset, rate-vs.-level functions did not consistently display rightward shifts in function during cooling. Sample size limitations preclude a thorough analysis of these differences, but it was the case that in some neurones only adapted functions shifted during cooling, whereas onset-functions did not; however, it was never the case that onset functions shifted when adapted functions did not. Moreover, in several neurones, the extent of cortical-cooling associated shift in the baseline, non-adapted (also known as

silence-adapted) state was smaller than in the adapted state. I never observed the opposite pattern. These data are consistent with the notion that neurones, when adapted, are more susceptible to corticofugal influence. This proposal is compatible with the view of the descending projections to IC as being involved in particular with neuronal plasticity (Gao & Suga 2000). However, unlike work over several decades by Suga and colleagues in bats, and more recent work in other species (Yan & Ehret 2002), my results suggest that cortex is not the origin of plasticity in IC, but rather a modulator of plasticity inherent to the afferent pathways of the auditory system up to and including IC. Thus my interpretation lies between that of Antunes and Malmierca (2011), who found no role for the descending systems in adaptation, and that of Suga and co-workers, who consider neural plasticity to be entirely dependent on descending pathways from cortex.

The difference between my results and those of other authors is likely to arise from three sources. First, most studies examining neuronal plasticity and corticofugal function employ cortical stimulation paradigms, whilst I employed cortical inactivation. Excitation might stimulate processes not present in my preparation. Second, the origin of plasticity might depend on its timescale. The data presented in this thesis concern adaptation, a form plasticity whose time-scale I found to be on the order of hundreds of milliseconds. The plasticity discussed more usually in corticofugal literature lasts for seconds to minutes. It may be that cortex only modulates very short-term plasticity (i.e. spike-rate adaptation) in the IC, but engenders longer term forms of plasticity therein. Finally, the difference in results could arise from interspecies variation, since very little cortex stimulation work has been carried out in guinea pig (but see Torterolo et al. 1998), with the vast majority being carried out in bat (Gao & Suga 1998; Zhou & Jen 2000).

A few recent studies have however examined subcortical adaptation in the context of cortical deactivation. For example, recordings in rat MGB using cryoloop deactivation of cortex have suggested that stimulus-specific adaptation (SSA) is not affected by cortical deactivation (Antunes and Malmierca, 2011), although other neuronal properties are affected. The authors concluded, as I do, that subcortical adaptation is not ‘inherited’ from cortex but results from processes occurring between cochlear and thalamus. Work by Bäuerle and colleagues, however, using muscimol inactivation of cortex, found that SSA is reduced in gerbil IC in the absence of cortical input. The data presented in the current study in guinea pig IC investigates adaptation to sound level stimuli, rather than to tones employed in these thalamic studies, and finds, in contrast to both these studies, that adaptation is potentiated during IC deactivation, implying that cortex has a ‘restraining’, excitatory, role in modulating adaptation. Other data in accord with the possibility that corticofugal modulation has a specific role during adaptation comes from comparisons of the effects of corticofugal inactivation over the course of adaptation of neuronal responses to 100ms tones. Greater changes in rate-vs.-level functions were observed during cortical inactivation when the firing rates of the functions were calculated from the second 50ms of a 100ms stimulus (Popelár et al. 2003). In addition, Antunes and Malmierca (2011) found that whilst inactivation of cortex did not alter SSA in thalamus, the extent of corticofugal modulation of non-adaptive neural responses was correlated with the amount of SSA that neurones displayed.

#### ***6.4.5 Laterality of cortical input***

Pathways from cortex can reach IC by a number of routes. Both contralateral and ipsilateral cortices project to IC neurones. Whilst previous studies have selectively

activated both cortices independently whilst recording in IC (Tortero et al. 1998), no previous studies have compared the effects of deactivating ipsilateral or contralateral cortices. Therefore the physiology of the contralateral corticofugal pathways has been largely ignored prior to the current work. It was not the aim of this thesis to examine this pathway in isolation comprehensively. However, I did record a small number of IC neurones during exclusively contralateral, and exclusively ipsilateral deactivation. Interestingly, for both experimental designs, 1/3 neurones displayed rightward shifts in rate-vs.-level function similar to those observed during bilateral cooling, in which almost all neurones displayed such shifts. If these results are supported by further data, this implies that individual neurones may receive either ipsilateral or bilateral input subserving the same function with respect to sound level representation in the adapted state: deactivating either contralateral or ipsilateral inputs therefore results in changes in functions in some neurones, whereas deactivating both sides results in changes in the majority of neurones. In support of this notion, a cortical activation study in guinea pig IC found only minor differences in IC responses when stimulating ipsilateral versus contralateral cortex (Tortero et al. 1998).

#### **6.4.6 Neuronal coding**

During cortical cooling, sound level coding accuracy, measured using Fisher Information, tended to decline across all levels. Moreover, the peak of the Fisher Information tended to shifted to the right, away from the mean sound level, suggesting that corticofugal pathways tend to increase accuracy of level coding around the mean level of the environmental sound level distribution. This was observed in individual neurones and across the population: it was striking that when cortical inputs were removed, population Fisher Information remained almost flat, at its lowest values, across all levels of the high probability region of

the 51dB stimulus, but with cortex active, Fisher Information increased over the entire range of the high probability region, reaching a peak just above it, as found in previous work (Dean et al 2005). Moreover, this distinct population peak was missing in the cortex-cooled condition, in which the population Fisher Information for the 51dB stimulus appeared to saturate, rather than peak and decline. It appears that corticofugal input to the IC leads to a sharp peak of coding accuracy just above the mean sound level, and that without such input, coding accuracy is decreased overall. Rather than peaking sharply, Fisher Information rises across levels well above the mean, never achieving a distinct peak value. Thus, when cortical inputs to IC are active, adaptation in the IC leads to increased accuracy of sound level discrimination, and this increase is highly focussed around more probable levels. When these inputs are removed, the increase in accuracy is reduced, and this increase occurs at levels well above the probable levels, and fails to reach a peak. To my knowledge, no previous studies have analysed the role of corticofugal pathways in terms of its effects on neuronal coding accuracy in the midbrain.

### ***6.5 Spike rate adaptation: depth and time course***

The adaptation stimulus allowed examination of the effects of cortical cooling on steady-state rate-vs.-level functions from two stimulus distributions, with high-probability regions centred on 51dB and 75dB, as discussed above. By switching between these two stimulus distributions repeatedly, I were able to examine the time course of adaption, both with and without active corticofugal pathways. Time-constants fit to the spike rates averaged across switches to each distribution were highly correlated with the time course of shifts in rate-vs.-level functions, reflecting the reconfiguration of neuronal input-output functions. In general, I

found that adaptation was rapid, and that cortex can either slow or speed up adaptation in individual neurones; its overall effect, as inferred from the effects of deactivation, may be to make the population adapt more rapidly to a change in stimulus statistics. However, the overall direction of change due to cortical activity is a tentative finding: the main finding is that cortex plays some role in altering the time course of midbrain adaptation.

### ***6.5.1 Cortical influence on depth of adaptation***

Following a switch to the 75dB stimulus distribution, firing rate increased sharply then declined more slowly to a steady state. I quantified the amount of adaption by comparing onset and steady-state firing rates. ‘Onset’ here refers to the initial spike rate after a switch away from the 51dB stimulus to the 75dB stimulus. For the population of neurones recorded without cryoloops in situ, the mean percentage spike-rate reduction over the course of adaptation to the 75dB stimulus distribution was 58%; for the cryoloop experiments, in the warm condition, mean reduction was 60%, suggesting that these two populations are comparable and may be representative of the IC as a whole.

Cortical cooling led to significant reductions in both the ‘onset’ rate (i.e. response to new distribution whilst neurone was still adapted to the previous distribution) and adapted spike rates across the neuronal population. This reduction in both parameters resulted in no significant change in the percentage of adaptation (i.e. difference between onset and adapted rates) across the population. It appears that whilst cortical cooling leads to overall reductions in spike rate, it results in alterations to both ‘onset’ and steady-state responses equally. These spike-rate data reflect the extent to which rate-vs.-level functions shifted between adaptation states, and accord with my analysis of rate-vs.-level function threshold

shifts: I found no significant differences in the increase in threshold when switching to the 75dB distribution from the 51dB distribution, when comparing cortex warm and cortex cool conditions.

### ***6.5.2 Cortical influence on time course of adaptation***

With corticofugal pathways intact, following a switch to the 75dB stimulus distribution, spike rate adaptation occurred with a mean time constant, across neurones, of 159.7ms. Adaptation of mean firing rate to increased variance or kurtosis has been investigated in cat IC, and occurs with a time constant of 140ms or 260ms, respectively (Kvale & Schreiner 2004). Although I assessed adaptation to the mean, rather than variance or kurtosis, using noise rather than pure tones, and changed sound level over longer time scales, the similarity in time course between the two studies suggests that adaptation over hundreds of milliseconds is characteristic of the adjustment of IC responses to stimulus statistics.

During cortical cooling, the mean time constant increased to 288ms, reflecting the tendency of a majority of neurones to adapt more slowly without cortical input: in one neurone the time constant increased from 200 to over 800ms. However, a minority of neurones adapted more quickly without cortical input, one neurone's time constant decreasing to 19ms, among the fastest observed across all conditions. Consistent with this finding, a recent study found that cortical deactivation led to a reduction in latency of auditory neuronal responses in thalamus (Antunes and Malmierca, 2011). Thus, it appears that cortical input has a tendency to increase the speed of adaptation in the midbrain across the population, but may either increase or decrease the speed of adaptation in individual neurones. It would be premature, however, to conclude from these experiments that cortex has a role in speeding up adaptation in IC. Data are averaged over a small number of neurones, since in most cases the time course of

adaptation failed to recover in the rewarm condition to warm values, and thus most neurones were excluded from analysis. Though the increase in time constant during cooling was significant, it is possible that with more data, a higher proportion of neurones would be found to adapt more quickly during cooling, and the difference in mean values across the population would be reduced. However, the finding of bidirectional cortical control of IC adaptation time course seems robust, and has not before been reported.

In addition to an increase in mean, the variance of time-constants across the population increased significantly during cooling, suggesting that without corticofugal input, there was a tendency for a greater spread of time constant values. A recent study by Nakamoto and colleagues (2010) found that cortical deactivation decreases the vector strength of the IC temporal response to a louder harmonic complex when presented simultaneously with a quieter complex. Popelár and colleagues (2003) found, in rat IC, that cortex improves temporal responses on a time-scale sufficient to alter neuronal synchronization. A temporal, synchronizing role for corticofugal pathways has also been found in the visual thalamus (Villa et al. 1991). The current study extends these findings to suggest that cortex can also modulate temporal responses on the order of hundreds of milliseconds.

What might be the function of corticofugal pathway-induced alterations in the cross-population distribution of adaptation time constants? Other studies have found that the mean of adaptation time constants depends on time-scales in the stimulus (Fairhall et al. 2001). I did not find a similar dependence on time-scales in the stimulus. However, it is possible that cortex is sensitive to some aspect of the stimulus I have not varied, and, via corticofugal pathways, brings time-constants in the IC towards a common value in response to this unknown aspect of

the stimulus. For example, it may be the case that the mean level of the stimulus alters adaptation time constants, and that this alteration is under corticofugal control. This possibility could be tested by repeating experiments using distributions with different means and comparing time constants with those found in the current study.

In summary, although I found that cortical deactivation does alter the time course of adaptation, tending to slow it down, the time scale remains on the order of hundreds of milliseconds, which appears characteristic of adaptation in IC (Dean et al, 2008; Kvale & Schreiner 2004). Therefore, cortex seems to be responsible for modulating time course via corticofugal efferents, but only within limits set by mechanisms inherent to ascending pathways. The functional implications of this finding are several: for example, it has been shown in locusts that neuronal filter properties depend on adaptation time course and can result in the generation of intensity invariance (Benda & Hennig 2008); such invariance has been found in songbird area L, an homologue of primary auditory cortex (Billimoria et al. 2008). My data suggest that cortex may alter subcortical adaptation time course, which may render its own inputs more intensity-insensitive. Further, adapting neurones, by filtering out certain frequencies, are able to differentiate signals of particular frequencies from background noise (Benda et al. 2005). Clearly, if cortex alters filter properties of midbrain neurones, it would alter neuronal representation of background noise versus signal. It would be of interest to test whether this potential corticofugal modulation is one mechanism whereby the ability to identify particular signals from a noisy background is placed under attentional control. This would require an awake, behaving animal preparation with cryoloops surgically implanted, as has been previously used in cat (Lomber & Malhotra 2008). Data from Seluakumaran and

colleagues (2008) suggests that the MOC pathways improves signal-in-noise discrimination in IC neurones, and Nakamoto and colleagues have found that corticofugal pathways results in greater differences in representation of louder harmonic complexes presented concurrently with quieter complexes (2010). These data, together with data in the current study and the literature linking adaptation to filter properties of neurones, support the possibility that corticofugal pathways may alter signal processing in midbrain through an effect on adaptation time course-dependent filter properties.

### ***6.5.3 Adaptation to a reduction in mean sound level***

For those neurones in which it could be measured, adaptation to a reduction in mean level also occurred over hundreds of milliseconds when cortex was active. When cortex was inactive, this time course could not be measured, due to the increased thresholds occurring during cortical cooling. Time constants were fit to the mean firing rate following a switch, and this rate was dominated by the response to levels in the high probability region. In the cortex warm condition, following a switch to the 51dB distribution, thresholds often shifted from well above 51dB downwards, to lie within the high probability region, so that a change to this distribution resulted in a sudden decrease, followed by a slower increase in firing rate. However, in the cortex-cool condition, although there was usually a decrease in threshold following a switch to the 51dB stimulus distribution, this decrease rarely resulted in the threshold lying within the 51dB stimulus high-probability region. Since firing rates are dominated by responses to sound levels in this region, these higher thresholds meant that firing rates never increased appreciably following a switch to this distribution in the cortex cool condition.

In the cortex warm condition, this argument applied only to some neurones; for others, time constants could be fit, and neurones tended to adapt more rapidly to an increase than to a decrease in mean level. Such asymmetry is observed in auditory nerve fibre (ANF) responses to isolated tones (Harris & Dallos 1979) and for adaptive processes arising after binaural integration in the brainstem (Ingham & McAlpine 2004). Such time course asymmetry has been shown for other forms of adaptation; for example, visual responses adapt more quickly to an increase in stimulus variance than to a decrease (Smirnakis et al. 1997; Fairhall et al. 2001). Thus, the asymmetry I report appears to reflect a general property of adaptation.

#### ***6.5.4 Relation of adaptation time course to characteristic frequency***

The time course of adaptation to an increase in mean level was negatively correlated with neuronal CF. An outstanding question is whether the relation to CF reflects a physiological constraint of the system, or is functionally relevant - linked, for example, to the representation of natural sound environments salient to the guinea pig. It was not possible to test whether this relationship remained consistent when corticofugal pathways were deactivated, due to the smaller population of neurones recorded. It is possible, given that these pathways alter the time course, that this BF-relation is no longer present when they are inactivated. Further work will address this possibility.

#### ***6.5.5 Multiple time-scales of adaptation in the IC***

In addition to the rapid adaptation described above, I observed a slow adaptation in the present study, with an average time constant of 12s. The range of

adaptation time courses I report indicates that the adjustment of neuronal response at this level of the auditory pathway can access several time-scales, as has been found in auditory cortex (Ulanovsky *et al.*, 2004). These time courses appear to be in part under corticofugal control, in that the rapid component associated with a switch to a louder stimulus distribution is modified by descending pathways.

### **6.6 Neuronal recovery post-cooling**

34/54 neurones failed to recover firing patterns to their original, pre-cooled state. This was in part due to brain movement and consequent loss of neuronal isolation. Another reason for this finding was likely because I assessed 'recovery' according to adapted firing rates. It may be the case that adaptation processes require a longer recovery time than baseline responses. I found that neurones could recover baseline functions, recorded prior to the adaptation functions in the rewarm condition, even when adapted functions had not recovered. This observation, that a neurone can appear recovered from the effects of inactivation when probed with a baseline, as opposed to an adapting, stimulus, suggests a possible specific mechanism of action of the descending pathways during adaptation. The rightward shift in rate-vs.-level functions may thus be a product of two mechanisms affected by descending, cortical input: one adaptation-independent mechanism, and one adaptation-dependent mechanism. The adaptation dependent mechanism appears to recover more slowly than the other mechanism. This finding is consistent with cortical excitation studies demonstrating hours-long effects of cortical activation on midbrain plasticity (Yan & Ehret 2001).

A subset of neurones (n=3) displayed 'rebound' rate-vs.-level functions, which moved further to the left during recovery than during the initial warm condition. Antunes and Malmierca (2011) made a similar observation, and

interpreted this as being caused by a higher synaptic release probability during rewarming, which may well account for my observations (Volgushev et al, 2004).

### ***6.7 Mechanisms of adaptation and corticofugal modulation***

Adaptation, the decline in neuronal spike-rate over the course of sustained stimulation, can occur by a variety of mechanisms. Recent work in the locust has demonstrated that the time course of adaptation is different in neurones whose functions are distinct, and these different expressions of adaptation are subserved by different mechanisms; the time course of these mechanisms is reflected in the time course of the adaptation (Hildebrandt et al. 2009) I observed that the effect of deactivating cortex was to alter the time course of adaptation, and its effects on coding, in the IC. Other studies implying a role for descending pathways in adaptation include that by Popelár (2003), who found changes in sustained responses in 35% of the neurones in rat IC following AC inactivation by tetrodotoxin, and more recent work by Bäuerle et al. (2011) which found stimulus-specific adaptation in gerbil MGB was altered by cortical deactivation. These studies, and my own, suggest that cortex modulates adaptation processes in the IC itself or in centres upstream of IC. Forms of adaptation are displayed at sites upstream of the IC, including the auditory nerve (Westerman & Smith 1984) the CN (Bleeck et al. 2006) and the medial superior olive (Tzounopoulos & Kraus 2009); mechanisms underlying these effects may contribute to the adaptation I observe. Such mechanisms may be intrinsic to the neurone (e.g. channel based adaptation), or act presynaptically (e.g. synaptic depression); either of these classes of mechanism may be subject to network influences, including corticofugal modulation. Work in locusts suggests that adaptation mechanisms can vary greatly even in anatomically closely related neurones, though clearly this cannot be extrapolated to mammals (Hildebrandt et al. 2009). My results suggest

that at some stage in the ascending pathway, the efferent network does intervene with the effect of modulating spike-rate adaptation. This observation, and the definition of the time course, will assist future work in identifying the basis of the adaptation, by constraining the possibilities to mechanisms operating over comparable time-scales and prompting the search for mechanisms which can be subject to corticofugal influences. What might these mechanisms be?

The rapid adaptive effects shown here occur over a similar time-scale to adaptation resulting from synaptic depression, for example in somatosensory cortex (Chung et al. 2002; Higley & Contreras 2006). On the other hand, in olfactory cortex, synaptic depression is associated with much longer timescales, from seconds to hundreds of seconds (Best & Wilson 2004). Synaptic depression in the IC *in vitro*, however, occurs over hundreds of milliseconds (Wu et al. 2004), an appropriate timescale for the spike rate adaptation I observe. Adaptation of synaptic strength within the IC itself may thus contribute to the rapid effects I describe.

Alternatively, the rapid adaptation of IC responses following an increase in mean level is suggestive of medial olivocochlear (MOC) efferent effects, which modulate outer hair cell activity over a similar time course (Boyev et al. 2002; Backus & Guinan 2006; Guinan 2006) and indeed adjust ANF rate-vs.-level functions (Guinan & Stankovic 1996). This mechanism may be particularly susceptible to cortical influences, and has been shown to have functional consequences for IC neurones, such as altering representation of signals in noise (Seluakumaran et al, 2008). However, the MOC appears to be largely inactivated by urethane anaesthesia (Dean, I, personal communication), rendering its involvement in my experiments unlikely.

In addition to synaptic influences, intrinsic mechanisms may play a role in adaptation. Intrinsic, channel-based adaptation, can arise through activity-dependent potassium conductances in visual cortical neurones (Carandini & Ferster 1997; Sanchez-Vives et al. 2000a; Sanchez-Vives et al. 2000b); such conductances are intrinsic to some IC neurones (Sivaramakrishnan & Oliver 2001). However, it is unlikely that the conductances described in visual cortex underlie the rapid component of adaptation I observe since they operate over seconds. Such conductances may, however, underlie the slow adaptation I observe; indeed, the proportion of IC neurones displaying slow adaptation (36%) is similar to the proportion expressing these conductances and showing adapting firing patterns *in vitro* (29%; Sivaramakrishnan and Oliver, 2001). It remains possible that intrinsic conductances underlie rapid adaptation: the link between fast adaptation and intrinsic conductances was recently affirmed in the locust Lobular Giant Movement Detector (LGMD), where an intrinsic calcium-activated potassium current was found to underlie spike-frequency adaptation on a time-scale of tens of milliseconds, (Peron & Gabbiani 2009b; Peron & Gabbiani 2009a) raising the possibility that intrinsic conductances might also underlie the rapid adaptation I observe.

Intrinsic mechanisms may be subject to corticofugal control: it is known that noradrenergic inputs can modify the slow afterhyperpolarization (AHP) in guinea pig thalamic neurones (McCormick & Prince 1988). The slow AHP is a potassium-channel dependent conductance thought to underlie some forms of spike-rate adaptation (Sanchez-Vives et al. 2000b). Interestingly, the IC projection to cochlear nucleus is in part noradrenergic (Behrens et al. 2002). It is possible that cortical influences on IC activate CN-projecting IC noradrenergic fibres which could alter CN adaptation and therefore improve neuronal coding upstream

of (i.e. more peripherally than) IC. Consistent with this is the finding that, in thalamus, noradrenaline reduces the amount of adaption on a timescale of tens to hundreds of milliseconds, encompassing the range of adaptation time constants I find in IC (McCormick & Prince 1988). Testing this noradrenergic hypothesis of corticofugal modulation of midbrain adaptation requires several further experimental steps, including investigation of whether corticofugal fibres ending in IC can activate IC noradrenergic inputs to CN, and further, whether these inputs can alter the expression of adaptation of rate-vs.-level functions in the CN.

In addition to seeking mechanisms of adaptation subject to corticofugal control, mechanisms must be sought that can explain the relation to neuronal CF, which may arise from an adaptive mechanism that varies in time course along the tonotopic axis. The time course asymmetry between increases and decreases in mean level also must be explained mechanistically. For example, whilst MOC effects show an opposite asymmetry (Backus and Guinan, 2006), and therefore are unable to account fully for the IC adaptation, synaptic depression has a complementary time course asymmetry to that shown here (Dobrunz et al. 1997; Chung et al. 2002).

### ***6.8 Anatomy of observed corticofugal effects***

The current study has shown that removal of corticofugal activity alters activity in the central nucleus of the IC (ICC). This suggests one function for the cortex-ICC pathway whose presence has been inferred through retrograde tracing in guinea pigs (Coomes et al., 2005). I found that IC neurones can be modulated either by ipsilateral or contralateral cortical deactivation, which is evidence of a functional role for the contralateral pathway discovered by Coomes and colleagues (2005).

Alternatively, the effects I observe may act through other, polysynaptic pathways. These include intra-collicular pathways, such as cortex→IC (external nucleus)→ICC. In addition, cortical descending fibres contact the IC bilaterally, and may affect the contralateral IC via commissural fibres (Aitkin & Phillips 1984; Saldaña et al. 1996; Coomes et al. 2005). Finally, descending pathways may have their primary action via brain structures peripheral to IC: a subset of cochlear nucleus neurones which receive descending input, project directly to IC, ipsilaterally, contralaterally, or bilaterally (Schofield & Coomes 2005). Future work should locate the anatomical position of neurones recorded in IC with the aim of recording from external nucleus as well as ICC in order to investigate this circuitry.

Several lines of evidence suggest that the direct corticocollicular pathway is excitatory (Saldaña et al. 1996; Feliciano and Potashner 1996). However, not all anatomical data is consistent with an excitatory pathway: Schofield (2009) found non-pyramidal corticofugal fibres that may have been inhibitory. In addition, the presence of IC interneurons also implies that, whether corticofugal fibres are inhibitory or excitatory, their final effect on a given IC neurone may be in either direction. My data support the view that excitatory corticofugal feedback is predominant: I find that corticofugal activity serves to increase spike rates across the neuronal dynamic range. My data may also in part result from the presence of a second, indirect excitatory pathway, consisting of cortical projections to neurones of tegmental nuclei; the same neurones that receive these projections send cholinergic inputs to the ipsilateral IC (Schofield & Motts 2009).

## **6.9 Further considerations and study limitations**

### **6.9.1 Urethane anaesthesia**

Although commonly used in small-animal experiments due its minimal effects on cardiorespiratory function, urethane is known both to potentiate  $\gamma$ -aminobutyric acid (GABA) and glycine receptors and to inhibit N-methyl-D-aspartate (NMDA) and  $\alpha$ -amino-3-hydroxy-5-methyl-4-isoxazolepropionic acid (AMPA) receptors (data based on a recombinant-receptor, xenopus oocyte preparation which reflects receptor subsets found in CNS; Hara and Harris, 2002). However, Hara and Harris found that all changes to receptors were modest in comparison with other anaesthetics. For example, whereas urethane decreased responses of 10% of NMDA receptors, ketamine decreased responses in 80% of receptors. Urethane is thought to exert its anaesthetic effect by modest alterations in a wide variety of receptors rather than a large reduction in a single receptor. Nonetheless, it is important to note that part of the adaptation processes or the corticofugal-associated alterations in adapted rate-vs.-level functions I observed, may in turn be influenced by urethane anaesthesia. As mentioned above, unpublished studies by Dr I Dean suggest that urethane may abolish MOC activity, which in turn might cause differences between my findings and the awake behaving preparation. As with all work in anaesthetised preparations, my data need to be interpreted as pertaining to the anaesthetized state, and applied to the awake state with care.

### **6.9.2 Control experiments: temperature**

An important finding of the current study was the small decline in temperature in the midbrain when cortex was cooled, according with recent work by Coomber and colleagues in the guinea pig (2011). Although care was taken to minimise this by maintaining cortical temperature as high as possible, it is nonetheless possible

that a small decrease in temperature in the IC was sufficient to reduce firing rates and contribute to the effects found in this study. Although previous studies have found that neuronal firing rates do not decrease appreciably above 24°C in vivo, in vitro work has revealed that vesicle depletion begins with any temperature drop, though depletion rapidly increases below 24°C (Yang et al. 2005). Control experiments in the current study showed that, when cortex is kept above 10°C, placing the cryoloop on cortex overlying IC does not lead to any changing in firing rates. This suggests that the effect is not due to temperature decreases, but further controls would confirm this. For example, IC could be cooled directly using a modified cryoloop with narrow profile and cooling limited to the tip. Alternatively, the study could be repeated using another method of cortical deactivation, although other methods – such as surgical ablation, or drug administration, are not easy to reverse.

Although the current study calibrated the effect of the cryoloop with respect to temperature spread at different levels within AC, I did not measure systematically the spread of cooling across the entire cortical surface. However, the data of Coomber and colleagues (2011) suggests that effective temperature drops are limited to the AC, including belt auditory areas, when using a cryoloop of similar dimensions to my own (Coomber et al. 2011). Whilst my employment of bilateral loops may tend to increase spread of cooling, I used a relatively warm temperature in comparison to other studies, which would tend to counteract such spread.

### **6.9.3 Data collection and neural recording limitations**

Whilst my study is robust in some areas, the small data set of recovered neurones mean that several of its conclusions must be taken as preliminary and subject to modification by further work. This low number reflected several technical challenges. First, the time taken to present the adaptation stimuli before, during, and after cooling, was often longer than a neurone could be held in isolation. Second, even if neurones were held this long, some did not recover pre-cooling responses after cortical cooling within the time window allotted. Third, in certain animals the brain retracted tens of microns when cortex was cooled, presenting a challenge to maintaining isolation. However, this effect was in general no more extensive a shift in position than typically occurs over the course of a long neuronal recording in which the brain typically descends a small amount. Finally, bilateral craniotomies tend to cause a general instability of the brain tissue, thereby rendering isolation more challenging. Agar failed to improve this situation, and future work should address the challenge of filling the craniotomy with a substance firm enough to reduce brain movement but soft enough to admit electrodes with deforming them.

### **6.9.4 Analysis limitations**

The analysis of data of Fairhall and colleague (2001), as well as data from other species and sensory systems on adaptation (Brenner et al. 2000; Maravall et al. 2007), points to a limitation in my analysis. I assessed neuronal input-output relationships only between current firing rate and sound level in the current 50ms bin. It is highly likely that sound levels more distant in time would have influenced current sound level; I did not assess this possibility. By contrast, the studies mentioned above tend to use reverse correlation to take account of the

dependency of current spiking on the full stimulus history. I were limited in this regard by my small number of repeats per data point (to a minimum of ~10), due to the division of repeats among 30 sound levels and because most of these levels were only chosen with a probability of 0.2. My visualisations of adapted rate-vs.-level functions are thus temporally incomplete representations of the evolving relationship between stimulus and response.

### **6.9.5 Interpretation of function**

Results from several adaptation studies in the blowfly indicate that adaptation leads to information transmission that approaches the physical limits imposed by entropy (Brenner et al. 2000; Fairhall et al. 2001). The question then arises: if insect neurones can adapt so precisely to stimulus statistics, why in mammalian brains is a cortex necessary to improve subcortical adaptation? One possibility is that adaptation, in addition to its information processing advantages, may be useful in minimizing neuronal energy expenditure (Laughlin 2001). Indeed, this may have been the primary evolutionary drive for the development of neuronal adaptation in mammalian, but not necessarily in insect, neurones. In this scheme, it may be that cortical inputs transform neuronal adaptation from an energy-saving mechanism into a phenomenon for adjusting the dynamic range of neurones according to environmental demands. Consistent with this notion is the finding that in the brains of senescent cats, where energy expenditure is of greater importance, adaptation occurs to a greater extent (Hua et al. 2009). In these cat brains, stimulus selectivity is poorer (Hua et al. 2006), a finding which the author suggest may be due to excessive adaptation.

### **6.10 Summary model and future work**

Adaptation of rate-vs.-level functions in the IC may be more useful in the presence of cortical input. The decrease in firing rate associated with cortical

cooling has the effect of attenuating the apparent benefit adaptation confers on level coding accuracy. My findings imply that adaptation is inherent to IC and/or more peripheral centres, and does not originate with descending inputs. Combined with recent work suggesting less marked rate-vs.-level function adaptation in the auditory nerve than in IC, this implies that rate-vs.-level adaptation is a process potentiated at successive auditory centres to produce the adaptation observed in IC (Wen et al. 2009) and above. The current work, by removing cortical inputs, in effect ‘unmasked’ the ascending pathway tendency towards adaptation.

The data may thus be viewed as an exception to descending systems research that posits that plasticity arises at subcortical sites as a result of cortical feedback (Gao & Suga 2000) and is more in accord with recent work suggesting that subcortical adaptation arises subcortically (Antunes and Malmeirca, 2011) and can be modified by descending inputs (Bäuerle et al. 2011). My finding that adaptation is transformed by corticofugal pathways from a decrease in sensitivity over common sound levels into a potentially useful tool for neuronal sound level representation extends understanding both of the mechanisms underlying adaptation, and of the functions of auditory cortex and its subcortical projections.

Cortical deactivation results in adapted rate-vs.-level functions shifting rightwards with increases in threshold and decreases in dynamic range. Cortical deactivation also slows neuronal adaptation across the population of IC neurones. These two processes are summarised in Figure 6.1, a simple processing diagram emphasising that unopposed adaptive drive might have severe ethological consequences, in this case preventing a thirsty deer from hearing a tiger’s approach above the background noise of the stream.

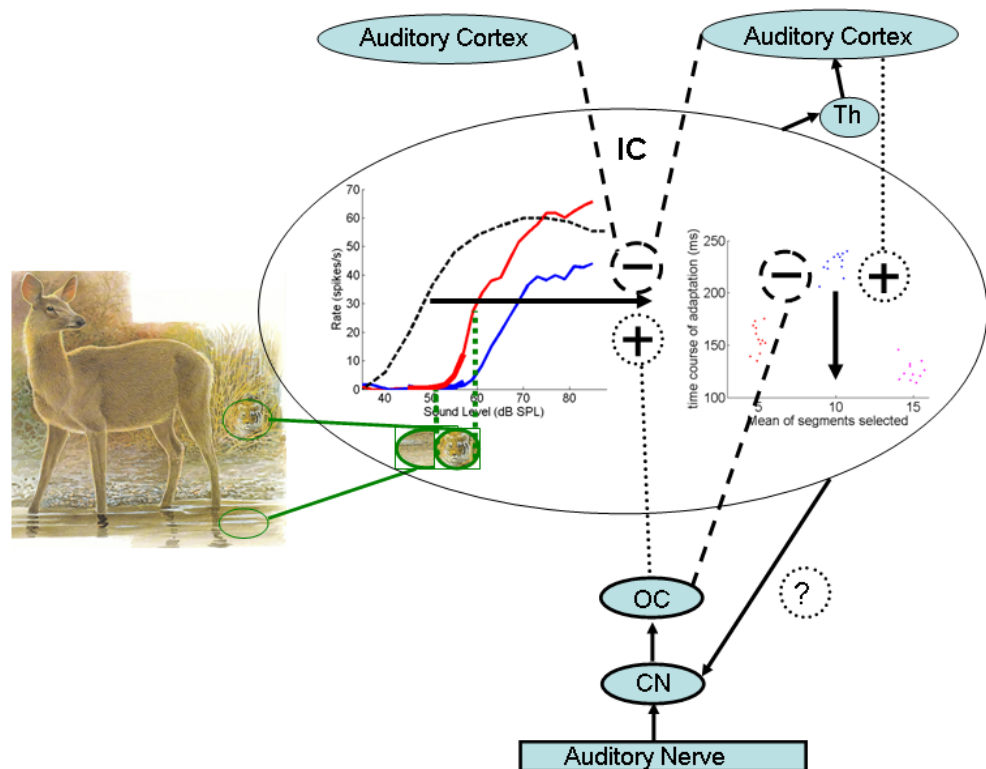


**Figure 6.1 Utility of adaptation in IC depends on the interaction of bottom-up and top-down processes: a balanced model of adaptation.** Ascending pathways act to shift rate-vs.-level functions along the abscissa to higher sound levels, and to decrease the rate of this adaptation. Descending pathways counteract both these actions, restraining the extent of rate-vs.-level function shift and increasing the speed of spike rate adaptation. The balance of these two opposing inputs to IC results in adaptation which usefully and rapidly improves coding around the mean sound level – in this case ensuring that the deer has the best possible chance of discriminating the sound of a padding tiger from the background noise of flowing water and wind-rustled grass. Graph on left: rate-vs.-level functions for a single neurone for the baseline, from-silence stimulus (dashed black line), the 51dB stimulus (red line) and the 51dB stimulus during cortical cooling (blue), which reflects the unopposed actions of the ascending auditory pathway. Note that the amount of contribution of more peripheral sites to adaptation in the IC, and the amount occurring within the IC, is at present not known. The pathway from IC to CN is shown, although its functional role in my data remains to be assessed. CN: cochlear nucleus. OC: Olivary complex. Th: Thalamus. For clarity, only unilateral ascending pathway is shown.

These two findings could reflect two separate cortical mechanisms exerting control over IC responses to sound in noisy environments. Since my data suggest that cortex may boost IC responses to particular sound levels, corticofugal pathways may function to help pick out signals based on their mean sound level,

or on the relation of their mean level to that of the background. In addition, corticofugal pathways could help extract particular signals based on their modulation frequencies, by adjusting the filter properties of the neurone to match those of the signal via adjustment of adaptation time-course.

The central finding advanced in this thesis is that the aptness of adaptation for adjusting neuronal rate-vs.-level functions to match environmental demands, depends on the descending pathways. Without these pathways, adaptation still occurs, but excessively so, such that it seems no longer to match neuronal response ranges with the range of sound levels in the environment. This finding requires support by further work in other auditory areas, and in other sensory systems, and to undertake the experiments in an awake, behaving, animal model. Thus it would be possible to assess any behavioural benefits of IC adaptation, as well as the extent to these may be diminished when corticofugal pathways are deactivated. This would reveal the functional consequences which occur when adaptation is driven solely by subcortical processes, unconstrained by cortical feedback.

# BIBLIOGRAPHY

---

- Adams, J.C., 1980. Crossed and descending projections to the inferior colliculus. *Neuroscience Letters*, 19(1), 1-5.
- Adrian, E.D., 1926. The impulses produced by sensory nerve endings: Part I. *The Journal of Physiology*, 61(1), 49-72.
- Aitkin, L.M. & Phillips, S.C., 1984. The interconnections of the inferior colliculi through their commissure. *The Journal of Comparative Neurology*, 228(2), 210-216.
- Andolina, I.M., Jones, H.E., Wang, W. & Sillito A.M., 2007. Corticothalamic feedback enhances stimulus response precision in the visual system. *Proceedings of the National Academy of Sciences of the United States of America*, 104(5), 1685-1690.
- Antunes, F.M. & Malmierca, M., 2011. Effect of auditory cortex deactivation on stimulus-specific adaptation in the medial geniculate body. *Journal of Neuroscience*, 31 (47), 17306-17316.
- Arnault, P. & Roger, M., 1987. The connections of the peripeduncular area studied by retrograde and anterograde transport in the rat. *The Journal of Comparative Neurology*, 258(3), 463-476.
- Backus, B.C. & Guinan, J.J., 2006. Time course of the human medial olivocochlear reflex. *The Journal of the Acoustical Society of America*, 119(5 Pt 1), 2889-2904.
- Bäuerle, P., von der Behrens W., Kössl M., & Gaese B.H., 2011. Stimulus-specific adaptation in the gerbil primary auditory thalamus is the result of a fast frequency-specific habituation and is regulated by the corticofugal system. *The Journal of Neuroscience*, 31(26): 9708:9722
- Bajo, V.M. & Moore, D.R., 2005. Descending projections from the auditory cortex to the inferior colliculus in the gerbil, *Meriones unguiculatus*. *The Journal of Comparative Neurology*, 486(2), 101-116.
- Bajo, V.M. et al., 2007. The ferret auditory cortex: descending projections to the inferior colliculus. *Cerebral Cortex (New York, N.Y.: 1991)*, 17(2), 475-491.
- Bajo, V.M., Nodal, F.R., Moore, D.R. & King, A.J., 2010. The descending corticocollicular pathway mediates learning-induced auditory plasticity. *Nature Neuroscience*, 13(2), 253-260.
- Bal, R., Gree, G.G., Rees, A. & Sanders, D.J., 2002. Firing patterns of inferior

colliculus neurones-histology and mechanism to change firing patterns in rat brain slices. *Neuroscience Letters*, 317(1), 42-46.

Behrens, E.G., Schofield, B.R. & Thompson, A.M., 2002. Aminergic projections to cochlear nucleus via descending auditory pathways. *Brain Research*, 955(1-2), 34-44.

Benda, J. & Hennig, R.M., 2008. Spike-frequency adaptation generates intensity invariance in a primary auditory interneuron. *Journal of Computational Neuroscience*, 24(2), 113-136.

Benda, J. & Herz, A.V.M., 2003. A universal model for spike-frequency adaptation. *Neuronal Computation*, 15(11), 2523-2564.

Benda, J., Longtin, A. & Maler, L., 2005. Spike-frequency adaptation separates transient communication signals from background oscillations. *The Journal of Neuroscience*, 25(9), 2312-2321.

Best, A.R. & Wilson, D.A., 2004. Coordinate synaptic mechanisms contributing to olfactory cortical adaptation. *The Journal of Neuroscience*, 24(3), 652-660.

Billimoria, C.P., Kraus, B.J., Narayan, R., Maddox, R.K. & Sen, K., 2008. Invariance and sensitivity to intensity in neuronal discrimination of natural sounds. *The Journal of Neuroscience*, 28(25), 6304-6308.

Bleeck, S., Sayles, M., Ingham, N.J. & Winter, I.M., 2006. The time course of recovery from suppression and facilitation from single units in the mammalian cochlear nucleus. *Hearing Research*, 212(1-2), 176-184.

Boyev, K.P., Liberman, M.C. & Brown, M.C., 2002. Effects of anesthesia on efferent-mediated adaptation of the DPOAE. *Journal of the Association for Research in Otolaryngology: JARO*, 3(3), 362-373.

Brenner, N., Bialek, W. & de Ruyter van Steveninck, R., 2000. Adaptive rescaling maximizes information transmission. *Neuron*, 26(3), 695-702.

Buresova, O, Marusyeva, A.M., Bures J., & Fifkova E., 1964. The influence of cortical spreading depression on unit activity in the colliculus inferior of the rat.. *Physiologia Bohemoslovenica*, 13, 227-235.

Carandini, M. & Ferster, D., 1997. A tonic hyperpolarization underlying contrast adaptation in cat visual cortex. *Science*, 276(5314), 949-952.

Cao, X.-J., and Oertel, D. (2005). Temperature affects voltage-sensitive conductances differentially in octopus cells of the mammalian cochlear nucleus. *J. Neurophysiol.* 94, 821-832

Chung, S., Li, X. & Nelson, S.B., 2002. Short-term depression at thalamocortical synapses contributes to rapid adaptation of cortical sensory responses in

vivo. *Neuron*, 34(3), 437-446.

- Coomes, D.L., Schofield, R.M. & Schofield, B.R., 2005. Unilateral and bilateral projections from cortical cells to the inferior colliculus in guinea pigs. *Brain Research*, 1042(1), 62-72.
- Coomber, B., Edwards, D., Jones, S., Shackleton, T., Goldschmidt, J., Wallace, M. & Palmer, A., 2011. Cortical inactivation by cooling in small mammals. *Frontiers in Systems Neuroscience*, 5, 1-10.
- Costalupes, J.A., Young, E.D., Gibson, D.J., Effects of continuous noise backgrounds on rate response of auditory nerve fibers in cat, 1984. *Journal of neurophysiology*, 51(6), 1326-1344.
- de Boer, J. & Thornton A.R., 2008. Neuronal correlates of perceptual learning in the auditory brainstem: efferent activity predicts and reflects improvement at a speech-in-noise discrimination task. *Journal of Neuroscience*, 28(19):4929–4937
- Dean, I., Robinson, B.L., Harper N.S., & McAlpine D., 2008. Rapid neural adaptation to sound level statistics. *Journal of Neuroscience*, 28(25), 6430-6438.
- Dean, I., Harper, N.S. & McAlpine, D., 2005. Neural population coding of sound level adapts to stimulus statistics. *Nature Neuroscience*, 8(12), 1684-1689.
- Diamond, I.T., Jones, E.G. & Powell, T.P., 1969. The projection of the auditory cortex upon the diencephalon and brain stem in the cat. *Brain Research*, 15(2), 305-340.
- Dobrunz, L.E., Huang, E.P. & Stevens, C.F., 1997. Very short-term plasticity in hippocampal synapses. *Proceedings of the National Academy of Sciences of the United States of America*, 94(26), 14843-14847.
- Dyan, P. & Abbott, L.F., 2001. *Theoretical neuroscience: computational and mathematical modelling of neural systems* (MIT Press, Cambridge, Massachusetts).
- Fairhall, A.L., Lewen, G., Bialek, W. & de Ruyter van Steveninck, R.R., 2001. Efficiency and ambiguity in an adaptive neuronal code. *Nature*, 412(6849), 787-792.
- Feliciano, M. & Potashner, S.J., 1995. Evidence for a glutamatergic pathway from the guinea pig auditory cortex to the inferior colliculus. *Journal of Neurochemistry*, 65(3), 1348-1357.
- Gao, E. & Suga, N., 1998. Experience-dependent corticofugal adjustment of midbrain frequency map in bat auditory system. *Proceedings of the National Academy of Sciences of the United States of America*, 95(21), 12663-12670.
- Gao, E. & Suga, N., 2000. Experience-dependent plasticity in the auditory cortex

and the inferior colliculus of bats: role of the corticofugal system. *Proceedings of the National Academy of Sciences of the United States of America*, 97(14), 8081-8086.

- Gibson, D.J., Young, E.D., and Costalupes, A, 1985. Similarity of dynamic range adjustment in auditory nerve and cochlear nuclei. *Journal of Neurophysiology*, 53(4), 940-958.
- Guinan, J.J. & Stankovic, K.M., 1996. Medial efferent inhibition produces the largest equivalent attenuations at moderate to high sound levels in cat auditory-nerve fibers. *The Journal of the Acoustical Society of America*, 100(3), 1680-1690.
- Guinan, J.J., 2006. Olivocochlear efferents: anatomy, physiology, function, and the measurement of efferent effects in humans. *Ear and Hearing*, 27(6), 589-607.
- Harris, D.M. & Dallos, P., 1979. Forward masking of auditory nerve fiber responses. *Journal of Neurophysiology*, 42(4), 1083-1107.
- Hardingham, N.R., and Larkman, A.U. (1998). The reliability of excitatory synaptic transmission in slices of rat visual cortex in vitro is temperature dependent. *The Journal of Physiology* 507, 249-256.
- Hashemi-Nezhad, M., Wang, C., Burke, W., Dreher, B., 2003. Area 21a of cat visual cortex strongly modulates neuronal activities in the superior colliculus. *The Journal of Physiology*, 550(Pt 2), 535-552.
- Hara, K., & Harris RA (2002). The anaesthetic mechanism of urethane: the effects on neurotransmitter-gated ion channels. *Anaesthesia and Analgesia*, 94(2), 313-8
- He, J., 1997. Modulatory effects of regional cortical activation on the onset responses of the cat medial geniculate neurones. *Journal of Neurophysiology*, 77(2), 896-908.
- He, J., 2003a. Corticofugal modulation on both ON and OFF responses in the nonlemniscal auditory thalamus of the guinea pig. *Journal of Neurophysiology*, 89(1), 367-381.
- He, J., 2003b. Corticofugal modulation of the auditory thalamus. *Experimental Brain Research*. 153(4), 579-590.
- Higley, M.J. & Contreras, D., 2006. Balanced excitation and inhibition determine spike timing during frequency adaptation. *The Journal of Neuroscience*, 26(2), 448-457.
- Hildebrandt, K.J., Benda, J. & Hennig, R.M., 2009. The origin of adaptation in the auditory pathway of locusts is specific to cell type and function. *The Journal of Neuroscience*, 29(8), 2626-2636.

- Hua, T., Tang, C., Wang, Z. & Chang, S., 2009. Enhanced adaptation of visual cortical cells to visual stimulation in aged cats. *Neuroscience Letters*, 451(1), 25-28.
- Hua, T., Li, X., He, L., Zhou, Y., Wang, Y., Leventhal, A.G., 2006. Functional degradation of visual cortical cells in old cats. *Neurobiology of Aging*, 27(1), 155-162.
- Huffman, R.F. & Henson, O.W., 1990. The descending auditory pathway and acousticomotor systems: connections with the inferior colliculus. *Brain Research. Brain Research Reviews*, 15(3), 295-323.
- Ingham, N.J. & McAlpine, D., 2004. Spike-frequency adaptation in the inferior colliculus. *Journal of Neurophysiology*, 91(2), 632-645.
- Jasper, H., Ajmone-Marsan, C. & Stoll, J., 1952. Corticofugal projections to the brain stem. *A. M. A. Archives of Neurology and Psychiatry*, 67(2), 155-171.
- Jen, P.H., Sun, X. & Chen, Q.C., 2001. An electrophysiological study of neuronal pathways for corticofugally inhibited neurones in the central nucleus of the inferior colliculus of the big brown bat, *Eptesicus fuscus*. *Experimental Brain Research*, 137(3-4), 292-302.
- Kvale, M.N. & Schreiner, C.E., 2004. Short-term adaptation of auditory receptive fields to dynamic stimuli. *Journal of Neurophysiology*, 91(2), 604-612.
- Laughlin, S.B., 2001. Energy as a constraint on the coding and processing of sensory information. *Current Opinion in Neurobiology*, 11(4), 475-480.
- Lim, H.H. & Anderson, D.J., 2007. Antidromic activation reveals tonotopically organized projections from primary auditory cortex to the central nucleus of the inferior colliculus in guinea pig. *Journal of Neurophysiology*, 97(2), 1413-1427.
- Linden, R. & Rocha-Miranda, C.E., 1983. Organization of the visual thalamus: corticothalamic projections from the primary visual area in the opossum. *Brazilian Journal of Medical and Biological Research*, 16(3), 247-260.
- Lomber, S.G., Payne, B.R. & Horel, J.A., 1999. The cryoloop: an adaptable reversible cooling deactivation method for behavioral or electrophysiological assessment of neuronal function. *Journal of Neuroscience Methods*, 86(2), 179-194.
- Lomber, S.G. & Malhotra, S., 2008. Double dissociation of 'what' and 'where' processing in auditory cortex. *Nature Neuroscience*, 11(5), 609-616.
- Luo, F., Wang, Q., Kashani, A., Yan, J., 2008. Corticofugal modulation of initial sound processing in the brain. *The Journal of Neuroscience*, 28(45), 11615-11621.
- Ma, X. & Suga, N., 2007. Multiparametric corticofugal modulation of collicular

- duration-tuned neurones: modulation in the amplitude domain. *Journal of Neurophysiology*, 97(5), 3722-3730.
- Maravall, M., Petersen, R.S., Fairhall, A.L., Arabzadeh, E. & Diamond M.E., 2007. Shifts in coding properties and maintenance of information transmission during adaptation in barrel cortex. *PLoS Biology*, 5(2), e19.
- McCormick, D.A. & Prince, D.A., 1988. Noradrenergic modulation of firing pattern in guinea pig and cat thalamic neurones, in vitro. *Journal of Neurophysiology*, 59(3), 978-996.
- Meltzer, N.E. & Ryugo, D.K., 2006. Projections from auditory cortex to cochlear nucleus: A comparative analysis of rat and mouse. *The Anatomical Record. Part A, Discoveries in Molecular, Cellular, and Evolutionary Biology*, 288(4), 397-408.
- Mitani, A., Shimokouchi, M. & Nomura, S., 1983. Effects of stimulation of the primary auditory cortex upon colliculogeniculate neurones in the inferior colliculus of the cat. *Neuroscience Letters*, 42(2), 185-189.
- Moriizumi, T. & Hattori, T., 1991. Pyramidal cells in rat temporoauditory cortex project to both striatum and inferior colliculus. *Brain Research Bulletin*, 27(1), 141-144.
- Motts, S.D. & Schofield, B.R., 2009. Sources of cholinergic input to the inferior colliculus. *Neuroscience*, 160(1), 103-114.
- Mulders, W.H.A.M., Seluakumaran, K. & Robertson, D., 2008. Effects of centrifugal pathways on responses of cochlear nucleus neurones to signals in noise. *The European Journal of Neuroscience*, 27(3), 702-714.
- Murphy, P.C. & Sillito, A.M., 1987. Corticofugal feedback influences the generation of length tuning in the visual pathway. *Nature*, 329(6141), 727-729.
- Nakamoto, K.T., Jones, S.J. & Palmer, A.R., 2008. Descending projections from auditory cortex modulate sensitivity in the midbrain to cues for spatial position. *Journal of Neurophysiology*, 99(5), 2347-2356.
- Nakamoto, K.T., Shackleton, T.M. & Palmer, A.R., 2010. Responses in the Inferior Colliculus of the Guinea Pig to Concurrent harmonic series and the effect of Inactivation of Descending Controls. *Journal of Neurophysiology*, 103: 2050–2061.
- Normann, R.A. & Werblin, F.S., 1974. Control of retinal sensitivity. I. Light and dark adaptation of vertebrate rods and cones. *The Journal of General Physiology*, 63(1), 37-61.
- Ohzawa, I., Sclar, G. & Freeman, R.D., 1985. Contrast gain control in the cat's visual system. *Journal of Neurophysiology*, 54(3), 651-667.

- Oliver, D.L., Winer, J.A., Beckius, G.E. & Saint Marie, R.L., 1994. Morphology of GABAergic neurones in the inferior colliculus of the cat. *The Journal of Comparative Neurology*, 340(1), 27-42.
- Orman, S.S. & Humphrey, G.L., 1981. Effects of changes in cortical arousal and of auditory cortex cooling on neuronal activity in the medial geniculate body. *Experimental Brain Research. Experimentelle Hirnforschung. Expérimentation Cérébrale*, 42(3-4), 475-482.
- Peron, S. & Gabbiani, F., 2009a. Spike frequency adaptation mediates looming stimulus selectivity in a collision-detecting neuron. *Nature Neuroscience*, 12(3), 318-326.
- Peron, S.P. & Gabbiani, F., 2009b. Role of spike-frequency adaptation in shaping neuronal response to dynamic stimuli. *Biological Cybernetics*, 100(6), 505-520.
- Perrot, X., Ryvlin, P., Isnard J., Guénot, M., Catenoix, H., Fischer, C., Manguie, F., & Collet, L., 2006. Evidence for corticofugal modulation of peripheral auditory activity in humans. *Cerebral Cortex*, 16(7), 941-948.
- Phillips, D.P. and Hall, S.E., 1986. Spike-rate intensity functions of cat cortical neurons studied with combined tone-noise stimuli. *J. Acoust. Soc. Am.*, 80, 177-187.
- Popelár, J., Nwabueze-Ogbo, F.C. & Syka, J., 2003. Changes in neuronal activity of the inferior colliculus in rat after temporal inactivation of the auditory cortex. *Physiological Research / Academia Scientiarum Bohemoslovaca*, 52(5), 615-628.
- Rees, A. and Palmer, A.R., 1988. Rate-intensity functions and their modification by broadband noise for neurons in the guinea pig inferior colliculus. *J Acoust. Soc. Am.*, 83(4), 1488-1497.
- Romanski, L.M. & LeDoux, J.E., 1993. Information cascade from primary auditory cortex to the amygdala: corticocortical and corticoamygdaloid projections of temporal cortex in the rat. *Cerebral Cortex*, 3(6), 515-532.
- Saldaña, E., Feliciano, M. & Mugnaini, E., 1996. Distribution of descending projections from primary auditory neocortex to inferior colliculus mimics the topography of intracollicular projections. *The Journal of Comparative Neurology*, 371(1), 15-40.
- Sanchez-Vives, M.V., Nowak, L.G. & McCormick, D.A., 2000a. Cellular mechanisms of long-lasting adaptation in visual cortical neurones in vitro. *The Journal of Neuroscience*, 20(11), 4286-4299.
- Sanchez-Vives, M.V., Nowak, L.G. & McCormick, D.A., 2000b. Membrane mechanisms underlying contrast adaptation in cat area 17 in vivo. *The Journal of Neuroscience*, 20(11), 4267-4285.
- Schiff, S.J. & Somjen, G.G., 1985. The effects of temperature on synaptic

- transmission in hippocampal tissue slices. *Brain Research*, 345(2), 279-284.
- Schofield, B. & Motts, S., 2009. Projections from auditory cortex to cholinergic cells in the midbrain tegmentum of guinea pigs. *Brain Research Bulletin*, 80(3), 163-170.
- Schofield, B.R., 2009. Projections to the inferior colliculus from layer VI cells of auditory cortex. *Neuroscience*, 159(1), 246-258.
- Schofield, B.R., 2010. Projections from auditory cortex to midbrain cholinergic neurons that project to the inferior colliculus. *Neuroscience*, 166(1), 231-240.
- Schofield, B.R. & Coomes, D.L., 2005. Projections from auditory cortex contact cells in the cochlear nucleus that project to the inferior colliculus. *Hearing Research*, 206(1-2), 3-11.
- Schofield, B.R. & Coomes, D.L., 2006. Pathways from auditory cortex to the cochlear nucleus in guinea pigs. *Hearing Research*, 216-217, 81-89.
- Seluakumaran, K., Mulders W., & Robertson D., 2008. Unmasking effects of olivocochlear efferent activation on responses of inferior colliculus neurones. *Hearing Research*, 243: 35–46.
- Sillito, A.M. et al., 1994. Feature-linked synchronization of thalamic relay cell firing induced by feedback from the visual cortex. *Nature*, 369(6480), 479-482.
- Sivaramakrishnan, S. & Oliver, D.L., 2001. Distinct K currents result in physiologically distinct cell types in the inferior colliculus of the rat. *The Journal of Neuroscience*, 21(8), 2861-2877.
- Smirnakis, S.M., Berry, M.J., Warland, D.K., Bailek W., & Meister, M., 1997. Adaptation of retinal processing to image contrast and spatial scale. *Nature*, 386(6620), 69-73.
- Suga, N., Gao, E., Zhang, Y., Ma, X., & Olsen, J.F., 2000. The corticofugal system for hearing: recent progress. *Proceedings of the National Academy of Sciences of the United States of America*, 97(22), 11807-11814.
- Suga, N., 2008. Role of corticofugal feedback in hearing. *Journal of Comparative Physiology. A, Neuroethology, Sensory, Neuronal, and Behavioral Physiology*, 194(2), 169-183.
- Sun, X., Chen, Q.C. & Jen, P.H., 1996. Corticofugal control of central auditory sensitivity in the big brown bat, *Eptesicus fuscus*. *Neuroscience Letters*, 212(2), 131-134.
- Syka, J. & Popelár, J., 1984. Inferior colliculus in the rat: neuronal responses to stimulation of the auditory cortex. *Neuroscience Letters*, 51(2), 235-240.

- Syka J., Popelár J., Kvasnák E., and Astl J., (2000). Response properties of neurons in the central nucleus and external and dorsal cortices of the inferior colliculus in guinea pig. *Exp Brain Res.*, 133(2): 254-66.
- Tortorolo, P., Zurita, P., Pedemonte M., Velluti, R.A., 1998. Auditory cortical efferent actions upon inferior colliculus unitary activity in the guinea pig. *Neuroscience Letters*, 249(2-3), 172-176.
- Trevelyan, A.J., and Jack, J. (2002). Detailed passive cable models of layer 2/3 pyramidal cells in rat visual cortex at different temperatures. *The Journal of Physiology* 539, 623-636.
- Tzounopoulos, T. & Kraus, N., 2009. Learning to encode timing: mechanisms of plasticity in the auditory brainstem. *Neuron*, 62(4), 463-469.
- Villa, A.E., Rouiller E.M., Zurita S.P., de Ribaupierre, Y., & de Ribaupierre F., 1991. Corticofugal modulation of the information processing in the auditory thalamus of the cat. *Experimental Brain Research*, 86(3), 506-517.
- Volgushev M., Kudryashov I., Mukovski M., Niesmann J., & Eysel UT., 2004. Probability of transmitter release at neocortical synapses at different temperatures. *Journal of Neurophysiology*, 92: 212-220.
- Volgushev, M., Vidyasagar, T.R., Chistiakova, M., and Eysel, U.T. (2000a). Synaptic transmission in the neocortex during reversible cooling. *Neuroscience* 98, 9-22.
- Volgushev, M., Vidyasagar, T.R., Chistiakova, M., Yousef, T., and Eysel, U.T. (2000b). Membrane properties and spike generation in rat visual cortical cells during reversible cooling. *The Journal of Physiology* 522, 59-76.
- Wallace, M.N., Rutkowski, R.G. & Palmer, A.R., 2000. Identification and localisation of auditory areas in guinea pig cortex. *Experimental Brain Research*, 132(4), 445-456.
- Watkins, P.V. & Barbour, D.L., 2008. Specialized neuronal adaptation for preserving input sensitivity. *Nature Neuroscience*, 11(11), 1259-1261.
- Watkins, P.V. & Barbour, D.L., 2011. Level-Tuned Neurones in Primary Auditory Cortex Adapt Differently to Loud versus Soft Sounds. *Cerebral Cortex*, 21(1), 178-90.
- Wen, B. et al., 2009. Dynamic Range Adaptation to Sound Level Statistics in the Auditory Nerve. *Journal of Neuroscience*, 29(44), 13797-13808.
- Westerman, L.A. & Smith, R.L., 1984. Rapid and short-term adaptation in auditory nerve responses. *Hearing Research*, 15(3), 249-260.

- Winer, J.A. & Prieto, J.J., 2001. Layer V in cat primary auditory cortex (AI): cellular architecture and identification of projection neurones. *The Journal of Comparative Neurology*, 434(4), 379-412.
- Winer, J.A., 2005. Decoding the auditory corticofugal systems. *Hearing Research*, 207(1-2), 1-9.
- Winer, J.A., Chernock, M.L., Larue, D.T. & Cheung, S.W., 2002. Descending projections to the inferior colliculus from the posterior thalamus and the auditory cortex in rat, cat, and monkey. *Hearing Research*, 168(1-2), 181-195.
- Winer, J.A. & Lee, C.C., 2007. The distributed auditory cortex. *Hearing Research*, 229(1-2), 3-13.
- Winer, J.A., Miller, L.M., Lee, C.C., & Schreiner, C.E., 2005. Auditory thalamocortical transformation: structure and function. *Trends in Neurosciences*, 28(5), 255-263.
- Wong, D. & Kelly, J.P., 1981. Differentially projecting cells in individual layers of the auditory cortex: a double-labeling study. *Brain Research*, 230(1-2), 362-366.
- Wu, S.H., Ma, C.L. & Kelly, J.B., 2004. Contribution of AMPA, NMDA, and GABA(A) receptors to temporal pattern of postsynaptic responses in the inferior colliculus of the rat. *The Journal of Neuroscience*, 24(19), 4625-4634.
- Xiao, Z. & Suga, N., 2002. Modulation of cochlear hair cells by the auditory cortex in the mustached bat. *Nature Neuroscience*, 5(1), 57-63.
- Yan, J. & Ehret, G., 2001. Corticofugal reorganization of the midbrain tonotopic map in mice. *Neuroreport*, 12(15), 3313-3316.
- Yan, J. & Ehret, G., 2002. Corticofugal modulation of midbrain sound processing in the house mouse. *The European Journal of Neuroscience*, 16(1), 119-128.
- Yan, J., Zhang, Y. & Ehret, G., 2005. Corticofugal shaping of frequency tuning curves in the central nucleus of the inferior colliculus of mice. *Journal of Neurophysiology*, 93(1), 71-83.
- Yang, X. et al., 2005. Cooling blocks rat hippocampal neurotransmission by a presynaptic mechanism: observations using 2-photon microscopy. *The Journal of Physiology*, 567(Pt 1), 215-224.
- Zhou, X. & Jen, P.H., 2000. Brief and short-term corticofugal modulation of subcortical auditory responses in the big brown bat, *Eptesicus fuscus*. *Journal of Neurophysiology*, 84(6), 3083-3087.

# ACKNOWLEDGEMENTS

---

I present this thesis with gratitude to David McAlpine and Isabel Dean for their unstinting support both within the lab and without. This research would not exist without their enthusiasm and care.

The work was supported by MRC and BBSRC grants and use was made of Deafness Research UK and Brain travel grants to present preliminary data at conferences.